1-1-2003

Analytical modeling of the shear behavior of reinfored concrete exterior beam-column joints

Reza Sadjadi
Ryerson University

ANALYTICAL MODELING OF THE SHEAR BEHAVIOR OF REINFORCED CONCRETE EXTERIOR BEAM-COLUMN JOINTS

By

Reza Sadjadi
B.Sc., Tehran Polytechnic, IRAN, 1992

A thesis

Presented to Ryerson University

in partial fulfillment of the

requirement for the degree of

Master of Applied Science

in the Program of Civil Engineering

Toronto, Ontario, Canada, 2003

National Library
of Canada

Bibliothèque nationale
du Canada

Acquisitions and
Bibliographic Services

Acquisisitons et
services bibliographiques

395 Wellington Street
Ottawa ON K1A 0N4
Canada

395, rue Wellington
Ottawa ON K1A 0N4
Canada

Canadä

AUTHOR'S DECLERATION

I hereby declare that I am the sole author of this thesis.

I authorize Ryerson University to lend this thesis to other institution or individuals for the purpose of scholarly research.

I further authorize Ryerson University to reproduce this thesis by photocopying or by other means, in total or in part, at the request of other institution or individuals for the purpose of scholarly research.

BORROWERS PAGE

Name	Address	Signature	Date

ANALYTICAL MODELING OF THE SHEAR BEHAVIOR OF REINFORCED CONCRETE EXTERIOR BEAM-COLUMN JOINTS

BY: REZA SADJADI
MASTER OF APPLIED SCIENCE
CIVIL ENGINEERING, RYERSON UNIVERSITY
SEPTEMBER 2003

ABSTRACT

In reinforced concrete structures, failure of beam-column joint was observed as one of the major causes of damage of those structures during earthquakes. Non-ductile detailing of reinforcement in the joint in terms of inadequate shear reinforcement in the joint panel or insufficient anchorage of the beam bars within the joint region are the main causes of deficiency in the performance of joints during an earthquake.

The objectives of this study are to compare different aspects of modeling the nonlinear behavior of exterior beam-column joints and also to propose a new model for the shear behavior of exterior joints. Two well-known computer programs for nonlinear dynamic analysis of the structures DRAIN-2DX (element type 15) and IDARC2D are used. The advantages of using each one for the beam-column joints in the reinforced concrete structures, and the effect of modeling features on the response of beam-column joints are discussed.

ACKNOWLEDGEMENTS

I would like to express my profound gratitude and great appreciation to my research supervisor, Dr. R. Kianoush, for his encouragement, valuable advise, constructive suggestions, tireless guidance, and enduring patience throughout this study.

Finally, I would like to express my sincere appreciation to my father, mother, and sister for their endless love and support. This thesis is dedicated to them.

TABLE OF CONTENTS

LIST OF TABLES

LIST OF FIGURES

LIST OF SYMBOLS

AMLB	Parameter defining the clear length of the beam, plus the length of two rigid arms.) [IDARC2D]
AMLC	Parameter defining the clear length of the column, plus the length of two rigid arms) [IDARC2D]
CEFF	Effectiveness of confinement for typical hoop arrangements in IDARC2D
EC	Initial Young's Modulus of concrete) [IDARC2D]
E13N	Post Yield Flexural Stiffness (negative)) [IDARC2D]
E13P	Post Yield Flexural Stiffness (positive) [IDARC2D]
EPSH	Strain at start of hardening (%)[IDARC2D]
EPSO	Strain at maximum stress of concrete (%)[IDARC2D]
EPSU	Ultimate strain in compression [IDARC2D]
ES	Modulus of elasticity [IDARC2D]
ESH	Modulus of strain hardening [IDARC2D]
FC	Unconfined compressive strength [IDARC2D]
FS	Yield strength [IDARC2D]
FT	Stress at tension cracking [IDARC2D]
FSU	Ultimate strength [IDARC2D]
HBD	Stiffness degrading parameter (ductility based) [IDARC2D]
HBE	Strength degrading parameter (energy-controlled) [IDARC2D]
HC	Strength degrading parameter [IDARC2D]
HS	Slip or crack closing parameter [IDARC2D]
PCN	Cracking Moment (negative) [IDARC2D]
PCP	Cracking Moment (positive) [IDARC2D]
PYP	Yield Moment (positive) [IDARC2D]
PYN	Yield Moment (negative) [IDARC2D]
RAMB1	Rigid Arm at beam's left end [IDARC2D]
RAMB2	Rigid Arm at beam's right end [IDARC2D]
RAMC1	Rigid Arm at column's bottom [IDARC2D]
RAMC2	Rigid Arm at column's top [IDARC2D]

UUN	Ultimate Curvature (negative) [IDARC2D]
UUP	Ultimate Curvature (positive) [IDARC2D]
UYN	Yield Curvature (negative) [IDARC2D]
UYP	Yield Curvature (positive) [IDARC2D]
ZF	Parameter defining the slope of the falling branch
A_g	Gross cross-section area
As	Area of reinforcement
b'	Width of confined core measured to outside of hoops.
b_{Joint}	Joint panel width
C's	Compressive force in steel bar (beam)
C'_C	Compressive force in concrete (beam
d'	Depth of cross-section
E	The elastic modulus of concrete
E_S	Modulus of elasticity of steel
f'_c	Maximum compressive strength of the concrete in 28 days
F_c	Internal diagonal compressive stresses in the joint zone
f'_{cc}	Confined concrete strength
f_{max}	Strength capacity prior to bar fracture
f_s	Stress in the still
f'_t	Lateral confining pressure produced by steel ties
F_t	Internal diagonal tensile stresses in the joint zone
f_u	Peak strength in steel
f_y	Yield strength of steel
I	Rectangular section moment of inertia
J_b	The value of the stress resultants normalized effective depth
P_u	Axial force on the column
S	Spacing of hoops
S_h	Spacing of hoops
T	Tensile strength in the longitudinal beam bar (Top)
T`	Tensile strength in the longitudinal beam bar (Bottom)
V_C	Column shear force

σ_y The yield strength of steel

ε_{50c} The strain corresponding to stress of 0.5 f'_c

ε_c The maximum strain of concrete

ε_{cc} Compressive concrete strain corresponding to f'_{cc}

ε_u Strain at which peak strength is achieved

ε_{max} Strain at which fracture occurs

ε_s Strain of steel

ε_{sh} Strain at which strain hardening initiates

ε_u The ultimate strain of steel

λ Reinforcement over-strength factor

ρ_s Ratio of volume of transverse reinforcement to volume of concrete measured to outside of hoops

Chapter 1

INTRODUCTION

1.1 Background

Major seismic events during the last few decades have continued to demonstrate the destructive power of earthquakes. Buildings, bridges, industrial facilities, and other structures are damaged or destroyed, often with high loss of life and great economic loss. Due to building codes prior to 1970, many reinforced concrete frame structures were designed only for gravity load or for inadequate lateral loads than the loads specified by the current seismic codes. Even there is evidence of structures designed according to the current code, but collapsed because the designer was inexpert in earthquake resistive design (The parking garage at California State University, Northridge, shown in Figure 1-1).
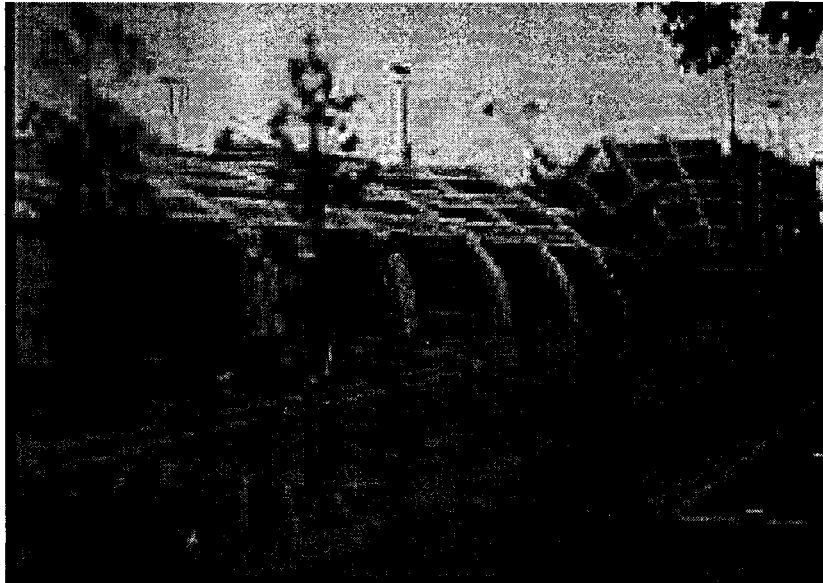
Figure 1-1 The parking garage at California
University, Northridge State
http://www.ngdc.noaa.gov/seg/hazard/slideset

In reinforced concrete structures, failure of beam-column joint was observed as one of the major causes of damage or even collapse of those structures during earthquakes. Experimental investigation and observation of structural damage following recent earthquakes show that inadequately designed connections have the potential for producing inadequate structural response.

1

Non-ductile detailing of reinforcement in the joint in terms of inadequate shear reinforcement in the joint panel, or insufficient anchorage of the beam bars within the joint region are the main causes of deficiency in the performance of the beam-column joints during an earthquake.

The intersection between the beam and column defines a region of unique design, loading and behavior within a reinforced concrete frame under earthquake loading. Design procedures should begin to select from types of failures that are acceptable and others that are undesirable. For frame structure systems, flexural yielding of the beam prior to flexural yielding of the column is the desired response mechanism. Thus, under severe loading and if the connection is adequately designed, the beam could be expected to achieve significant post-yield flexural strength while the column flexural demands could be expected to approach values associated with nominal flexural strength. These actions imply substantial shear loading of the connection, which could result in connection damage or failure. With the proper design of columns and beams, it may be found that beam-column joints become the weakest part in the mechanism of resistance of the structure. It has been found that inelastic deformations within a joint during cyclic reversed loading may lead to rapid loss of both stiffness and strength.

Joints in general are unsuitable localities for energy dissipation. Capacity design, relevant to joints, must ensure that the over-strength input from beams that are connected is maintained with a minimum of inelastic deformation within the joint core. When it is accepted that the avoidance of irreparable deformations and damages under very severe seismic excitations is not economical, the attention is immediately focused on the various modes of structural failure that could result. Structural failures and consequent irreparable damage to be considered are not synonymous with structural collapse. Indeed the most important aim in earthquake resistant structural design is to minimize the likelihood of collapse under the most severe excitation that could be expected during the expected life of the structure. Moreover, the building structure should be designed in a controlled manner such that its behavior is ensured at predefined performance levels under earthquake loading and the design guidelines should imply the damage levels, which are expected to be achieved, or at least not be exceeded, when the structure is subjected to earthquake ground motion of specified intensity. In other word, the design objective can

be interpreted as providing a uniform interstory drift distribution over the height of the building (Gupta and Krawinkler, 2000), followed by reduction in unnecessary costs. These are the main objective criteria for the performance-based seismic design: minimum structure cost and uniform ductility demand over all stories.

Performance-based seismic design of buildings is a relatively new concept and is rapidly becoming widely accepted in structural engineering practice. There are uncertainties concerning the seismic demand and seismic capacity of the structure. Performance-based design is a more general design philosophy in which the design criteria are expressed in terms of achieving stated performance objectives when the structure is subjected to stated levels of seismic hazard. The performance targets may be a level of stress not to be exceeded, a load, a displacement, a limit state or a target damage state.

If connection design is inadequate for the shear load that develops under earthquake excitation, the connection may exhibit deteriorating stiffness and strength. This behavior may result in inadequate structural performance. The beam-column connection provides continuity between the beam and column elements, establishing a continuous load path in the frame. Thus, connection flexibility increases global structural flexibility. If the connection exhibits inelastic shear deformation or slip of reinforcement anchored in the connection, the increase in connection flexibility may be relatively large and may control structural response. Inelastic response mechanisms may result in deterioration of connection strength as well as stiffness.

1.2 Behavior of Beam-Column Joints

To investigate the load-deformation response of a beam-column connection, it is necessary to consider connection behavior at a localized level. Local response mechanisms that determine connection behavior include those associated with flexure of the beams and column that frame into the connection, load transfer between concrete and reinforcing steel and shear transfer in the connection core. The flexural response of the beams and column defines the global load demand on the connection. Beyond load demand, flexural response of the framing element determines the stress distribution in the

3

concrete and reinforcing steel at the perimeter of the connection and, as a result, affects the stress distribution in the connection core.

With load defined at the perimeter of the connection, the bond stress distribution defines the longitudinal steel stress distribution within the connection and thus the additional connection flexibility associated with extended yielding of the reinforcement. Bond response also determines the load distribution at the perimeter of the connection core. Inadequate bond strength may limit the capacity of the connection to transfer beam and column flexural loads resulting in a strength degrading response history under earthquake loading. In particular the consequences of bar slip within a joint can be very serious. It enhances interstorey drift and thus allows P-delta effects also to become more significant.

Finally, connection response may be determined by behavior of the connection core. Loading of connection core concrete comes through transfer of the concrete stress developed in beam and column flexural compression zones and through transfer of reinforcing steel compression and tension stress as distributed to the connection core through bond. These external loads combine to define a global connection shear load. Under severe reversed cyclic shear loading, concrete in the connection core may crack under high principal tensile stress, or crush under high principal compression stress. Also, accumulated damage in the connection core concrete from previous cycles may result in substantial inelastic deformation and strength loss.

1.3 Analytical Modeling of Beam-Column Joints

The main objective of any design method is the assessment of the safety and the serviceability of the structure during different load history. Because of the economic feasibility of using analytical model instead of obtaining data from destructive experimental tests, there is a need for an efficient and reliable analytical model, which predicts the behavior of such structures, and gives comparable results to experimental data. For modern complex structures, which are subjected to very complex load history during an earthquake, the safety and serviceability assessment of such structures should be based on accurate analytical model with reliable results. Much of the analyses in the past were based on the consideration of simple inelastic system to predict the response of the structure during earthquakes. When a member is designed for gravity loads, the

4

ultimate load level is usually designed to be in the elastic range, while in seismic design of the structures the critical elements must be ductile since the member is designed to go into the inelastic range. Moreover, the load-deformation relationship is not identical during successive cycles, because the elements degrade due to the accumulating damage of previous cycles.

Experimental investigation and observation of structural damage following recent earthquakes show that inadequately designed connections have the potential for producing inadequate structural response. The more the nonlinear behavior of beam-column joint is known and predictable, the better such undesirable damages could be prevented, and the appropriate retrofitting scheme could be selected. Estimates of the demands can be established through dynamic inelastic analyses of appropriate models. These models can be chosen to cover the practical range of values of the most significant parameters considered explicitly in design. The model should be based on accurate nonlinear dynamic analysis and real behavior of the elements. A number of nonlinear models have been developed for predicting the behavior of different structural elements during earthquakes. Most of the nonlinear models assume the beam-column connection to be rigid, regardless of the real behavior of the joint during shear degradation and bond deterioration. The behavior of the joint is then simulated by means of several inelastic springs, which have been calibrated by the results of experimental data. Since the contribution of the joint deformation to the overall performance of the structure is not negligible, therefore the mentioned model is not precise.

There are two rather valid major categories for the nonlinear dynamic analysis of reinforced concrete structures. One is to present the overall behavior of each structural component in terms of a macromodel. The second is to discretize each structural component into smaller units and then capture the overall behavior of the component in terms of the behavior of those smaller units.

A major aspect in modeling the nonlinear behavior of the components is how to consider the regions which yield and the regions which remain elastic in the structural components during the dynamic analysis. One common model (lumped plasticity model) is to consider the yielding of the element to be localized in the zero length regions in the elements' ends, which are called plastic hinges. The idea behind the other model (spread

plasticity model) is to assume the plastic hinges to form in the members' ends but allows some parts of the length of the element to go into inelastic deformation. DRAIN-2DX (Allahabadi and Powel, 1988) is a computer program for static and dynamic analysis of inelastic plane structures. The concept of lumped plasticity is implemented in the program (plastic hinge beam-column element). Yielding occurs only in the plastic hinges, that is; the element consists of an elastic beam, and two plastic hinges at the ends of the beam, and optional rigid end zone. The element has serious limitation. The inelastic axial deformation is not considered, and plastic hinges are assumed to yield only in bending. Thus using such element in the event of significant P-M interaction is not theoretically correct. Moreover modeling the behavior of reinforced concrete with lumped-plasticity idealization is not accurate, since inelastic deformation is observed throughout the non-zero length in the members' end. The hysteretic moment- curvature of the member is a combination of two parallel components: An elastic component, which provides the stiffness after yielding, and an elastic-plastic component. The bilinear resultant is specified in terms of moment rotation of the member ends, thus the model relies on the relation between curvature and end rotation, and ignores the real behavior of the connection of the elements in the joint zone. IDARC2D has the capability of using both lumped plasticity, and spread plasticity concepts. The formulations are based on macro-models in which most of the elements are represented as a comprehensive element with nonlinear behavior. Columns and beams are macro-model with inelastic flexural deformation and elastic shear deformation. The beam unlike the column does not take axial deformation.

The deformation in the joint which has a controlling role in the load-deformation of the structure is simulated by versatile hysteretic models, which are implemented in the program and are mainly controlled by parameters indicating the stiffness degradation, strength deterioration, and pinching of the hysteretic loops.

Based on the mentioned concepts, the nonlinear dynamic analysis of a structure or a part of a structure relies on simplified method. There were no consideration of the actual behavior and deformation of the joint. Thus for prediction of the behavior of the structure during an earthquake by each model, there are many unknown parameters which should be defined. These include; deformation- load relationship in the members' end, stiffness

degradation, strength deterioration, and pinching factors, and so on. To fill the gap between these analytical models and a finite element method model, a new model for the shear behavior of the joint is presented. The model is based on fiber formulation concept (DRAIN-2DX /element type 15) in which, each structural member is modeled by a single element, but the stress-strain relationship for each point is evaluated during the analysis of the several cross section comprising the main cross section of the element. In fiber element material nonlinearity can spread through the whole length of the element. The deformable part of the element is discretized into parallel fibers that are assumed to be stressed and strained uniaxially in the direction parallel to the direction of the longitudinal axis of the element. The behavior is monitored at the center of the cross section in each fiber.

In the proposed model, the joint region is considered to be the connection between the column and the beam end. The beam bar anchorage is assumed to be perfect. Thus bond slip of the beam bars is ignored and the shear is resisted only by a diagonal concrete strut mechanism. The local response mechanisms that control connection behavior are defined by the behavior of plain concrete, and reinforcing steel under general reversed-cyclic loading. Consideration of material behavior associated with development of the local response mechanisms defines the required material modeling capabilities of the proposed model. Connection response is determined by the applied loading at the connection perimeter as controlled by flexural demand in the beams and column, and the behavior of the reinforced concrete constituent materials.

1.4 Motivation

Reinforced concrete structures subjected to strong ground excitation may suffer failure in the beam-column joint. This could have detrimental contribution to the storey drift and also the performance of the whole structure. The more the nonlinear behavior of beam-column joint is known and defined, the better such undesirable damages could be predicted and prevented. The behavior of beam-column joints can be established through cyclic inelastic analyses of appropriate models. The model should be based on accurate nonlinear cyclic analysis and idealized behavior of the elements. Several models have been proposed for modeling the behavior of joints. Each model has some advantages and

some disadvantages in comparison to the other models. Most of the available structural software packages assume a rigid beam-column joint. Although this assumption is reasonable for well-designed and detailed joints, it is not valid for many of the existing buildings. Therefore, there is a persistent need to develop accurate models based on true behavior of the beam-column joints.

1.5 Objectives

The objectives of the present research are:

1. To discuss the behavior of the beam-column joints in terms of mechanisms of load resistance and failure

2. To model the behavior of exterior beam-column joints using two well-known computer programs for nonlinear dynamic analysis of the structures; DRAIN-2DX (Element type 15), and IDARC2D. Each of those programs has features of using the aforementioned modeling aspects. The advantages of using each one for the beam-column joints in the reinforced concrete structures, and the effect of modeling features on the response of beam-column joints are discussed.

1.6 Scope

The present study is focusing on the shear behavior of the exterior beam-column joints, as it is believed that the shear strength of exterior joints are more vulnerable than interior joints, which are confined by more beams and have better condition of the joint core confinement. To achieve the research objectives, the scope of this study is summarized as follows.

1. Study the behavior of beam-column joints in shear and discussing the parameters that have effects on the mechanisms of shear resistance and shear failure.

2. Model the behavior of exterior beam-column joint as macromodels in the nonlinear analysis program IDARC2D.

3. Propose a new analytical model for shear behavior of the exterior beam-column joint based on the true behavior of the joints and the parameters that have effects on the mechanisms of shear resistance and shear failure, using fiber modeling concept in nonlinear analysis program DRAIN-2DX.

1.7 Organization

This thesis is organized into 8 chapters. The objective of the study and an introduction to the concepts, which are used in this study are described in Chapter 1. Chapter 2 describes the material models for the constituent materials in a reinforced concrete element. Several material models for defining the relationships between stress and strain for both concrete and steel are discussed and the appropriate models for applying in the analyses are selected. Chapter 3 describes the response of a circular reinforced concrete column under the axial load and lateral displacement reversals. The analytical modeling of the test is done both in IDARC2D and DRAIN-2DX, and then the results are compared with the experimental results. Chapter 4 describes the behavior of the beam-column joints with reference to well-known mechanisms for behavior of joints in shear. Chapter 5 describes the fiber element concepts, which are implemented in the proposed model in this study in the program DRAIN-2DX (element 15).

In chapter 6 the proposed analytical model for shear behavior of the exterior beam-column joints is described in details. In chapter 7, the results of experimental tests on 4 exterior beam-column joints are presented. The procedures for analytical modeling of the test in IDARC2D and DRAIN-2DX are described, and then the results are compared with the experimental results. In chapter 8, conclusion of the study and recommendation for the future research are presented.

Chapter 2

MATERIAL MODELS

2.1 General

Reinforced concrete structures are made up of concrete and steel, which have different characteristics, concrete and steel. Steel can be considered a homogeneous material and its material properties can be well defined. Concrete is, on the other hand, a heterogeneous material made up of cement, mortar and aggregates. Its mechanical properties scatter widely and cannot be defined easily, but for the convenience of analysis and design, concrete is considered a homogeneous material in this study.

The response of reinforced concrete structures is determined by the response of the concrete and steel under the load applied to the elements. The complex nonlinear response is due to the nature of seismic induced loads and also phenomenon like cracking of the concrete under tension, crushing of concrete under compression, yielding of the steel, the condition of bond between concrete and steel, aggregate interlock at a crack, and dowel action of the reinforcing bar crossing a crack. Therefore, the local response mechanisms that control beam-column connection behavior are defined by the behavior of plain concrete, reinforcing steel under specified loading. The stiffness of concrete and reinforcing steel is formulated separately. The results are then superposed to obtain the element stiffness. Consideration of material behavior associated with development of the local response mechanisms defines the required material modeling capabilities of the proposed model. Connection response is then determined by response of the reinforced concrete material to the applied loading at the connection perimeter as controlled by flexural demand exerted by beams and column to the connection.

In the following each material is discussed and the application of the behavior of each constituent material in the proposed model is discussed.

2.2 Behavior of Concrete

The response of reinforced concrete structures is determined partly by the response of the concrete of which it is composed. Thus, analysis of structural response to

static or dynamic loading requires prediction of concrete response to variable load histories.

The fundamental characteristics of concrete behavior are established through experimental testing of plain concrete specimens subjected to specific, relatively simple load histories. Standardized tests may be used to define material parameters such as compressive strength, elastic modulus, and tensile strength. The results of these experimental investigations define a data set that may be used in development and calibration of the proposed model.

The idealization of concrete as a homogeneous body requires additional consideration for the case of concrete subjected to moderate through severe loading. At these load levels, the response of concrete is determined by the formation of continuous crack systems. Researches have shown that it is possible to maintain the idealization of concrete as a continuum in the presence of discrete cracks. In these models, the material damage (evident in reduced material strength and stiffness) associated with discrete cracking is distributed over a continuous volume of the material. Modeling of concrete as a continuum results in a model that is compatible with many existing computer codes. Under real situation of loading in the structure, concrete is seldom stressed uniaxially; however the assumption of uniaxial stress condition in modeling the plane frame structures can be justified.

Consideration of reinforced concrete frame structure suggests that the response of the system may be investigated through two-dimensional modeling. Under moderate to severe loading, concrete expansion may activate transverse reinforcement to provide confinement in the out-of-plane direction. Thus, for these systems, the response may be characterized by a generalized plane stress model for which the out-of-plane shear stresses are assumed to be zero while the normal stress is defined to be a fixed value. The response of plain concrete subjected to uni-axial tension may determine the response of reinforced concrete structural elements that are inadequately reinforced. Additionally, the deterioration of concrete tensile strength results in accelerated activation of reinforcing steel in all reinforced concrete structures. Thus, it is necessary to include representation of the deterioration of concrete tensile strength in a concrete constitutive model.

Concrete exhibits a large number of microcracks, especially, at the interface between coarser aggregates and mortar, even before subjected to any load. The presence of these microcracks has a great effect on the mechanical behavior of concrete, since their propagation during loading contributes to the nonlinear behavior at low stress levels and causes volume expansion near failure. Many of these microcracks are caused by segregation, shrinkage or thermal expansion of the mortar. Some microcracks may develop during loading because of the difference in stiffness between aggregates and mortar. Since the aggregate-mortar interface has a significantly lower tensile strength than mortar, it constitutes the weakest link in the composite system. This is the primary reason for the low tensile strength of concrete. This is the reason why the contribution of the tensile strength of concrete in comparison to the strength of the member in compression is assumed negligible.

The response of a structure under load depends to a large extent on the stress-strain relation of the constituent materials and the magnitude of stress. Since concrete is used mostly in compression, the stress-strain relation in compression is of primary interest. Such a relation can be obtained from cylinder tests with a height to diameter ratio of 2. The normal standard cylinder is 12 inch high by 6 inch in diameter and the compressive strength attained at 28 days usually ranges between 15 to 55 N/mm^2. The complete stress-strain history for concrete subjected to uniaxial compression provides data for use in characterizing the response of concrete to general loading. For a typical concrete mix subjected to monotonically increasing compressive strain, some important characteristics of the response include the following outlined by Mehta and Monteiro [1993].

1. The response of the plain concrete under increasing strain is linear-elastic until the load reaches approximately 30 percent of the peak compressive strength. This linear-elastic response corresponds to minimal, stable crack growth within the transition zone. A stable crack does not continue to grow under constant load.

2. Loading to compressive stress between 30 and 50 percent of peak compressive stress, results in some reduced material stiffness. Reduction in the material stiffness results from a significant increase in crack initiation and growth in the transition zone. Crack growth is stable in this condition.

3. Loading to compressive stress between 50 and 75 percent of peak compressive stress results in further reduction in material stiffness. The reduced stiffness is partly a result of crack initiation and growth in the *hcp*. Additionally, reduced material stiffness results from the development of unstable cracks that continue to grow when subjected to a constant load.

4. Concrete loaded to more that 75 percent of the peak compressive load responds with increased compressive strain under constant loading. This results from spontaneous crack growth in the transition zone and *hcp* and from the consolidation of microcracks into continuous crack systems.

5. Loading to compressive strains beyond that corresponding to the compressive strength results in reduced compressive strength. This response is a result of the development of multiple continuous crack systems.

For model development, this behavior may be simplified into three levels of response.

Concrete initially responds as an elastic material. Under increased loading, global microcracking results in reduced material stiffness. Eventually, further increase in compressive strain demand results in the development of multiple continuous crack systems and reduced strength. In Figure 2-1 a typical stress-strain curve for concrete in compression is shown.
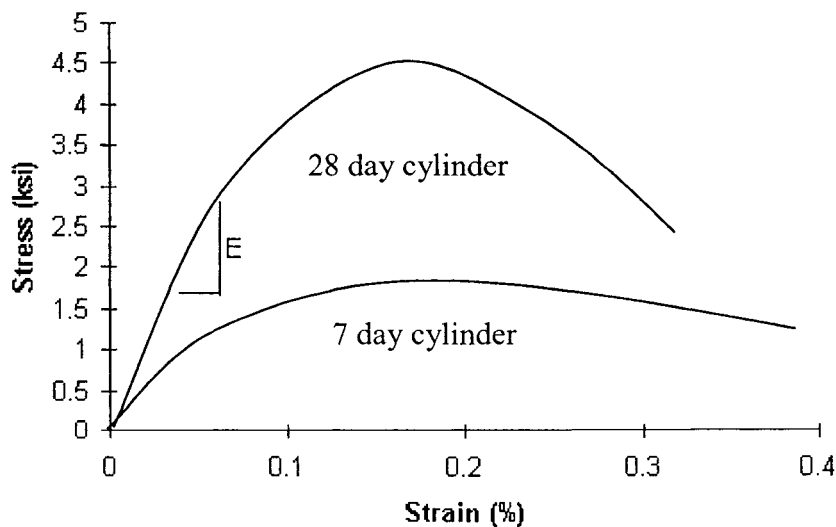
Figure 2.1 Typical stress-strain curve for concrete in compression

2.2.1 Concrete Models

The concrete model refers to the mathematical relationship between the stress and strain, like the one shown in Figure 2.1. The model is used in the analysis of the reinforced concrete structures. The experimental data suggest that a highly sophisticated analytical model is required to characterize concrete response under all possible load histories. Such a model may be impractical and computationally infeasible. In recent years there has been much effort fort developing analytical models that predict the response of plain concrete to specified loading accurately.

Early models relied on elasticity theory. More recently proposed models utilize general theories of solid mechanics including plasticity theory, damage theory and fracture mechanics. The majority of these proposed models predict particular aspects of concrete response with an acceptable level of accuracy and efficiency.

2.2.2 Stress-Strain Relationships for Confined Concrete in Compression

Much research has been conducted on stress-strain relationships for confined concrete by rectangular transverse reinforcement. Some of the better-known relationships especially for normal strength concrete are described by Chan (1995), Blume et al., (1961), Baker (1964) Roy and Sozen (1964), Soliman and Yu (1967), Sargin et al., (1971), Mander et al., (1988), Cusson and Paultre (1994), and Kent and Park (1971).

Chan (1995), proposed a tri-linear curve that is shown in Figure 2-2. The segments OA and AB are approximation of the curve for unconfined concrete, and segment BC is dependant on the transverse reinforcement.
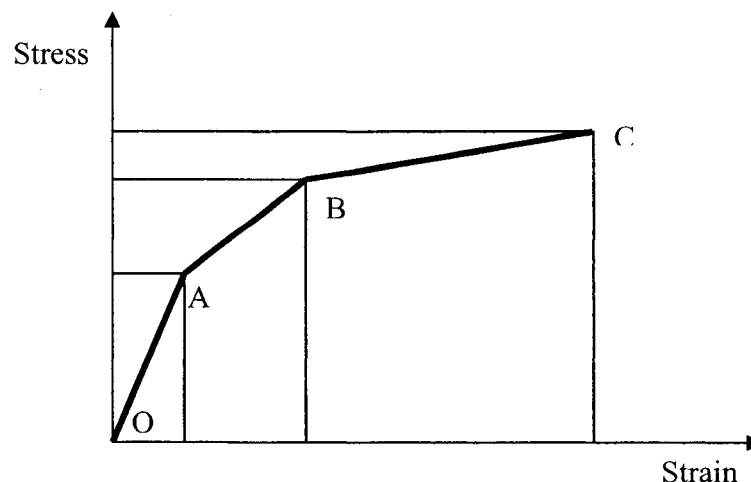
Figure 2-2 Stress-strain relationships proposed by Chan (1995)

14

Blume et al., (1961) also proposed the same curve as Chan but OA segment shows the relationship up to 0.85 f'_c, and AB, and BC segments are dependant on content and yield strength of the transverse reinforcement.

Baker (1964) proposed a parabola up to the maximum stress dependant on the strain gradient across the section and a horizontal branch, which is dependant on transverse reinforcement content. The curve is shown in Figure 2-3.
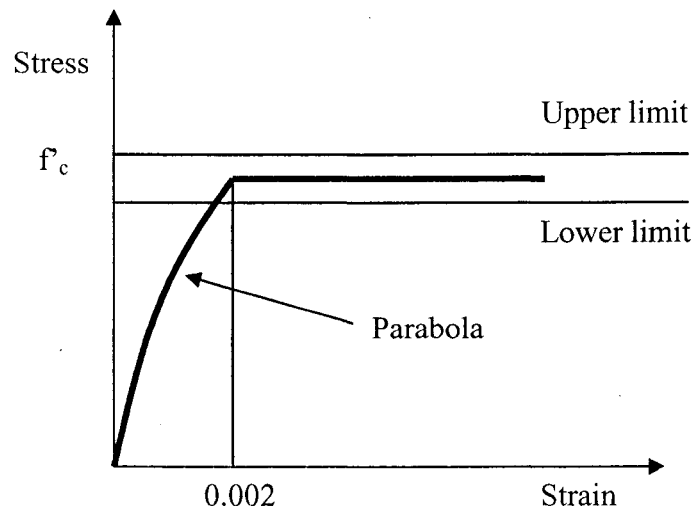
Figure 2-3 Stress-strain relationships proposed by Baker (1964)

Roy and Sozen (1964) suggested a curve that is shown in Figure 2-4, replacing the parabola with a straight line up to maximum stress and then a falling branch relating the stress at 0.5 f'_c to a strain, which is dependant on transverse reinforcement content.
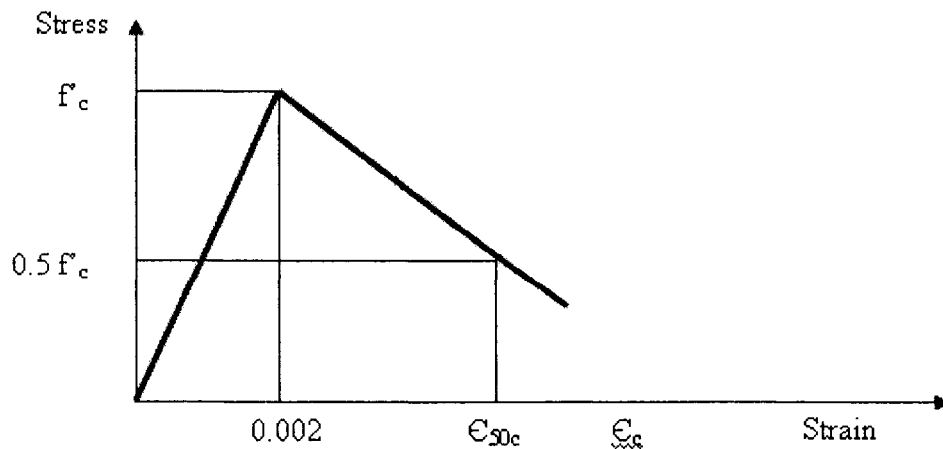
Figure 2-4 Stress-strain relationships proposed by Roy and Sozen (1964)

Soliman and Yu (1967), proposed a curve consisting of a parabola, a horizontal branch, and a falling branch relating the stresses and strains at critical points to content, spacing, and yield strength of transverse reinforcement. The relationship is shown in Figure 2-5.
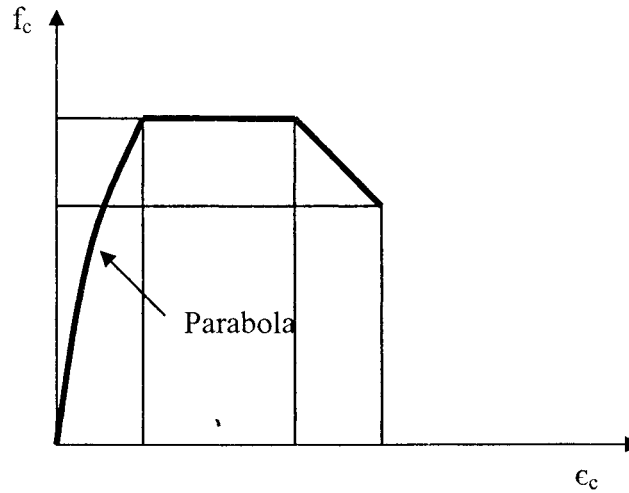
Figure 2 -5 Stress-strain relationships proposed by Soliman and Yu (1967)

Sargin, et al. (1971) proposed a continuous stress-strain curve related to content, spacing, and yield strength of transverse reinforcement, and also the concrete strength. The curve is shown in Figure 2-6.
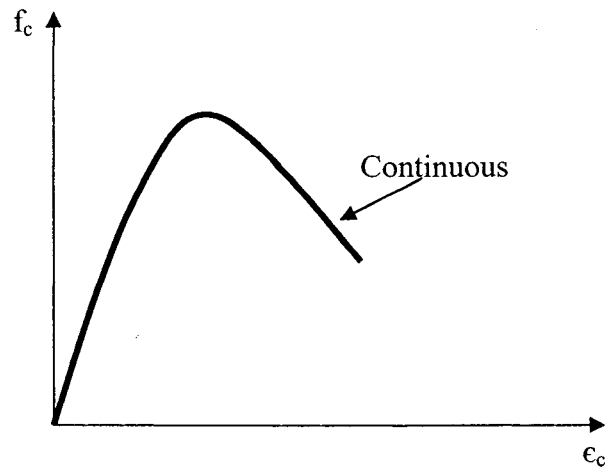
Figure 2-6 Stress-strain relationships proposed by Sargin et al.(1971)

The Mander (Mander et al., 1988) model, which is shown in Figure 2-7, is applicable to all section shapes and all levels of confinement. The stress-strain relationship for confined concrete is defined using the following equations.

16

$$f_c = \frac{f'_{cc}}{r-1+x^r}$$

$$f'_{cc} = f'_c \left(2.254 \sqrt{1+\frac{7.94 f'_l}{f'_c}} - \frac{2 f'_l}{f'_c} - 1.254\right)$$

$$x = \frac{\epsilon_c}{\epsilon_{cc}} \quad , \qquad \epsilon_{cc} = 0.002\,[1+5\,(f'_{cc}/f'_c - 1)]$$

$$r = \frac{E_c}{E_c - E_{scc}}$$

$$E_c = 5000 \sqrt{f'_c}\ \text{(MPa)} \qquad , \qquad E_{scc} = f'_{cc}/\epsilon_{cc}$$

Where: f'_c: Compressive Strength of the concrete

f'_t: Tensile Strength of the concrete

Consider first the generic stress-strain model below for monotonic loading of confined and unconfined concrete in compression from Mander et al., 1988. The shaded area in the stress-strain relationship of the Figure 2-7 characterizes the additional energy that can be absorbed in a confined section. The ratio of the maximum concrete strain in confined and unconfined concrete can range between 4 and 15.
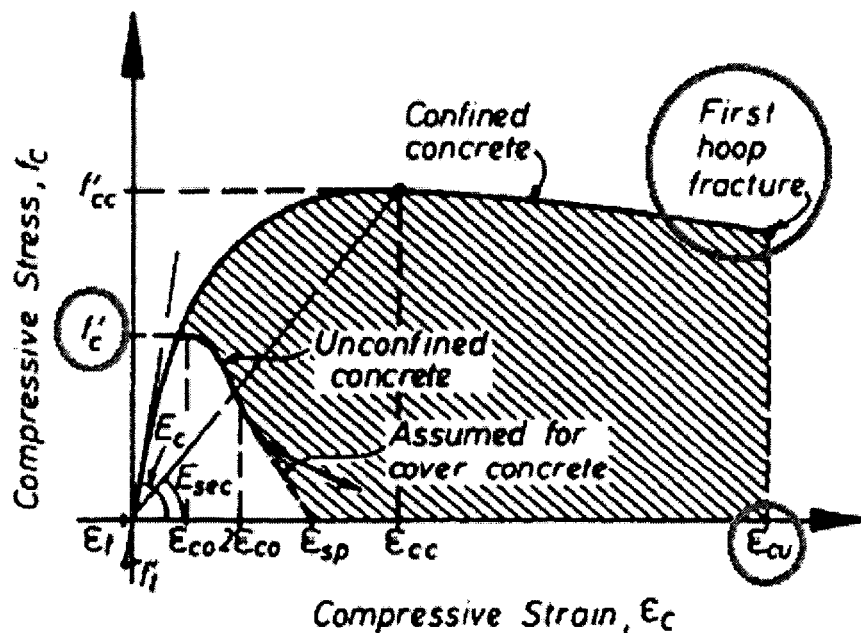
Figure 2-7 Stress-strain relationships proposed by Mander et al. (1988)

17

In Figure 2-7 the value of peak concrete stress, f'cc, is a function of the effective lateral confining pressure.

The material model for concrete model suggested by Cusson and Paultre (1994), as is shown in Figure 2-8 takes into account the different stress-strain curves of the concrete cover and the confined core. The model consists of a parametric strain-strain curve and a procedure to determine the parameters defining the curve, which are the strain, ϵ_{cc}, at peak confined strength, f'cc, and the strain, ϵ_{c50c}, when the post-peak stress drops to 50 % of the peak capacity. Furthermore, it does not assume that the stirrup yields; it estimates the actual stress in the stirrups at peak concrete stress. This model was further modified by assuming that at the strain ϵ_{c50c}, the confining steel is yielding.
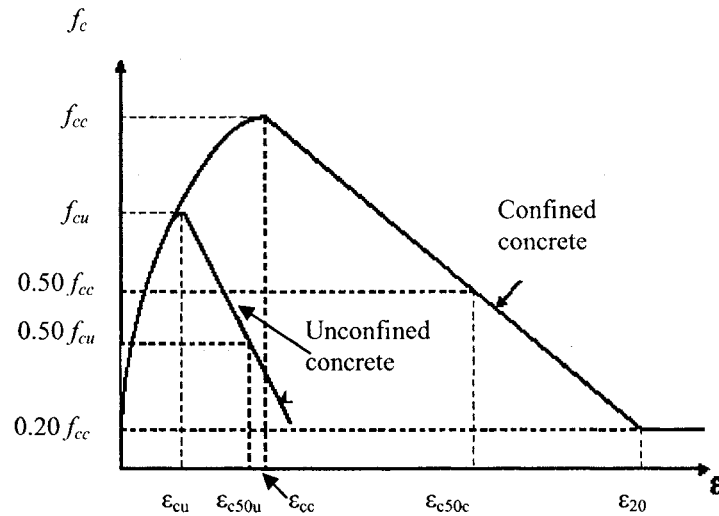
Figure 2-8 Stress-strain relationships proposed by Cusson and Paultre, 1994

The ascending branch, proposed by Popovics, is described by the following equation:

$$fc = fcc \left[\frac{k(\mathcal{E}c/_{\mathcal{E}cc})}{k - 1 + (\mathcal{E}c/_{\mathcal{E}cc})^k} \right] \qquad \mathcal{E}c \leq \mathcal{E}cc$$

$$k = \frac{Ec}{Ec - (^{fcc}/_{\mathcal{E}cc})}$$

Where k controls the initial slope and the curvature of the ascending branch, and E_c is the elastic modulus of concrete.

Kent and Park (Kent and Park, 1971) proposed the stress-strain curve for concrete confined by rectangular hoops. The curve is shown in Figure 2-9. The equations describing the branches are as follows:

Region AB: $\epsilon_c \leq 0.002$

$$f_c = f'_c \left[\frac{2\epsilon_c}{0.002} - \left(\frac{\epsilon_c}{0.002} \right)^2 \right]$$

The confining steel is assumed to have no effect on this part of the curve and on the strain at maximum stress which is conservatively taken as f'_c.

Region BC: $0.002 \leq \epsilon_c \leq \epsilon_{20c}$ $f_c = f'_c [1\text{-}Z (\epsilon_c\text{-}0.002)]$

Where: $Z = \dfrac{0.5}{\epsilon_{50u} + \epsilon_{50h} - 0.002}$

$$\epsilon_{50u} = \frac{3 + 0.002 f'_c}{f'_c - 1000}$$ $$\epsilon_{50h} = 0.75 \rho_s \sqrt{\frac{b''}{S_h}}$$

Where: f'_c = concrete cylinder strength in psi
ρ_s = ration of transverse reinforcement volume to volume of concrete core measured to outside of hoops
b'' = width of confined core measured to outside of hoops
S_h = spacing of hoops
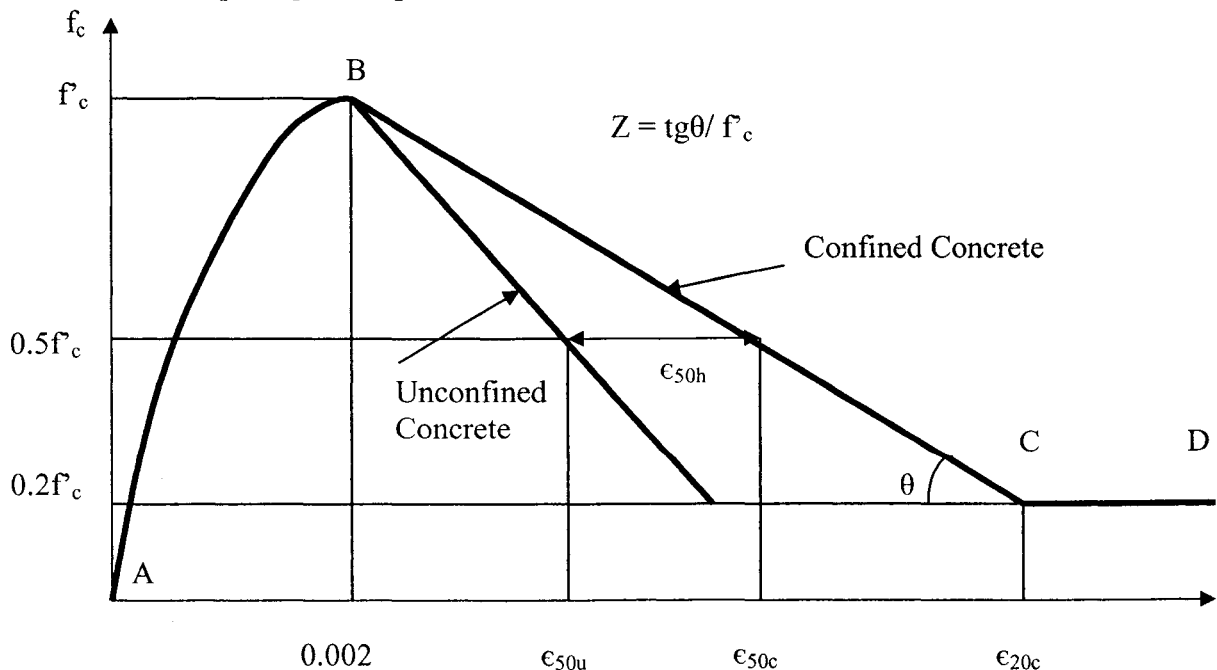
Figure 2-9 Stress-strain relationships proposed by Kent & Park (1971)

The parameter Z defines the slope of assumed linear falling branch, which is specified by the strain when the stress has fallen to 0.5 f'_c

Region CD: $\epsilon_{20c} \leq \epsilon_c$ $\qquad$ $f_c = 0.2 \, f'_c$

2.2.3 Stress-Strain Relationships for Confined Concrete in Tension

Flexure and splitting tests for determination of the tensile strength of the plain concrete result in a sudden failure of the test specimen, indicating the brittle nature of plain concrete in tension. However, if the deformation of the specimen is controlled in a test, a significant descending branch of the tensile stress-strain diagram can be developed beyond the strain corresponding to maximum tensile stress. Evans and Marathe (Evans, R.H., and Marathe, M.S, 1968) illustrated this behavior on specimens loaded in direct tension in a testing machine modified to control deformation. Figure 2-10 shows tensile stress-strain curves that include unloading beyond the maximum tensile stress.
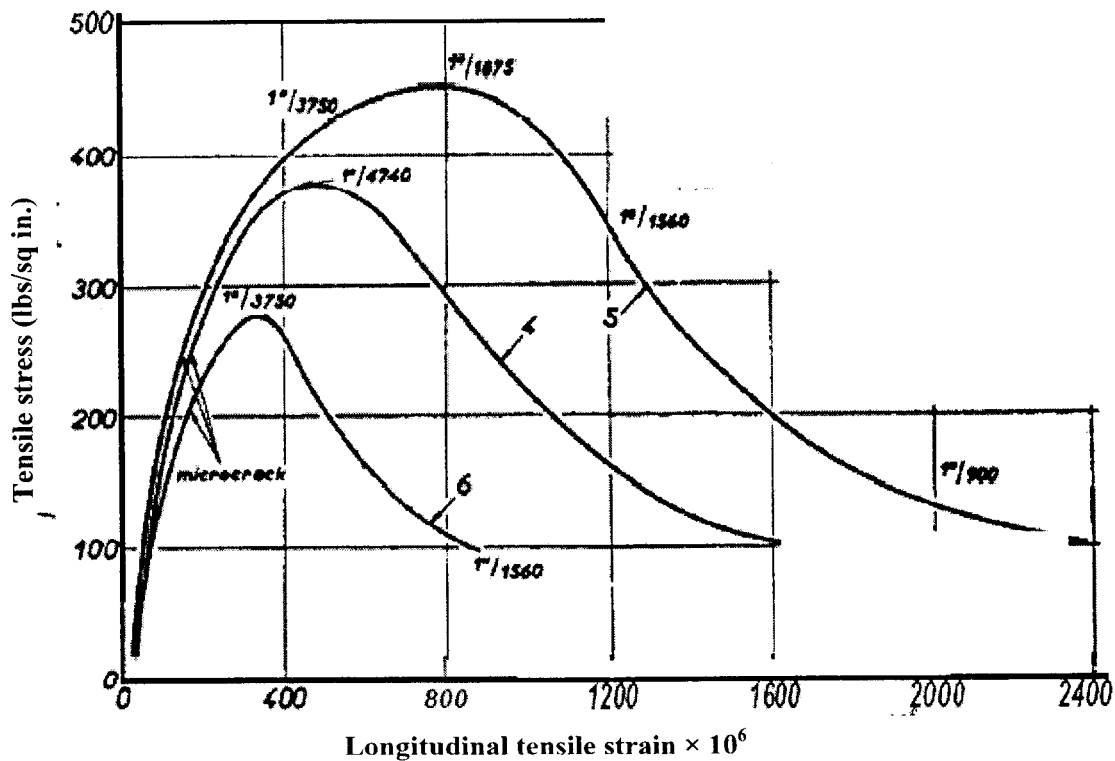
Figure 2-10 Relationship of tensile stress and longitudinal tensile strain for test specimens (ACI 224.2R-92, 2001)

Vebo and Gali (1977) proposed the relationship, which is shown in Figure 2-11 for stress-strain relationship for confined concrete in tension.

20

0.9f't

1

$E_c/2$

$f'_t = 0.62\sqrt{f'_c}$

0.45f't

0.75E_c

1

1

$E_c/20$

€₁   €₂   €₃
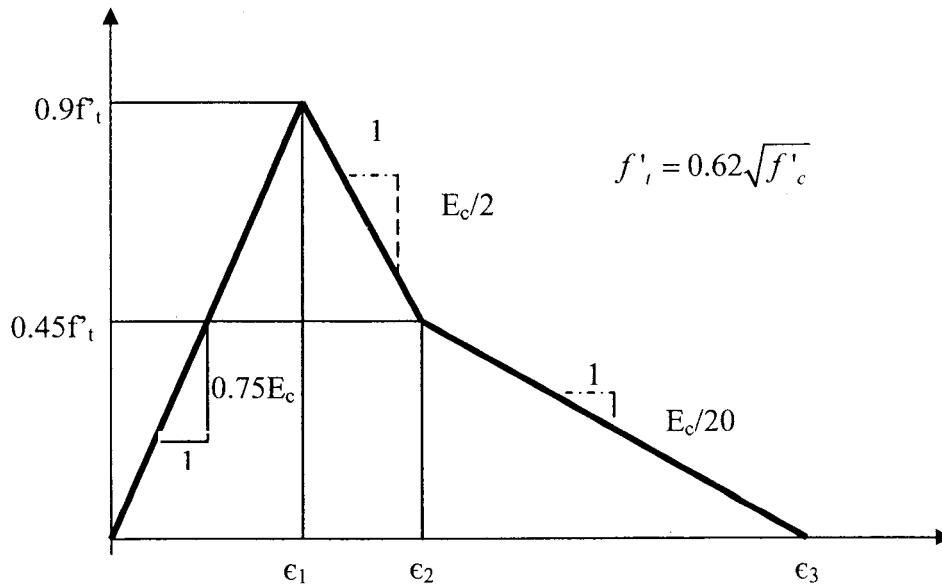
Figure 2-11 Stress-strain relationship in tension proposed by Vebo and Gali (1977)

2.3 Behavior of Reinforcing Steel

The behavior of reinforcing steel may control the response of reinforced concrete structural elements subjected to earthquake loading. The properties of reinforcing steel, unlike concrete, are generally not dependent on environmental conditions or time. Thus, the specification of a single stress-strain relation is sufficient to define the material properties needed in the analysis of reinforced concrete structures. (Kwak, H. G., Filippou, F. C. 1990). In predicting the response of reinforcing steel for analysis of reinforced concrete structures subjected to earthquake loading, it is necessary that an analytical model be developed on the basis of a the fundamental characteristics, which accounts for the behavior of steel in the range of force and deformation demands that the material may experience in an actual structure subjected to earthquake loading. Reinforcing steel in reinforced concrete structures carries load primarily along the axis of the bar. Reinforcement is relatively strong and stiff when loaded along the bar axis, and reinforced concrete members are designed to exploit this. Typically, loading of a volume of reinforced concrete results in cracking of the concrete and transfer of the tensile load to the reinforcement along the bar axis, perpendicular to the plane of the crack. In regions of variably oriented loading or relatively high shear loading, or both, cracked reinforced concrete may be loaded perpendicular to the axis of a reinforcing bar and parallel to an

21

established crack surface. This loading of the cracked reinforced concrete volume is referred to as shear friction, and activation of reinforcement perpendicular to the bar axis at a crack surface is referred to as *dowel action*.

Most research into the shear-friction response of reinforced concrete elements indicates that even for this type of loading, axial rather than dowel action dominates the response of the reinforcement perpendicular to the crack surface [Laible et al., 1977; Paulay and Loeber, 1977]. Under shear friction loading, a concrete crack must open substantially for sliding to occur. However, crack opening produces tensile stress in the reinforcing steel crossing the crack. These forces are equilibrated by a clamping force in the concrete that pushes the crack closed. Increased clamping force results in increased sliding frictional resistance along the crack surface.

Since steel reinforcement is used in concrete construction in the form of reinforcing bars or wire, it is not necessary to introduce the complexities of three-dimensional constitutive relations for steel. For computational convenience it even often suffices to idealize the one dimensional stress-strain relation for steel. Thus, axial stress in the steel rather determines response.

For the current study, the reinforcing steel is modeled as a uni-axial element and the dowel action of reinforcing steel is neglected. If reinforcing steel is modeled as an axial element, then experimental data defining the response of reinforcing steel to general, uni-axial loading are required for development, calibration and verification of the proposed model.

2.3.1 Behavior of Reinforcing Steel Subjected to Axial Loading

Figure 2-12, shows a typical engineering stress-strain history for reinforcing steel subjected to monotonically increasing strain demand. Important characteristics of this response include the following.

1- Initial response is linear-elastic for stress demand less than the initial yield strength.

2- For strain demand exceeding that corresponding to the initial yield strength, there is a slight drop in strength below the initial yield strength. Strength is maintained at this lower yield strength for moderate increase in strain demand. This range of response is referred to as the *yield plateau*, and the material yield strength typically is defined to be the average strength for loading within this strain range.

22
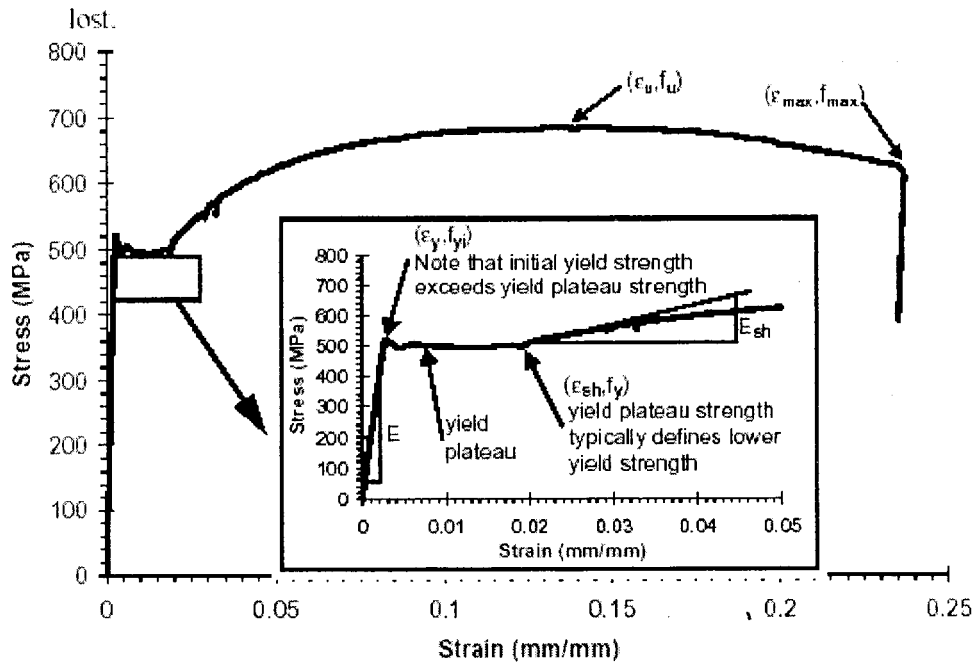
Figure 2-12 Tensile monotonic stress-strain history for typical reinforcing steel bar (Data for A706 Grade Reinforcement [Naito, 1991])

3- Increasing strain demand results in increased strength. This strain-hardening phenomenon is continued to a peak strength that typically exceeds the yield strength by thirty to sixty percent (Figure 2-12). The ratio of peak strength to nominal strength is a function of the steel specification, grade and batch composition, and has an important role in the shape of the hysteretic loops after yielding of the steel happens.

4- At severe tensile strain demand, reinforcement begins to neck and strength is reduced.

5- At a maximum strain demand, the steel reinforcement fractures and load capacity is lost.

This monotonic steel response may be defined by a few material parameters as identified in Figure 2-12. These include the elastic modulus, E; the lower yield strength, f_y; the strain at which strain hardening initiates, ε_{sh}; the strain at which peak strength is achieved, ε_u; the peak strength, f_u; the strain at which fracture occurs, ε_{max}, and the capacity prior to bar fracture, f_{max}.

As was mentioned, stress-strain curves for reinforcing steel bars used in concrete construction are obtained from tests of bars loaded monotonically in tension. For all practical purposes steel exhibits the same stress-strain curve in compression as in tension. The steel stress-strain relation exhibits an initial linear elastic portion, a yield plateau (i.e.

23

a yield point beyond which the strain increases with little or no increase in stress), a strain hardening range in which stress again increases with strain and, finally, a range in which the stress drops off until fracture occurs. The extent of the yield plateau is a function of the tensile strength of steel. High-strength, high-carbon steels, generally, has a much shorter yield plateau than relatively low-strength, low-carbon steels.

The modulus of elasticity of steel is given by the slope of the linear elastic portion of the curve, and is generally taken as 2×10^5 N/mm^2. The stress at the yield point, referred to as the yield strength, is a very important property of steel reinforcement and even in the design of reinforcement concrete elements. Sometimes yielding is accompanied by an abrupt decrease in stress, and the stress-strain diagram has the shape appearing in the Figure 2-13.
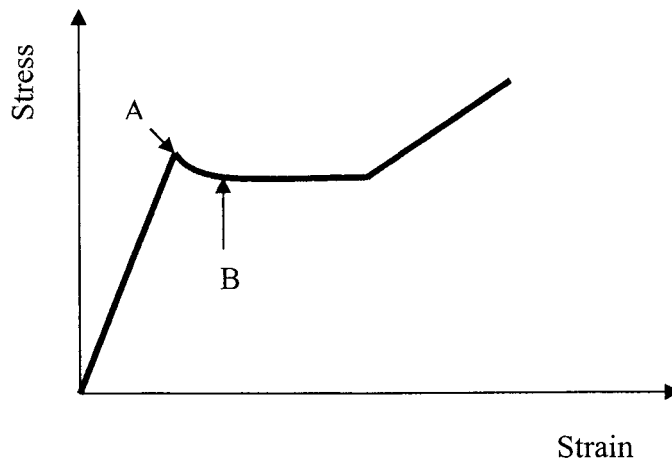
Figure 2-13 Upper and lower yield point in
stress-strain curve

In such case the stress at A and B are referred to as the upper and lower yield strengths, respectively. The position of the upper yield point depends on the speed of testing, the shape of the section, and the form of the specimen. The lower yield strength is usually considered to be the true characteristic of the material and is referred to simply as the yield strength.

The length of the yield plateau is generally a function of the strength of the steel. High-strength high-carbon steels generally have a much shorter yield plateau than lower strength low carbon steels. Similarly, the cold working of steel can cause the shortening

of the yield plateau to the extent that strain hardening commences immediately after the start of yielding.

The specified yield strength normally refers to a guaranteed minimum. The actual yield strength of the bars is usually somewhat higher than this specified value, which is usually being taken into account in terms of reinforcement *Overstrength factor*. In some cases (assessment of the seismic strength of members) it is undesirable to have yield strength much higher than that considered in the design (i.e. Overstrength factor much higher than unity). This is because the increased flexural strength of a member due to the reinforcement overstrength will produce increased shear forces acting on the member. This has a detrimental effect on the performance of joint resistance mechanism in the beam-column connections at ultimate load, which could result in a brittle shear failure of the member rather than the ductile flexural failure. Therefore, specifications for steel used in structures in seismic zones should also require that certain yield strength for a given grade of steel not to be exceeded. Some variation in response results from variability in steel specification and steel grade. However, experimental data show that two steel batches with the same specification and grade may have significantly different post-yield behavior.

As was mentioned, the stress-strain curves for steel in tension and compression are assumed to be identical. Tests have shown that this is a reasonable assumption. In design it is necessary to idealize the shape of stress-strain curve. Generally the curve is simplified by idealizing it as two straight lines as in Figure 2-14, ignoring the upper yield strength and the increase in strength due to strain hardening. This is the stress-strain curve for steel assumed by the ACI code (ACI 318-71). If the strain at the beginning of strain- hardening is much larger than the yield strain, this assumed curve gives very satisfactory results. This simplification is particularly accurate for steel (low carbon steel) having low yield strength. If the steel strain hardens soon after the onset of yielding, this assumed curve will underestimate the steel stress at high strains; in some cases it may be necessary to evaluate the steel stress at strains higher than yield, to more accurately assess the members' strength at large deformations. This is particularly true in seismic design, where ductility requirement may mean considering the possibility of reaching strain many times the yield strain.
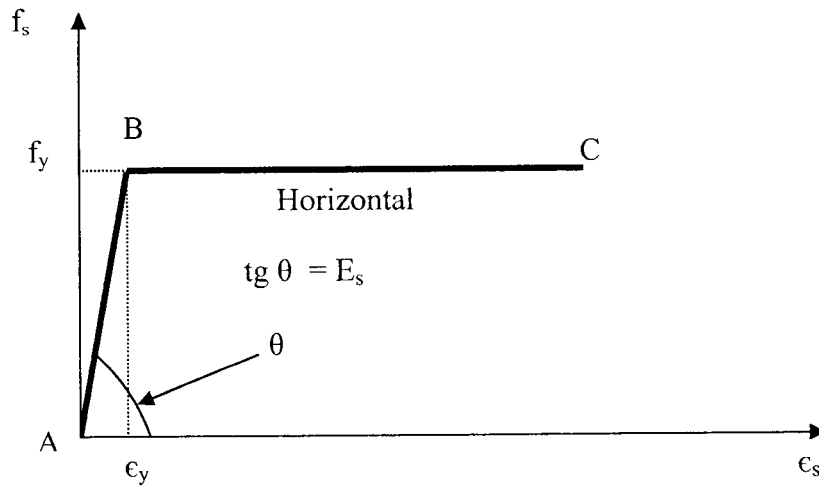
Figure 2-14 Elastic-perfectly plastic idealization for reinforcing steel
under tension or compression

More accurate idealizations for the stress-strain curve are given in Figure 2-15. Values for the stresses and strains at the start of yield, strain hardening, and tensile strength are necessary for use of such idealizations. These points can be located from stress-strain curves obtained from tests. As will be discussed later IDARC2D uses this tri-linear model for reinforcing steel.
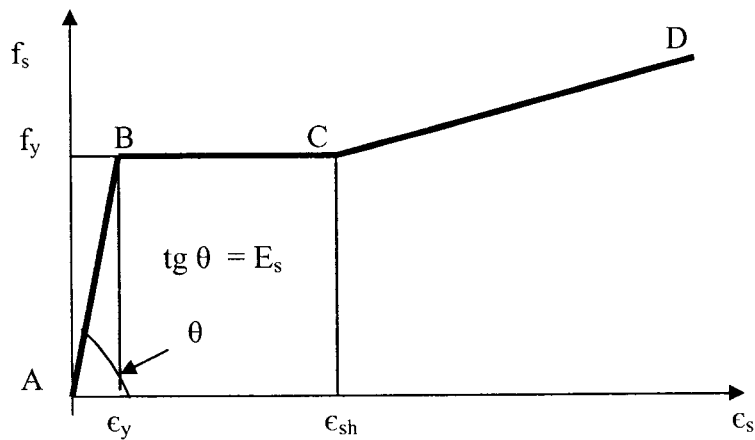
Figure 2-15 Tri-linear approximation for reinforcing steel
under tension or compression

Another assumption is that the reinforcing steel is modeled as a linear elastic, linear strain hardening material with yield stress as shown in Figure 2-16.

26
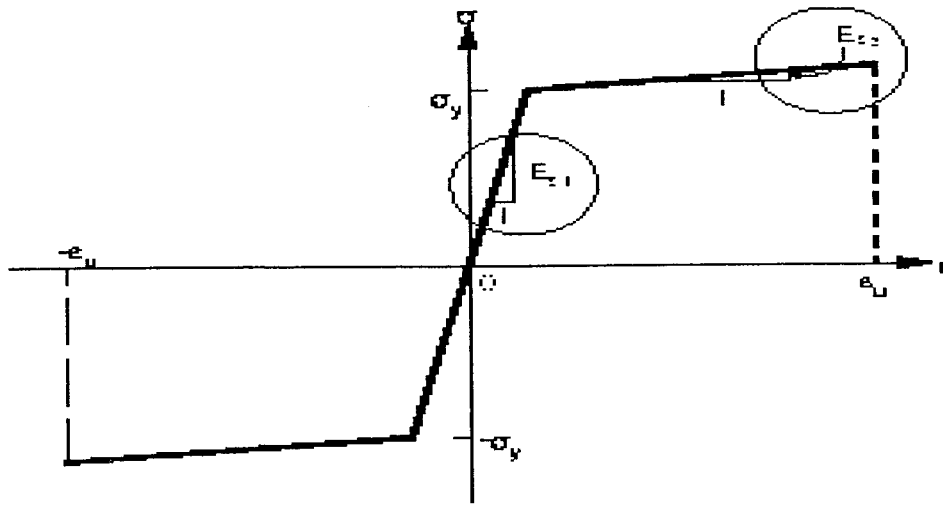
Figure 2-16 Linear elastic, linear strain hardening idealization for reinforcing steel.

The reasons for this approximation are: (1) the computational convenience of the model; (2) the behavior of RC members is greatly affected by the yielding of reinforcing steel when the structure is subjected to monotonic bending moments. Yielding is accompanied by a sudden increase in the deformation of the member. In this case the use of the (first model) elastic-perfectly plastic model leads to numerical convergence problems near the ultimate member strength. It is, therefore, advisable to take advantage of the strain-hardening behavior of steel in improving the numerical stability of the solution.

The assumption of a linear strain hardening behavior immediately after yielding of the reinforcement does not adversely affect the accuracy of the results, as long as the slope of the strain-hardening branch is determined so that the strain energy of the model is equal to the strain energy of the experimental steel stress-strain relation, such model has been successfully used in many analyses of reinforced concrete structures (Ngo and Scordelis 1967; Vebo and Gali 1977; Bashur and Darwin 1978). As will be discussed later the above model was adopted in modeling the reinforcing steel behavior in DRAIN-2DX program.

Figure 2-17 is a typical stress-strain curve for a steel specimen loaded either in axial tension or in compression to failure in a single run. If the load is released before the failure, the specimen will recover along a stress-strain path that is parallel to the original elastic portion of the curve. If loaded again, the specimen will follow the same path up to the original curve, as in Figure 2-18, with perhaps a small hysteresis and/or strain-hardening effect. The virgin curve is then closely followed, as if unloading had not occurred. Hence the monotonic stress-strain curve gives a good idealization for envelope curve for repeated loading of the same sign.
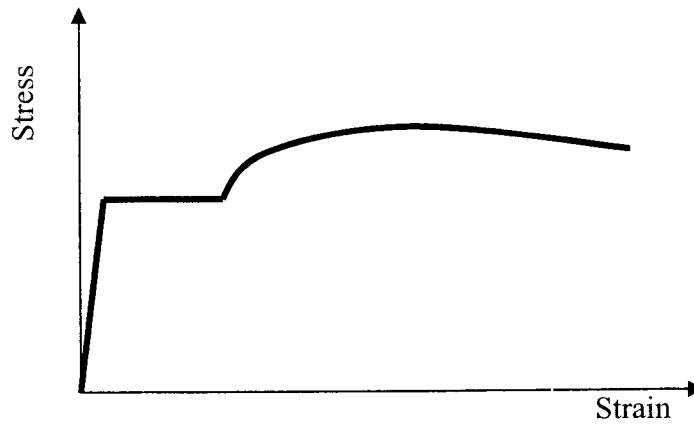
Figure 2-17 Typical stress-strain curve for steel reinforcement
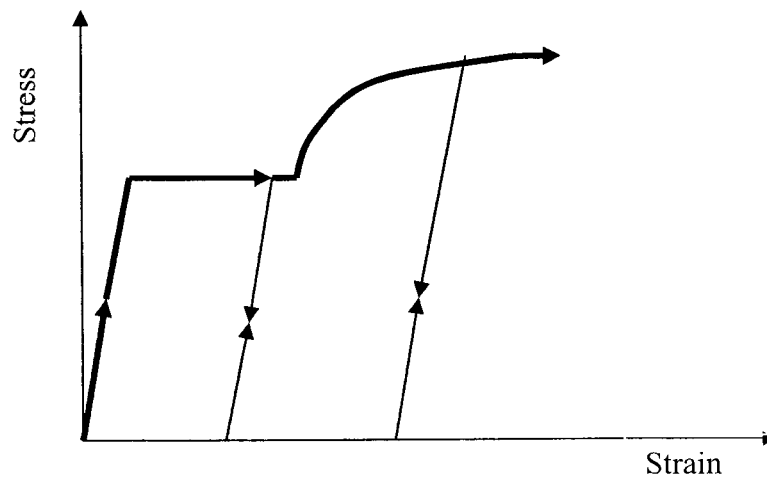
Figure 2-18 Stress-strain curve for steel under repeated loading

2.3.2 Reversed Stress Behavior for Steel

If reversed (tension-compression) axial loading is applied to a steel specimen in the yield range, a stress-strain curve of the type presented in Figure 2-19-a is obtained. Figure 2-19-b shows the *Bauschiger effect*, in which under reversed loading, the plastic deformation in compression occurs before negative yield strength. This steel behavior is strongly influenced by previous strain history; time and temperature. The unloading path follows the initial elastic slope. Thus, the often-used elastic-perfectly plastic idealization for reversed loading is only an approximation (Figure 2-20). Reversed loading curves are important when considering the effects of high intensity seismic loading on members.

(a) Typical Stress-Strain Curve under Cyclic Loading   **(b)** Bauschinger Effect
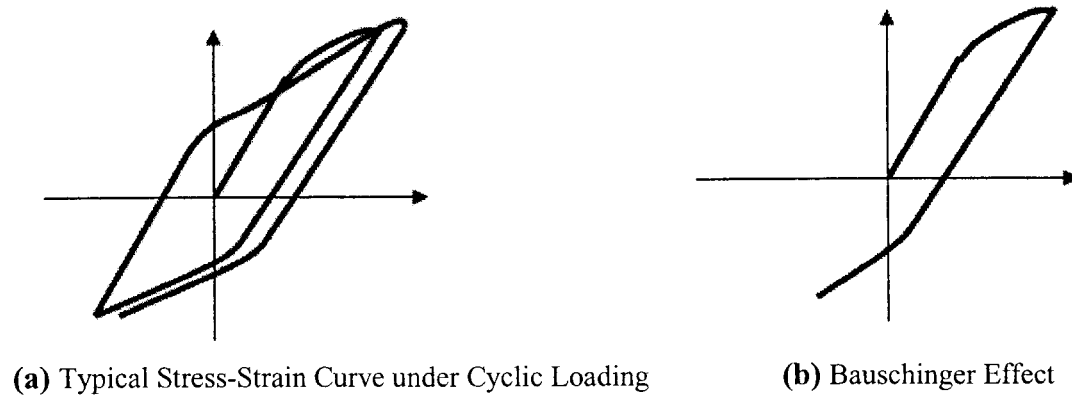
Figure 2-19 Reversed stress behavior for steel
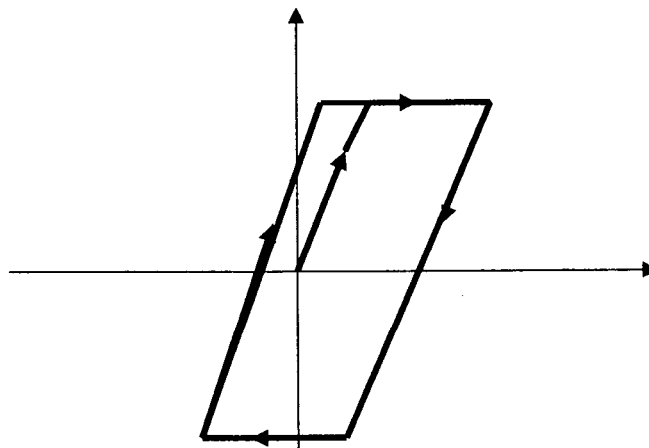
Figure 2-20 Elastic-perfectly plastic idealization for steel reinforcement under cyclic loading

29

As it can be seen in Figure 2-21, the engineering stress-strain history for reinforcing steel loaded in tension exhibits an elastic-plastic response with moderate strain hardening to a relatively high strain demand. However, severe strain demands ultimately result in necking of the reinforcement reduced engineering (Cauchy) stress capacity.
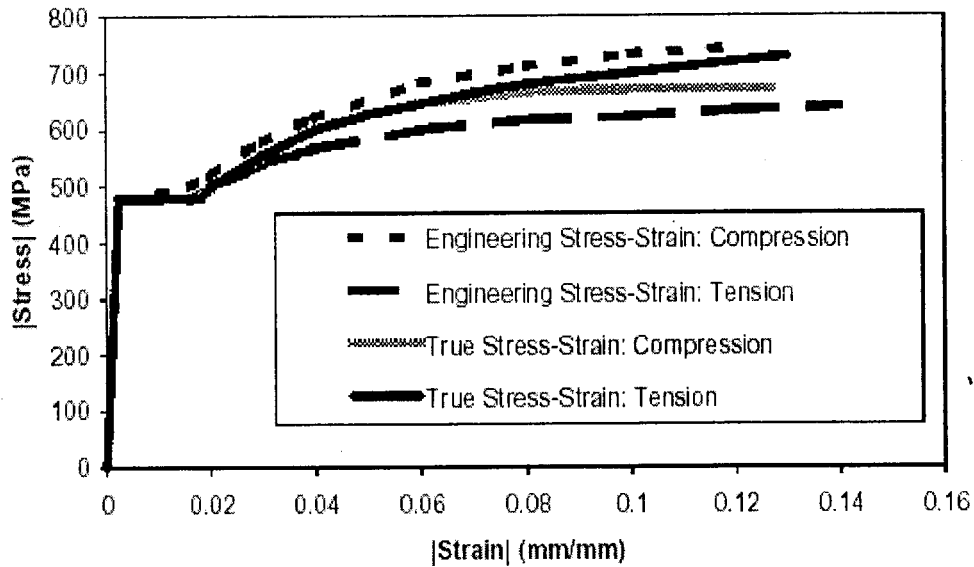
Figure 2-21 Engineering versus natural stress-strain history for reinforcing steel subjected to monotonic compression and tension loading (Data from Dodd and Restrepo-Posada [1995])

2.4   Application of the Material Behavior in Current Research

2.4.1 Application of the Material Behavior in IDARC2D

In the macro-model concept, which is adopted in IDARC2D the inelastic behavior is defined by means of force-deformation relationship to capture the overall behavior of the element. In theory, it is possible to define force-deformation relationship using constitutive models. However, constitutive laws hold true only for microscopic point in the material. For reinforced concrete as an inhomogeneneous material, it needs a very fine discretization of the member cross section to represent the material behavior in terms of local concrete-steel interaction. Such approach is not considered in IDARC2D because it is computationally intensive and time consuming especially in case of a frame structure with different element cross sections.

30

There are two options for defining the material properties in IDARC2D. The first option is by using fiber concept for structural elements. The program IDARC2D (Version 4.0) provides an option for users to input their own cross-section properties directly, and the program computes the moment-curvature internally. The properties for defining the stress-strain curve for unconfined concrete are shown in Figure 2-22. The moment curvature envelope describes the changes in force capacity with deformation during a nonlinear analysis. The cross section is divided into a number of fibers. The section is then subjected to increments of curvature and the strain distribution is obtained from compatibility and equilibrium.
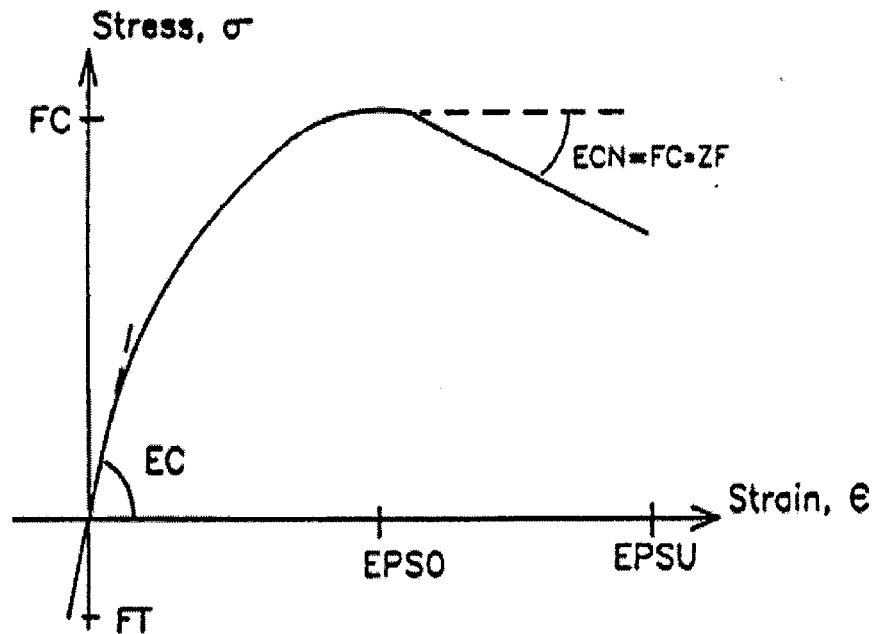
FC: Unconfined compressive strength
EC: Initial Young's Modulus of concrete
EPSO: Strain at maximum stress of concrete (%)
FT: Stress at tension cracking
EPSU: Ultimate strain in compression
ZF: Parameter defining the slope of the falling branch

Figure 2-22 Properties input data for concrete (IDARC2D)

In figure 2-23 the parameters needed for defining the stress-strain curve for reinforcing bar are shown.

FS: Yield strength
FSU: Ultimate strength
ES: Modulus of elasticity
ESH: Modulus of strain hardening
EPSH: Strain at start of hardening (%)
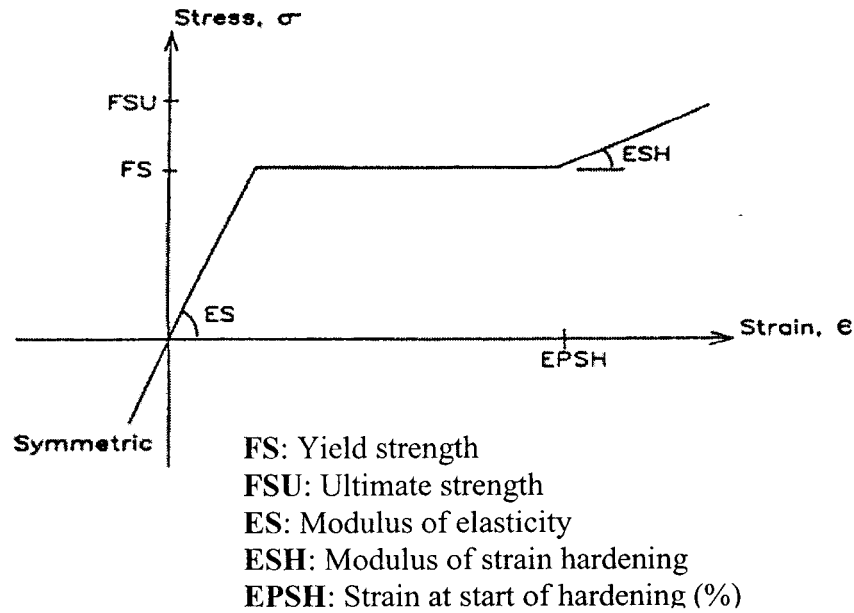
Figure 2-23 Properties input data for reinforcement (IDARC2D)

The second option requires complete moment-curvature envelope data to be provided by the user in the section where the element (column, beam) properties are specified. The required properties are those defined in Figure 2-24.

Note: Force = Moment or Shear
Deformation = Curvature, Rotation or Strain
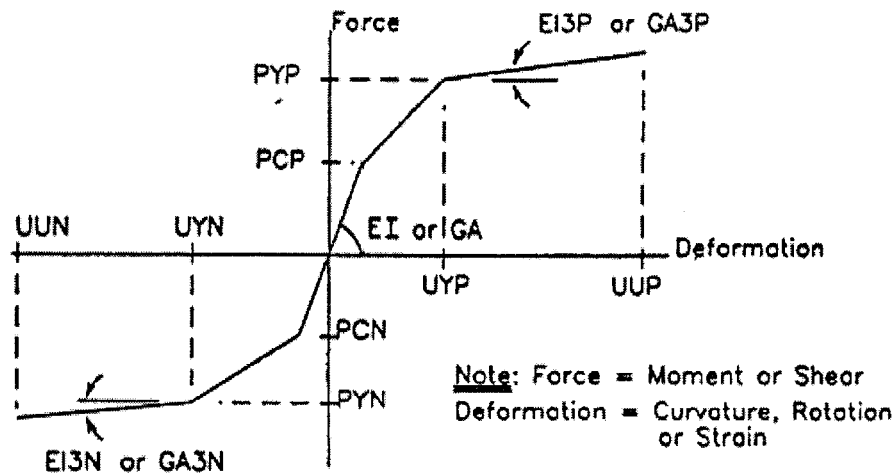
PCP: Cracking Moment (positive)	PCN: Cracking Moment (negative)
PYP: Yield Moment (positive)	PYN: Yield Moment (negative)
UYP: Yield Curvature (positive)	UYN: Yield Curvature (negative)
UUP: Ultimate Curvature (positive)	UUN: Ultimate Curvature (negative)
E13P: Post Yield Flexural Stiffness (positive)	E13N: Post Yield Flexural Stiffness (negative)

Figure 2-24 Input data for tri-linear user defined properties (IDARC2D)

32

In this study the first option is considered, because of the simplicity and availability of the required data in comparison to the second option.

2.4.2 Application of the Material Behavior in DRAIN-2DX

The material models in DRAIN-2DX account for yield of steel, including strain hardening, cracking and crushing of concrete and tension stiffening of the concrete. It is also possible to model a concrete, which takes no tensile force, which is needed in diagonal concrete struts in the joint. The concrete material properties are defined as points in the stress-strain curve in Figure 2-25. There is a maximum of 5 points for defining the stress-strain relationship in compression, and 2 points for defining the stress-strain relationship in tension.

The point with coordinates (S1C, E1C) refers to the cracking of the concrete and the point (S2C, E2C) refers to the maximum compression strength of the concrete. After the maximum strength point (S2C, E2C), the ascending branch defines the behavior of the concrete with negative modulus. It is important to note that the modulus should keep on decreasing, otherwise the program sends an error message and the analysis is not performed. The point (S3C, E3C) defines the ultimate strength of concrete under high strains. The horizontal branch shows the ability of concrete to sustain some strength at very large strains.
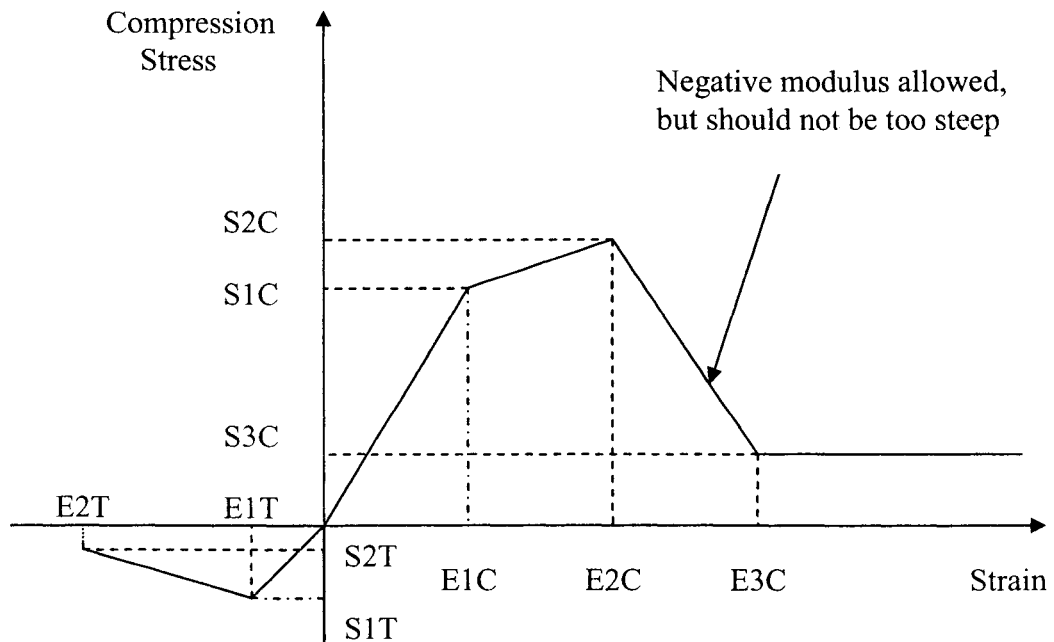
Figure 2-25 Properties input data for concrete (DRAIN-2DX)

33

By comparing the input format for defining the behavior of concrete to the mentioned models, for the concrete in compression, the curve proposed by Kent and Park (Kent and Park, 1971) and for concrete in tension, the relationship developed by Vebo and Gali (Vebo and Gali, 1977), which have been discussed in section 2-2 of this study have been adopted in this study.
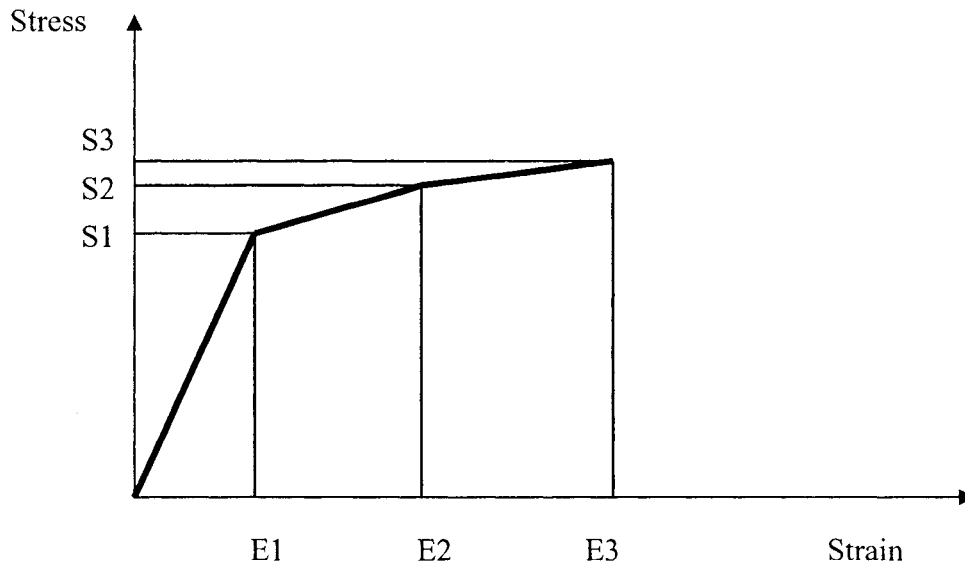
Figure 2-26 Properties input data for steel (DRAIN-2DX)

Figure 2-26 shows the input data for defining the behavior of steel in terms of stress-strain points. The program requires at maximum 5 points for defining the relationships between stress and strain. The program assumes same properties for steel in tension and compression. By comparison to the steel models discussed in section 2.3.1 the Linear elastic, linear strain hardening model for reinforcing steel as was depicted in Figure 2-16, was selected.

In the following chapter the example outlines the usage of above models in terms of modeling the behavior of a circular column under axial load and lateral displacement reversals.

Chapter 3
FULL SCALE BRIDGE PIER UNDER REVERSED CYCLIC LOAD

3.1 Experimental Test

A series of full-scale and scale model circular, spirally reinforced concrete bridge columns were subjected to cyclic inelastic lateral loading at the laboratories of the National Institute of Standards and Technology (Stone and Cheok, 1989; Cheok and Stone, 1990). These columns represent typical bridge piers deigned in accordance with CALTRANS (California State Department of Transportation) specifications. The piers were tested by applying slow cyclic lateral displacement with the axial load held constant. The column analyzed in this sample investigation is a full-scale circular bridge pier measuring 30' feet with an aspect ratio of 6.0 to exhibit flexural failure (Figure 3-1). The tests were performed using a displacement controlled quasi-static history as shown in Figure 3-2. The column was made of 5.2 ksi concrete (measured compressive strength at 28 days) and had a modulus of elasticity of approximately 4110 ksi.

The longitudinal reinforcement consisted of 25 D6 #14 (Grade 60 steel with an actual yield stress of 68.9 ksi and diameter of 0.552 inch) and elasticity modulus of 27438 ksi. The steel exhibited good ductility in the material testing with a 2% strain and a strain hardening of 1454 ksi before actual rupture. The cross-section in Figure 3-1 shows the reinforcement details. The purpose of this analysis is to simulate the characteristics of the hysteretic behavior and compare it with the experimental recorded response.

$A_g = 2827.43$ in^2
$A_s = 56.25$ in^2
$\rho_t = 0.0199$
$\rho_s = 0.0065$
Spiral = #5
Bars = # 14
1 in = 25.4 mm
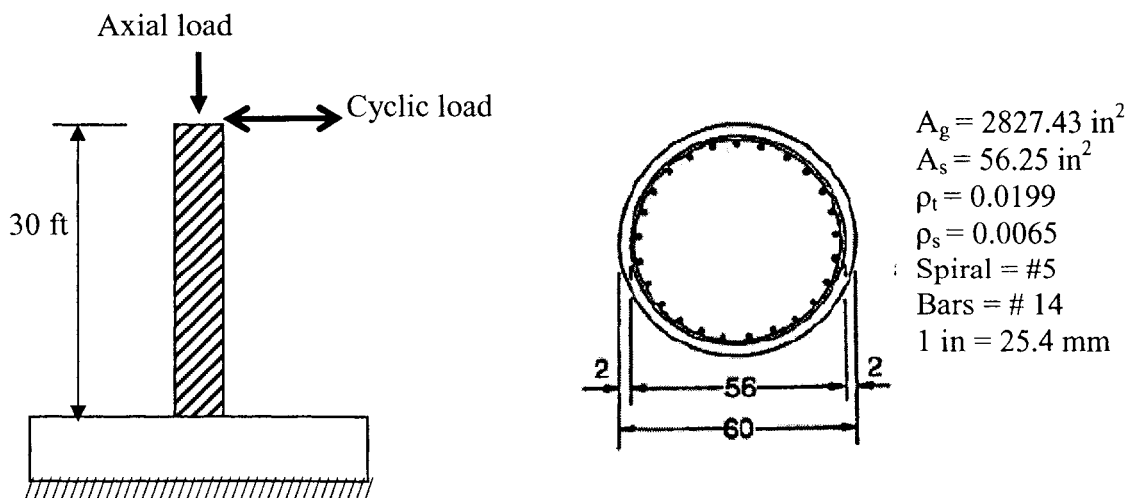
Figure 3-1 Configuration of full-scale bridge pier

35
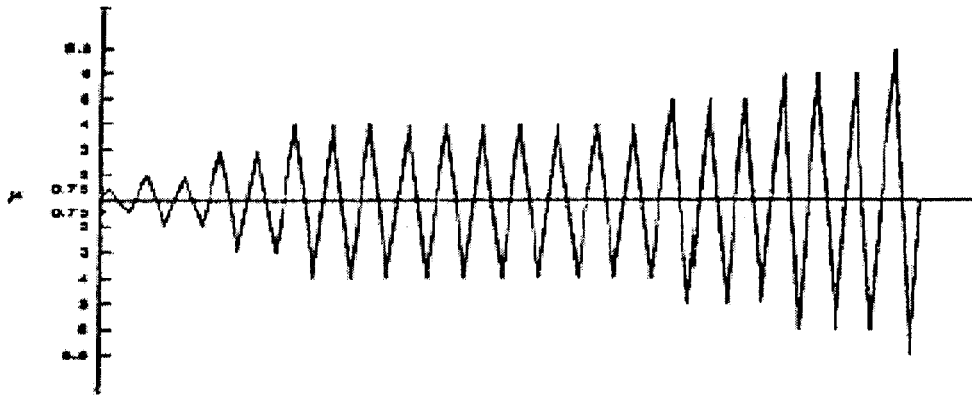
Figure 3-2 Loading sequence for full-scale flexure column

The specification of the column's properties are listed below:

Height of column = 30 ft = 360 in = 9144 mm

Diameter of column = 5 ft = 60 in = 1524 mm

Cover concrete = 2 in = 50.4 mm

Concrete compressive strength (28 days) = 5.2 ksi = 35.9 MPa

Modulus of elasticity of concrete = 4110 ksi = 28360 MPa

Diameter of longitudinal reinforcement = 1.693 = 43 mm

Diameter of transverse reinforcement = 0.625 in = 15.88 mm

Yield strength of longitudinal reinforcement = 68.9 ksi = 475.4 MPa

Modulus of elasticity of longitudinal reinforcement = 27438 ksi = 190000 MPa

Axial load = 1000 kips = 4545 KN

The result of the experimental data in terms of the relationship between shear force and displacement are shown in Figure 3-3
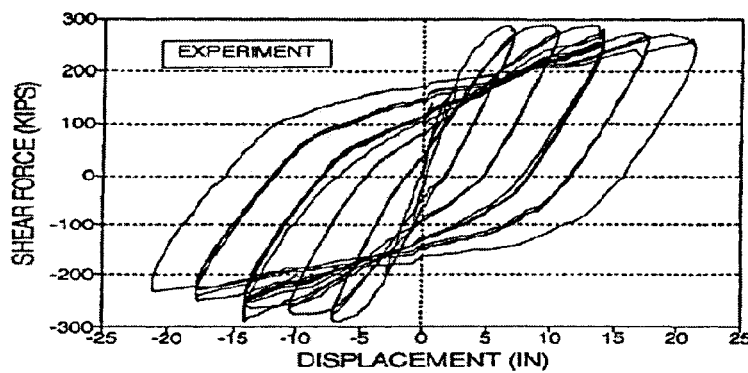
Figure 3-3 Observed response of the bridge pier under the specified loading

36

3.2 Modeling the Test in IDARC2D

The column specifications listed above are directly used for input file for IDARC2D.

In the following the part related to the specification of the column was selected from the input file (Case 1, IDARC2D Version 4.0 Manual).

FLOOR ELEVATIONS

360.0 in

CONCRETE PROPERTIES

1, 5.2, 4110.0, 0.2, 0, 0.0, 0.0

In the input section above 1 refers to the section properties type, which is 1, Concrete compressive strength (28 days) is taken as 5.2 ksi, and Modulus of elasticity of concrete is taken as 4110 ksi. The rest of the parameters are taken as default; that means Strain at maximum stress of concrete will be 2%, Stress at tension cracking will be 0.12*5.2= 0.624 ksi, Ultimate strain in compression (EPSU), and Parameter defining the slope of the falling branch (ZF), are internally calculated by the program according to the previously described model of Kent and Park.

$$ZF = \frac{0.5}{\epsilon_{50u} + \epsilon_{50h} - 0.002}$$

$$\epsilon_{50u} = \frac{3 + 0.002\, f'_c}{f'_c - 1000}$$

$$\epsilon_{50h} = \tfrac{3}{4}\, \rho_s \sqrt{\frac{b''}{S_h}}$$

b'= Width of confined core measured to outside of hoops.
S_h= Spacing of hoops
ρ_s = Ratio of volume of hoops to volume of concrete measured to outside of hoops

REINFORCEMENT PROPERTIES

1, 68.9, 103.6, 27438.0, 0.0, 0.0

In the input section above 1 refers to the section properties type which is 1, Yield strength of longitudinal reinforcement is equal to 68.9 ksi, Ultimate strength of longitudinal reinforcement is taken as 103.6 ksi, Modulus of elasticity of longitudinal reinforcement is 27438 ksi. The rest of the parameters are taken as default; that means: Modulus of strain hardening is: ESH = (ES / 60) ksi, which is equal to 27438/60 = 457.3 ksi, and the Strain at start of hardening will be 3.0%.

COLUMN DIMENSIONS

2, 1, 1, 1, 1, 360.0, 0.0, 0.0, 1000.0, 60.0, 2.5, 54.5, 25, 1.69, 0.625, 3.5

In the input section above, 2 refers to the section shape, which is circular, The 1, 1, 1, 1 refer to the column type set number, concrete type number, steel type number, and hyteretic rule number, respectively, because there is only one of each in the test specimen. The length of the column is taken as 360 inch, the axial load on the column is 1000 kips; rigid arm at the bottom and rigid arm at the top, are taken as zero because the column is fixed to the based from bottom and free at the top (program definition). The outer diameter of the column and the cover concrete to the center of the hoops are taken as 60 inch, and 2.5 inch, as detailed in the specifications of the test. The distance between centers of longitudinal bars is 54.5 inch, the number of the longitudinal bars is 25, the diameter of longitudinal and hoop bars are taken as 1.69 inch, and 0.625 inch, respectively. The spacing of the hoop bars is 3.5 inch.

HYSTERETIC MODELING RULES

1, 1, 1,9,0,0.1,1,2

The hyteretic parameters in IDARC2D are as following:

HC: Stiffness degrading parameter

HBD: Strength degrading parameter (ductility based)

HBE: Strength degrading parameter (energy-controlled)

HS: Slip or crack closing parameter

The ranges of above parameters are described in Table 3-1:

Table 3–1 Typical ranges of values for hysteretic parameters

HC	0.1	Severe degradation
	2.0	Nominal degradation
	10.0	Negligible degradation
HBD	0.0	No degradation
	0.1	Nominal deterioration
	0.4	Severe deterioration
HBE	0.0	No degradation
	0.1	Nominal deterioration
	0.4	Severe deterioration
HS	0.1	Extremely pinched loops
	0.5	Nominal pinching
	1.0	No pinching

38

Illustration of the Hysteretic Rule Parameters in IDARC2D

Stiffness Degradation: Experimental evidence indicates that stiffness degradation is best expressed as a function of attained ductility. The degradation is not obvious at small ductility. To model the reduced stiffness, all unloading branches were directed towards a common target point as shown in Figure 3-4(a).
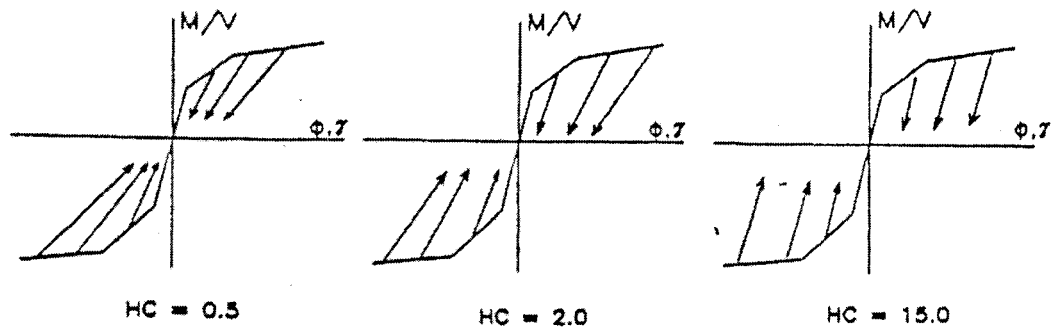
(a) Stiffness Degrading Parameter
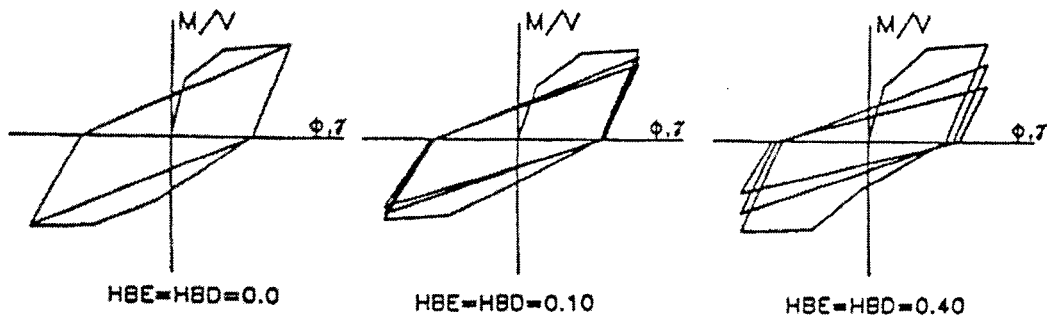
(b) Strength Deterioration Parameter
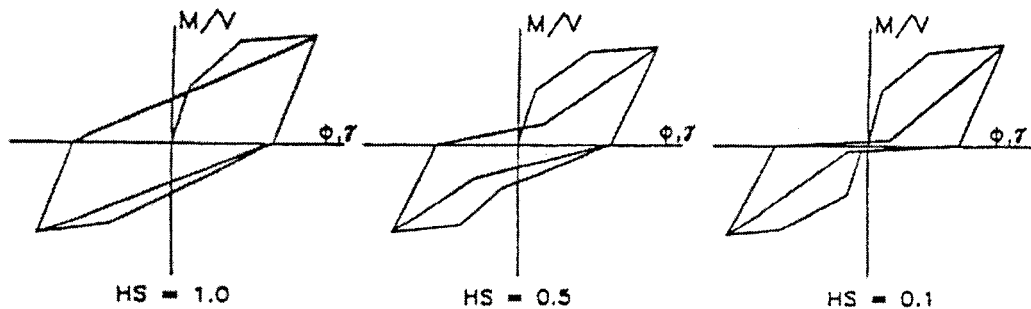
(c) Slip Control Parameter

Figure 3-4 Three-parameters hysteretic model in IDARC2D

Strength Deterioration: The modeling of strength decay is accomplished using two control parameters: ductility and dissipated hysteretic energy. Both parameters control the amount of strength loss per cycle till the previous maximum deformation is exceeded. Figure 3-4(b) shows the modeling of strength decay.

Pinching Behavior: Pinched loops are typical in cyclic RC member behavior due to the presence of high shear forces, or from the opening and closing of cracks, or the result of rebar slippage at beam column interfaces. This behavior is modeled using a third primary control parameter which reduces the target force as the load path crosses the zero force axis as shown in Figure 3-4(c).

For the circular column example, the modified three parameter vertex oriented hysteretic model was selected (the last parameter in the input data which is equal to 2), with a stiffness degradation coefficient HC=9.0 (very little degradation in the stiffness), strength degradation coefficient HBE=0.1; HBD=0.0 (very little deterioration in strength), and a pinching coefficient HS=1.0 (indicating no pinching). This hysteretic behavior can be related to the condition of the connection of the column to the base. Because of the volume of longitudinal and spiral transverse reinforcement and the well-detailed condition of the connection there is small failing effect of bar slippage or shear resistance deterioration of the connection. These parameters were estimated from the observed experimental data, and could be used to represent well-detailed section.

The quasi-static displacement control loading was applied to the column, and a static point load equal to 1000 kips was applied axially on the column. After the execution of the program, the load-displacement of the column top was obtained in the form of the hysteretic loops from the values from CYCLE.OUT file, and shown in Figure 3-5. Later in this chapter the analytical results will be compared to the experimental results. As was pointed out, this example was taken from the IDARC2D manual (the first case in the program validation section).
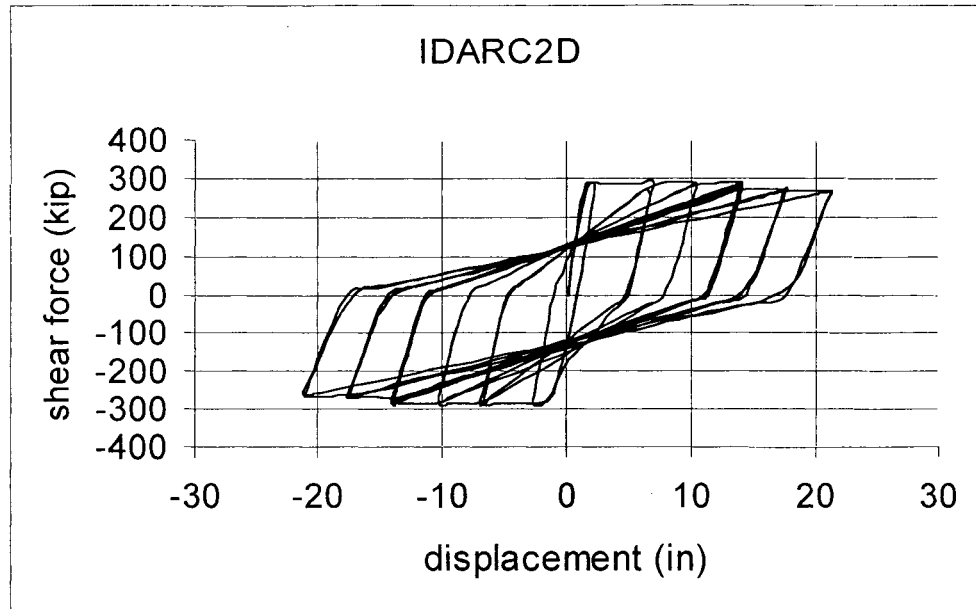
Figure 3-5 Shear force-Displacement relationships (IDARC2D)

IDARC2D program has the ability to analyze both circular and rectangular cross-sections. In the model based on fiber element concept, which is used in DRAIN-2DX there is no option of selecting the cross-section shape. The only parameters required for defining the cross-section properties are cross-sectional area of each fiber, and the distance of the fiber's centroid from the reference axis of the element. In section 3-3 the procedures for modeling the example in DRAIN-2DX are discussed.

3.3 Modeling the Test in DRAIN-2DX

In DRAIN-2DX (Fiber element) there is no provision for circular sections. The fiber concept will be discussed in details in Chapter-5. The circular column section was divided into 40 fibers with equal width. The reason for dividing the section into 40 fibers, as will be discussed in section 5.4, is to get accurate value for the moment of inertia of the cross-section. The area of each fiber and the area of reinforcement in each fiber section were obtained by using AUTOCAD14.

3.3.1 Procedures for AUTOCAD14

As shown in Figure 3-6, the circular section with 60 inch diameter was drawn and then 25 reinforcement bars were placed equally; using Array command and Polar option.

The section is then divided horizontally into 40 segments using Array command, Rectangle option.
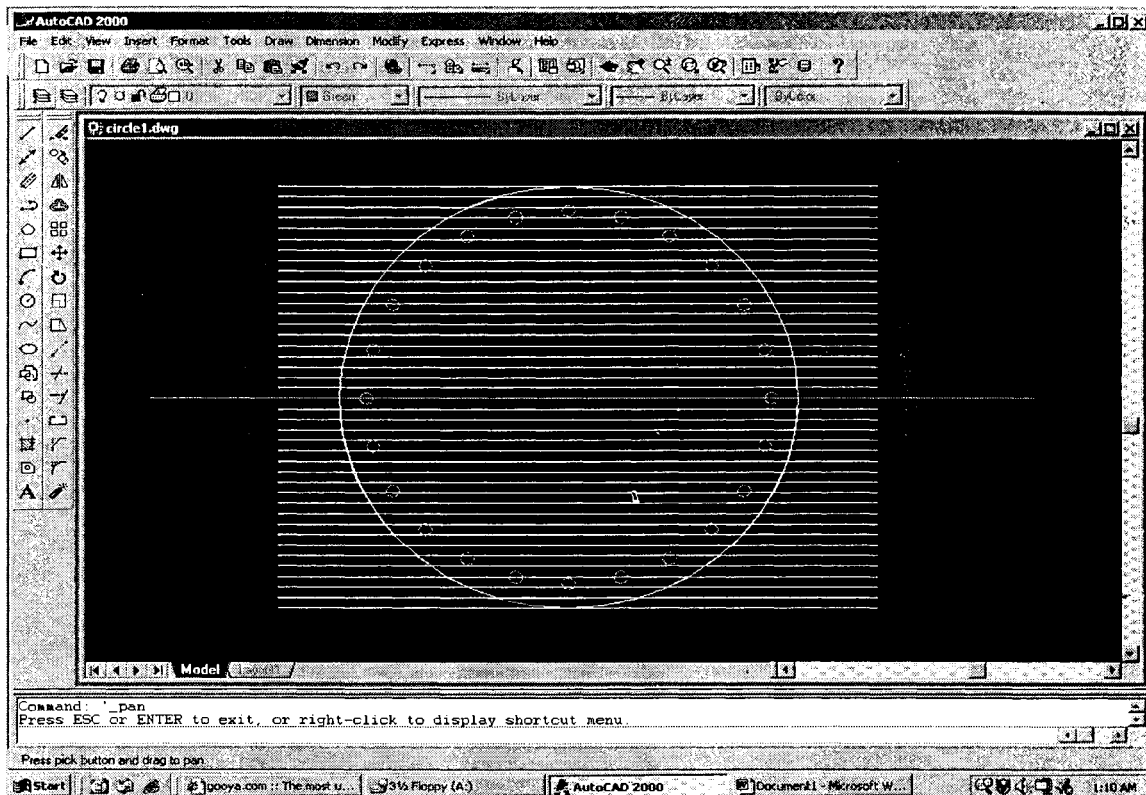
Figure 3-6 Column's cross-section in AUTOCAD14

The area of each segment was calculated, first by using Boundary command and pick point option, then by moving each segment away from the original section and finally by using area command and clicking on each segment.

The area of each segment and the distance from the center of the circle was obtained and then used as input data for the cross section type in the DRAIN-2DX program.

3.3.2 Constituent Material Behavior

Although the column is circular with spiral transverse reinforcement, but for concrete 3 points for compression, and 2 points for tension were approximated and obtained by using the Microsoft-Excel spreadsheet designed to calculate the required point from the concrete properties data according to the described Kent-Park model for rectangular column with transverse reinforcement. The data are shown in Table 3-2, and the stress-strain curve is shown in Figure 3-7.

Table 3-2 Concrete & reinforcement properties (N, mm)

f'$_c$	35.8	MPa
E (concrete)	28000	MPa
b'	1422	mm
d'	1422	mm
A$_s$	200	mm^2
S (spacing)	89	mm
f$_y$	475.4	MPa
E (steel)	190000	MPa
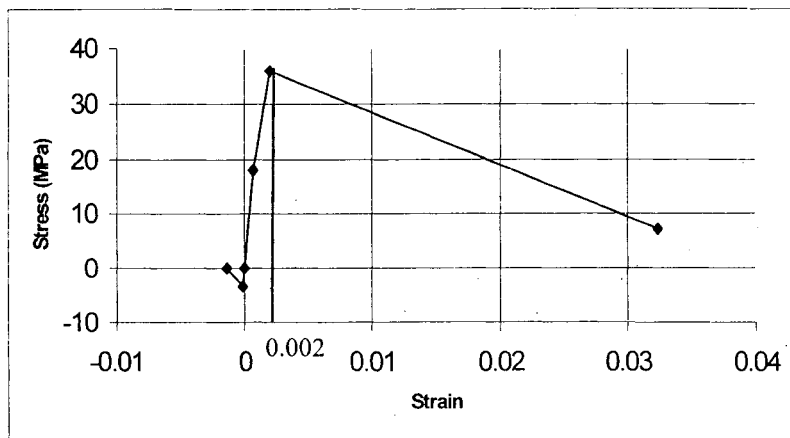
Figure 3-7 Stress-strain relationships for concrete

For reinforcing steel, two points, which are the same for tension and compression, were obtained from the material properties of steel as are shown in Table 3-2, and shown in Figure 3-8.
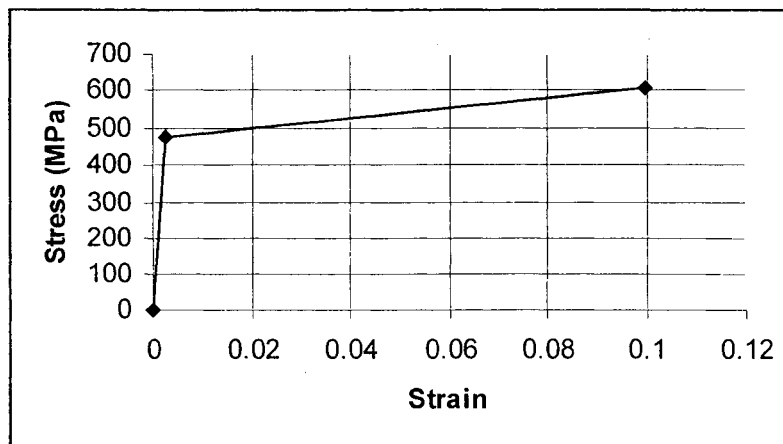
Figure 3-8 Stress-strain relationships for steel

43

The length of the plastic hinge, where the inelastic deformation was expected to occur within was assumed to be 15% the length of the column. The axial load of 4545 KN was applied to the column top and a horizontal quasi-static displacement loading was applied to the column. In the experiment each cycle was repeated many times, but due to the large size of the output files in DRAIN-2DX, in this study each cycle was performed once. The results in terms of load-displacement was obtained and graphed as can be seen in Figure 3-9.
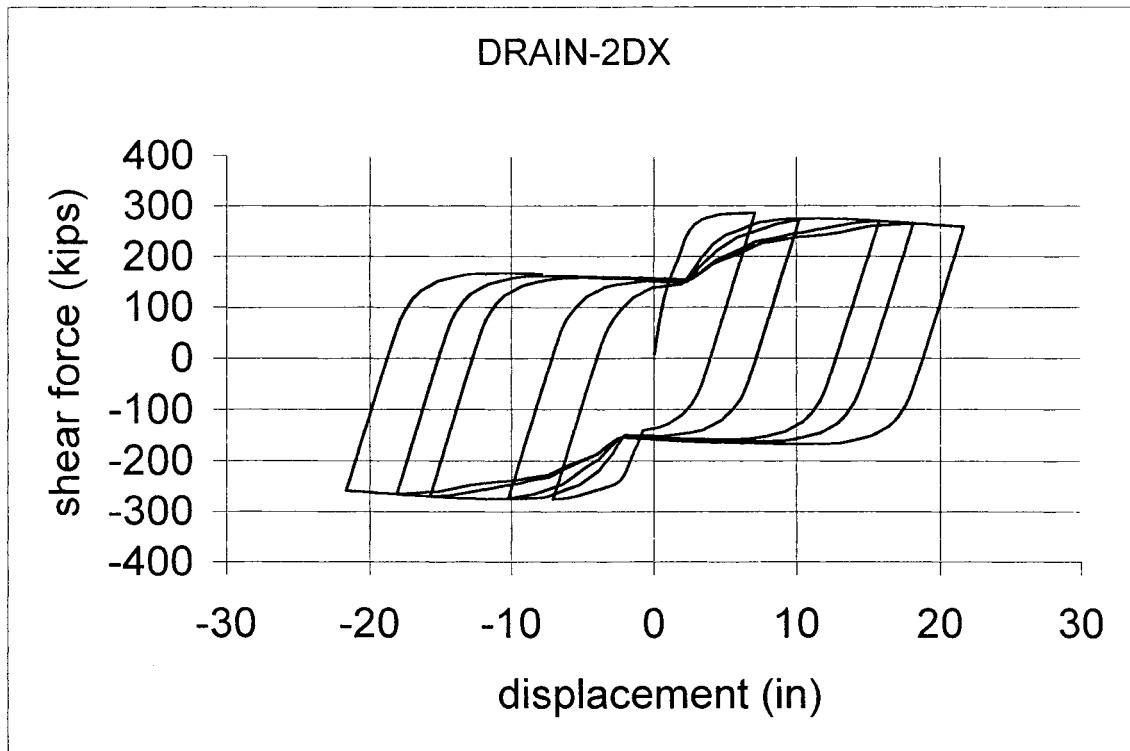
Figure 3-9 Shear force-displacement relationship (DRAIN-2DX)

3.4 Comparison of the Analytical Results with Experimental Evidence

In Figure 3-10, the predicted curve for shear force- displacement relationships obtained from analytical models using IDARC2D, and DRAIN-2DX are compared with the results of the experiment.
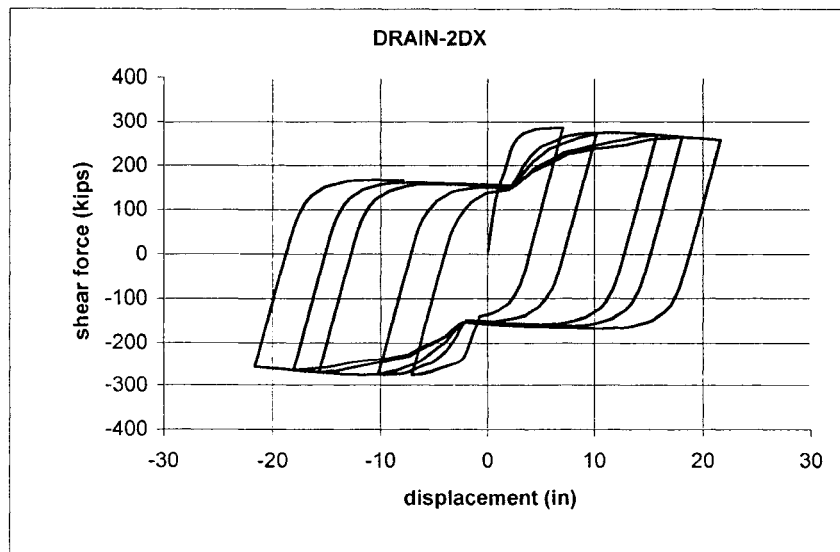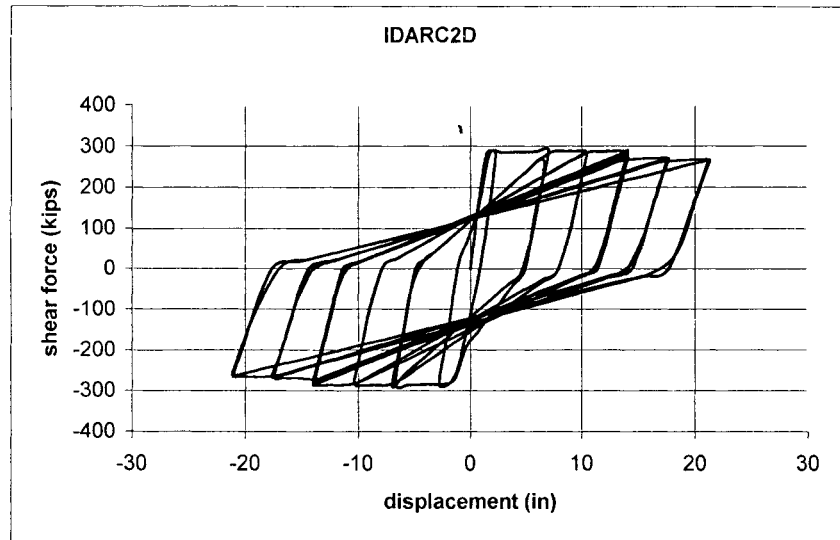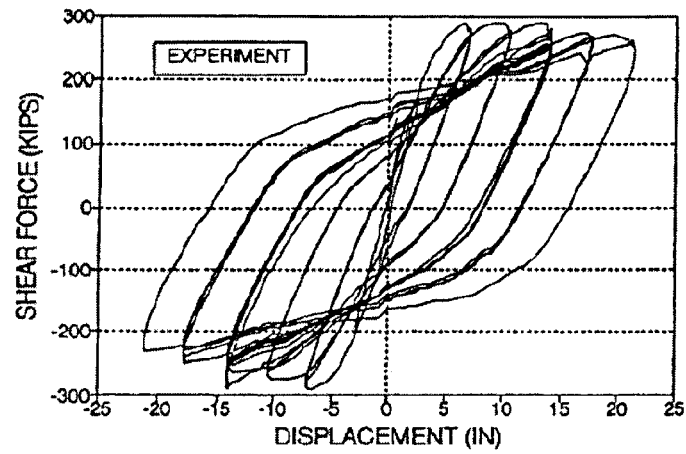
Figure 3-10 Comparison of experimental results and analytical results obtained by IDARC2D, and DRAIN2DX

Figure 3-10 shows that the analytical results correlated well with the experimental results. There was no numerical data found from the result of the experiment test in the reference or other sources. In IDARC2D, the maximum shear force sustained by the element is 289 kips at the top displacement of 7.06 inch. In DRAIN-2DX simulation, the maximum shear force sustained by the column is 286 kips at the displacement of 7.1 inch. At the maximum displacement of the test IDARC2D predicted the shear force of 266 kips at the displacement of 21.3 inch, while DRAIN-2DX predict the shear force of 259 kips at the same displacement. The maximum load, and the strain at maximum load and also the trend of gradual strength loss are well approximated with both programs. The bilinear curve in IDARC2D refers to the selection of bi-linear hysteretic curves, which compared with other hysteretic models gave the best comparable results to the experimental data.

Both programs are also able to predict the effects of various values of axial load on the column. In Figure 3-11, the behavior of the mentioned column under the same condition, but with axial load equal to 50% of that in the above example on the column, is obtained and compared graphically (i.e. axial load = %50*1000 = 500 Kips = 2272 KN). For the case of axial load equal to 50% of that in the first example, in IDARC2D simulation, the maximum shear force sustained by the element is 266 kips at the top displacement of 7.06 inch. In DRAIN-2DX simulation the maximum shear force sustained by the column is 269 kips at the displacement of 7.1 inch. At the maximum displacement of the test IDARC2D predicted the shear force of 246 kips at the displacement of 21.3 inch, while DRAIN-2DX predict the shear force of 253 kips at the same displacement. Both programs results indicate that; the increase in axial compressive load leads to increase in the flexural capacity, but a decrease in the ductility. This is in accordance with the results of a study on behavior of six large-scale circular reinforced concrete columns, with spiral confinement, under cyclic quasi-static lateral force, and axial load (Xiao. Y, Esmaeily-G.A, 2002), and also a study by Kent (Kent, 1969) on the hysteretic behavior of RC cantilever beams with different levels of axial load.
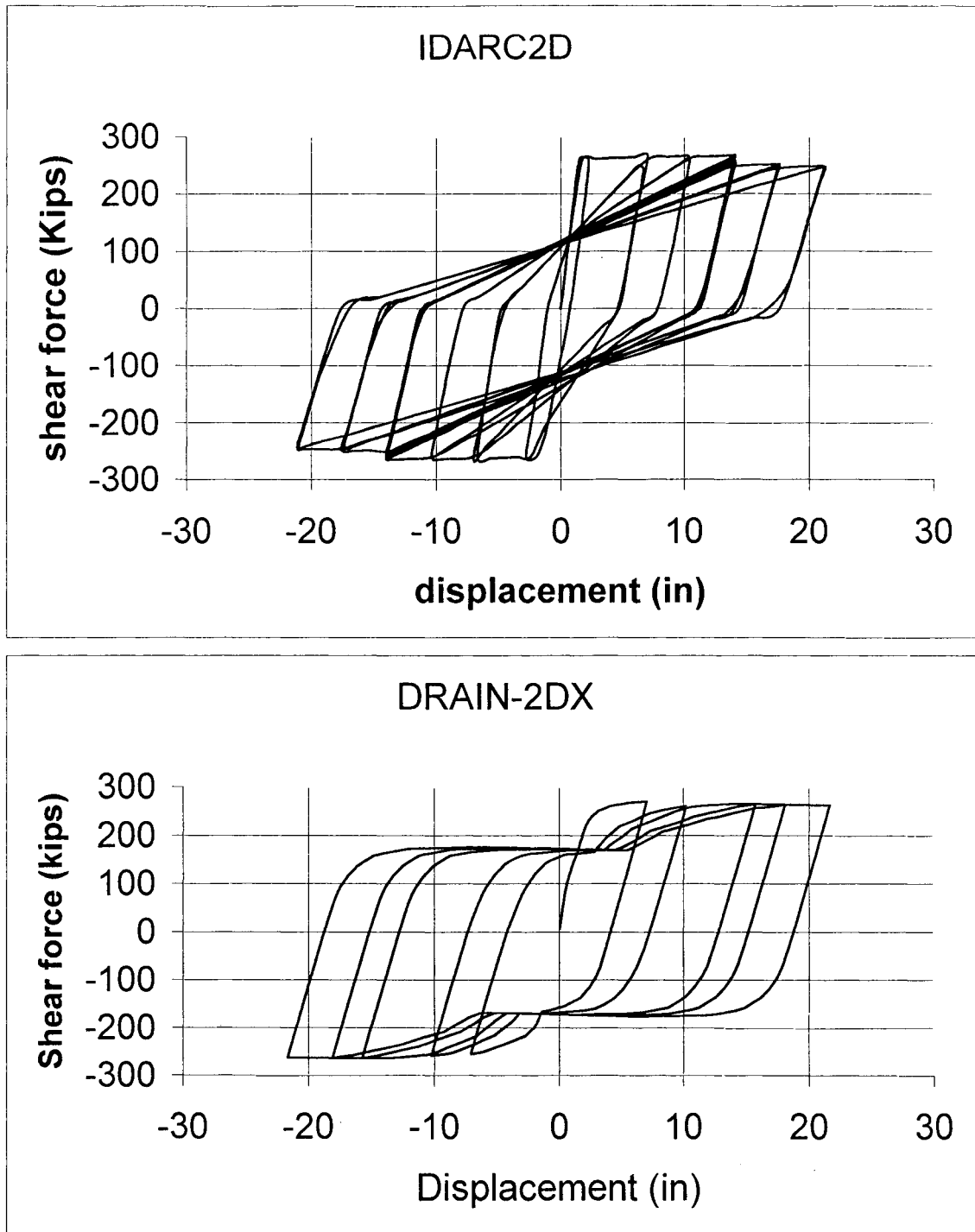
Figure 3-11 Shear force-displacement relationship (DRAIN-2DX & IDARC2D)

Chapter 4

BEAM-COLUM JOINT

4.1 General

In reinforced concrete structures, failure of beam-column joint was observed as one of the major causes of damage or even collapse of those structures during earthquakes. A beam-column joint should not fail during a strong earthquake because it provides continuity between the column and beams in the frame, and the gravity load must be sustained in the joint. Joints are difficult to repair after the earthquake; however, some damage should be tolerated if the damage does not cause detrimental effects on the overall behavior of the structure. The design of a joint against the gravity load and flexure is automatically satisfied if the column reinforcement is continued through the joint. However, the shear in a joint can be significantly different from that in the columns and beams, which frame into it. The joint should be designed against a brittle shear failure. At the same time, the anchorage of beam bars should be properly maintained to develop the weak-beam strong-column earthquake resistance mechanism.

Proper design of reinforced concrete beam-column connections is important for the behavior of the whole structure. With the proper design of element of the structure, the column could be designed so as to achieve ductile performance and significant post yield flexural strength, and the beam is expected to have flexural demands associated with nominal flexural strength, thus it may be found that beam-column joints become the weakest part in the mechanism, which provides resistance against seismic forces.

Under seismic excitation, the beam-column joint is subjected to horizontal and vertical shear stresses. The difference in signs of moments in beams and in columns at faces of the joint panel, at each load reversal, causes the joint to be subjected to high magnitude of shear stresses, whose magnitudes are typically many times higher than the stresses in the adjacent beams and columns at the face of the joint panel. The joint panel provides continuity between the column and beams in the frame, thus the connection flexibility leads to increased structural flexibility. It should also be noted the increase in connection flexibility and deformation due to bond loss, inelastic shear deformation, and cracks under high principal tensile stress or crush under high principal compression stress

may control the structure response. It has been found that inelastic deformations within a joint during cyclic reversed loading may lead to rapid loss of both stiffness and strength. The capacity of the column should not be jeopardized by possible strength degradation within the joint. Moreover, joint deformations should not significantly increase the storey drifts within a structure. Capacity design, relevant to joints, must ensure that the over-strength input from beams that are connected is maintained with a minimum of inelastic deformation within the joint core.

Due to reversals in the moments on the ends of beams at faces of the joint, the beam bars are in compression at one side, and at tension on the other side. The high bond stress is required to sustain these stresses across the joint panel. When these stresses are high, they may cause bond failure within the joint. In particular the consequences of bar slip within a joint can be very serious. It is enhancing interstorey drift and thus allows P-delta effects also to become more significant.

The behavior of the beam-column connections is complex and still not fully understood. The development of an analytical model, which has the capacity to account for the localized response mechanism that determines the global behavior of the structure, seems necessary for prediction of the response of the structures. These models range from simplified models that are appropriate for the design of beam-column joints to complex finite element models. All of these models require constituent material models and also some assumptions in terms of the joint behavior. These assumptions include the stress distribution at the boundary of the joint panel, bond stress distribution within the joint, and mechanism for shear transfer through the joint. Most of these models identify a load distribution that satisfies the equilibrium of forces, but not necessarily the compatibility. In other word the model is unable to consider localized response explicitly, thus is not powerful for investigating the complex behavior of the beam-column joint.

In finite element modeling, not only the sophisticated constituent material models are defined but also complex behavior of the joint like bar pullout and pinching behavior, stiffness and strength degradation of the joint can be modeled.

There are potentially a large number of parameters affecting joint capacity, and their full effect in joint behavior is still not fully understood, further, the advantages of new materials need to be continually evaluated. This makes it very difficult to cover all

the variables by experimental testing alone. A reliable analytical model could provide a significant contribution to a detailed, experimental study. Because of the economic feasibility of performing computer analysis on simulated structures and conditions, therefore the goal is to develop a robust, reliable model that could give comparable results to the experimental model, which could be utilized as an investigative tool in conjunction with the experimental program.

Methods for beam-column joint design have undergone many changes in the past years and are still evolving. Much of the studies in the past to predict structural damage during earthquakes had relied on the consideration of simple inelastic one-degree-of-freedom systems to predict the nonlinear response of actual structures. The reliable prediction of damage to a building during an earthquake requires the ability to perform accurate nonlinear dynamic analysis with realistic models of the structure under the simulated condition of the selected earthquake.

The response of the joint has a very complex behavior. It is mainly dependant on shear mechanism of the joint panel and the bond condition between concrete and reinforcement, which have controlling effects on the hysteretic behavior of the joint under earthquake cyclic loading. Hysteresis is a nonlinear phenomenon. Structures when subjected to dynamic loading under strong earthquake excitation usually exhibit hysteretic behavior. Different structural members and connections are deliberately designed and detailed to dissipate energy by hysteresis to increase the margin of safety against seismic collapse.

Joints in general are unsuitable regions for energy dissipation. The hysteretic behavior of the reinforced concrete beam-column joint depends on the behavior and interaction of the constituent materials under cyclic load reversals. Some examples of this interaction are the relative slip between steel and concrete in the form of pull out of reinforcement out of beam-column joint, cracks at the interface between beams and column joints, and slip or pinch which occurs as a result of crack closure. The hysteresis loop decays with the number of load reversals, resulting in a smaller resistance at the same peak displacement in each repeated loading cycle.

4.2 Mechanism of Shear Resistance in Joints

Experimental investigation of beam-column joints has been underway since the late 1960. In 1969, Hanson, et al. reported series of tests of beam-column joint and gave a definition of joint shear, which is widely accepted.

When plastic hinges are expected to develop in beams near the column in a ductile design, where strong column-weak beam philosophy governs, the joint must be capable of transferring large shear forces across the joint panel. The joint shear is the internal force acting on the free body cut at the horizontal line at the mid-height of the joint. The internal forces in the joint zone are shown in Figure 4-1. (Stresses applied by the columns' forces are not shown in the figure).

$$V_J = T + C`_C + C`_S - V_C \qquad (4-1)$$

By writing the equilibrium of forces in the left-hand beam: $T` = C`_C + C`_S$ (4-2)

By substituting in the equation (4-1) $\longrightarrow$ $V_J = T + T` - V_C$ (4-3)

Where: $C`_S$ = Compressive force in steel bar (beam)

         $C`_C$ = Compressive force in concrete (beam)

         T = Tensile strength in the longitudinal beam bar (Top)

         $T`$ = Tensile strength in the longitudinal beam bar (Bottom)

         V_C = Column shear force
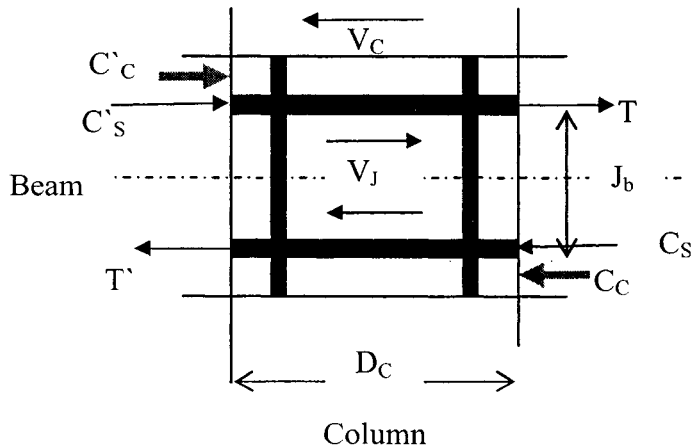
Figure 4-1 Stresses applied to an internal joint from adjacent beams

Several mechanisms for joint load transfer during an earthquake have been proposed. The most common and well-known mechanism, which was first discussed by

Paulay et al., (1992), is based on the compressive capacity of the joint concrete. This can be described as follows.

As Figure 4-2 shows, due to the seismic loads and the induced shears and moments in the beams and columns, the plastic hinges, imparts a significant shear in the joint. $V=dM/dX=2M_p$ / b_{Joint} (b_{Joint} is the width of the joint panel). This shear force as will be discussed later should be resisted and transferred by means of concrete compression struts, parallel to the shear cracks in the joint.
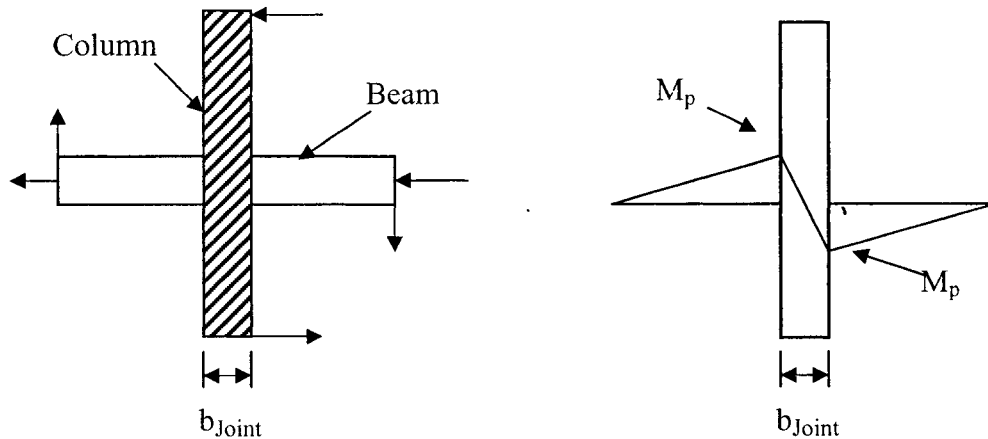
Figure 4-2 Beams' moment gradient around the joint

The compression strut model assumes that after the bond is lost due to the level of damage, the tension forces in the longitudinal reinforcements of beams and column are anchored on the opposite corners of the joint panel. This needs the assumption that the bond strength is mainly in the vicinity of beam and column flexural compression zone. These tensile forces are then combined with compression forces on each sides of the beam-column face and the resultants are then transferred through a diagonal compression strut. After the diagonal transferred shear exceeds the compressive strength of the cracked concrete in the joint, the joint shear resistance degrades. The transverse reinforcement has the role of confining the concrete core in the joint panel.

These are categorized as "main strut mechanism" and "sub-strut mechanism". The main strut is formed along the main diagonal of the joint panel as the resultant of the horizontal and vertical compression stresses acting at the beam and column critical sections. The main strut exists without regard to the bond situation of beam bars with the tensile stress in the vertical and horizontal reinforcement and the bond stresses within the

joint. The sub-strut mechanism is formed by diagonal compression stresses distributed uniformly within the panel region. The diagonal strut stresses must balance stresses along the beam and column exterior bars. If the bond is perfect along the beam reinforcement, the main strut mechanism transfers a part of shear nearly equal to the compression force of the top beam bar, and the sub-strut mechanism transfers the part nearly equal to the top beam bar tension force. Once the bond along the beam reinforcement deteriorates, the sub-strut mechanism starts to lose shear transfer ability, and gradually the effectiveness of the joint lateral reinforcement will degrade. The main strut mechanism carries the entire shear in the joint. The bond along the beam reinforcement inevitably deteriorates especially after the beam flexural yielding unless the strength and size of the reinforcement are strictly restricted. It is necessary to note that the reversed cyclic loading weakens the strut concrete and because the compressive strength is reduced by the increasing tensile strain perpendicular to the direction of the main strut.

Another method of joint shear transfer, which is often used in conjunction with the compression strut model, is the truss model. The truss model assumes that the forces developed in the face of the joint in the reinforcements of beams and columns are transferred through the joint panel by means of several tension (steel reinforcing ties), and compression (concrete struts) components. If it is assumed that the high demand on the perimeter of the joint panel cause concrete flexural cracks, and these cracks remain open during the load reversals, it seems that the reinforcement is the only load path for transferring the loads in beams and columns.

Main strut mechanism   Sub-strut mechanism   Truss mechanism
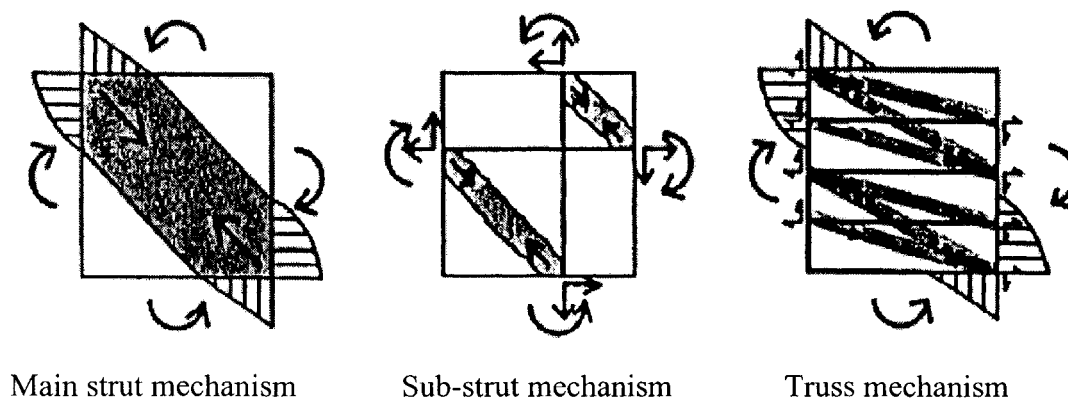
Figure 4-3 Strut and truss mechanism

53

The strut and ties model, which is shown in Figure 4-3 , and will be briefly explained assumes the load is transferred sequentially through a series of mentioned strut and ties. Another model proposed by Shiohara (Shiohara, 1998), is different from the above-mentioned model, and will be briefly explained. The model is based on the data obtained from tests of twenty-one reinforced concrete interior beam-column joints, failed in joint shear. The data indicated that there is increase in the joint shear even after apparent joint failure starts. The distance between stress resultants in beam at column face is reduced, resulting in reduction in beam moment and flexural resistance. This model identifies the deterioration of story shear to be a degrading of moment resistance of joint, originated from a finite upper limit of anchorage capacity of beam reinforcement through the joint core. In other word the data show that: when the story drift increases, the joint shear increases as well, causing the length of moment lever arm at the column face (J_b) to decrease.

The finite element modeling eliminates several limitations encountered with simple models. In finite element models the constitutive material behavior is developed either on the basis of previously well-defined models or on the basis of experimental data. Then the qualitative evaluation of the behavior and response of elements are used for identification of material characteristics to be implemented in the model. The development of the appropriate finite element techniques is the next step. Possible calibration for more complex system and the verification of the result with experimental data will be the last step.

In the following the two mentioned theory for the mechanism of joint that are referred to in this study are discussed.

4.3 Struts and Ties Model (T. Paulay, M. J. N. Priestly 1992)

4.3.1 Internal Joints

This mechanism was first discussed by Paulay, et al. (1992), and has been widely accepted and used as the joint mechanism in shear.

The resistance of shear forces in a joint core can be based on two mentioned mechanisms, the principal compression strut model, and the truss model.

An interior beam-column joint is considered where for simplicity no axial force is considered. The joint shear was calculated according to equation (4-3):

$$V_J = T + T` - V_C \qquad (4\text{-}4)$$

The top bars in the joint panel as is depicted in Figure 4-4, are assumed to be anchored by the bond force (U) throughout the joint.

$$U = C`_s + T \qquad (4\text{-}5)$$

Top Reinforcement

C`s   T

U

Joint Panel
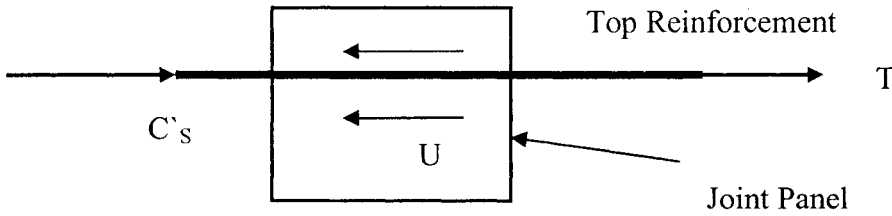
Figure 4-4 Stress condition on the top bars

During a cyclic loading, the level of damage and also the poor bond between the bars and concrete leads to the debonding of the top bars, so the bond force becomes zero and the tension forces in the longitudinal reinforcements of beams and column are anchored on the opposite corners of the joint panel.

$$U = 0 \quad \longrightarrow \quad T = -C`_s \qquad (4\text{-}6)$$

This means that the top bars are in tension throughout the joint panel.

$$T` = C`_C + C`_s$$

$$T = -C`_s \quad \longrightarrow \quad T` + T = C`_C \qquad (4\text{-}7)$$

Substituting into (1) : $V_J = T - T + T + T` - V_C \quad \longrightarrow \quad V_J = T + T` - V_C \qquad (4\text{-}8)$

By comparing equations (4-3), and (4-8) it is concluded that the bond deterioration along the beam bars in the joint has no effect on the total horizontal shear force acting on the joint core. (Hakuto, et al. 2000). A good and complete model should be applicable at all levels of loading, from low levels of demands when the stresses are in elastic domain, to high levels of damage when stresses and strains go beyond elasticity. Considering the section of joint panel and the external stresses acting on different faces of the section on the selected part of the frame in Figure 4-5, the forces on the perimeter of the joint panel, and the compression strut are shown in Figure 4-6.
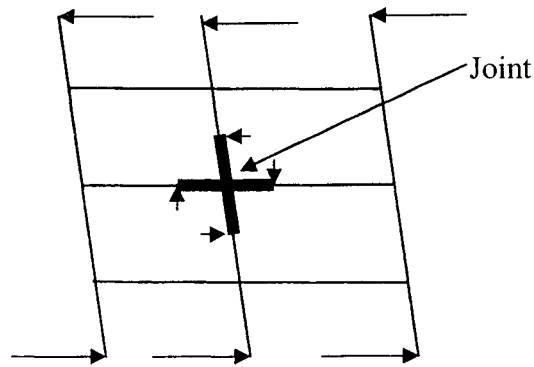
Figure 4-5 Forces on an interior joint
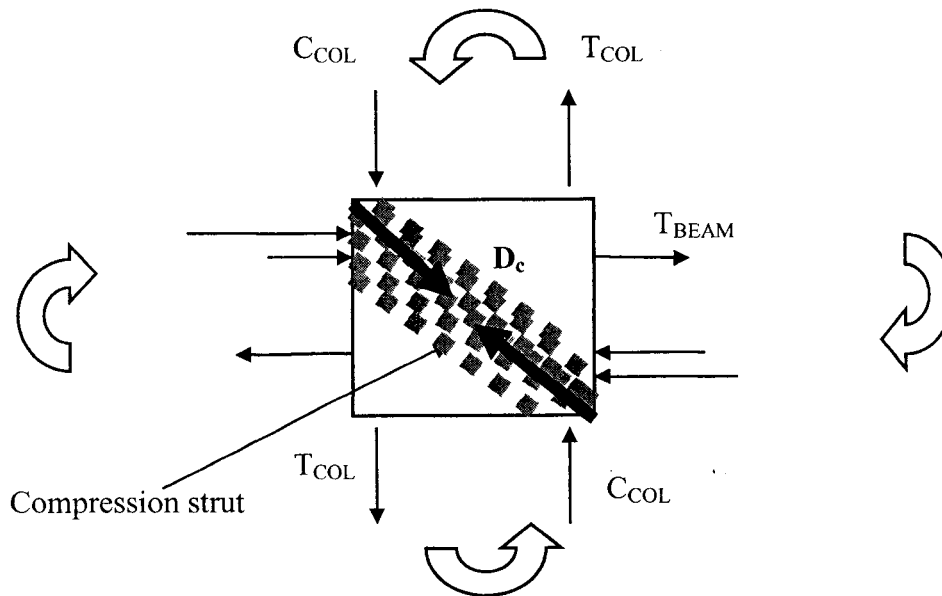
Figure 4-6 Diagonal compression strut

As it is shown in Figure 4-6, the moments at the ends of beams and columns at the face of joint, produce compression and tensile stresses in the concrete and reinforcement at different faces of the joint panel. The diagonal compression force is mobilized by concrete compression forces at the two opposite corners of the joint core and also by some bond forces transferred from the beam and column reinforcement approximately over length within the shaded area.

The strut mechanism transfers shear forces via a diagonal concrete strut, which sustains compression only and is assumed to be inclined at an angle close that of potential

diagonal corner to corner plane. The contribution of this mechanism, sustaining a diagonal compression force, is sometimes referred to as the "shear carried by the concrete" the notations V_{Sh}, and V_{Sv} are used to present the horizontal and vertical joint shear forces resisted by this mechanism, respectively. The moments and shear forces generated during an earthquake produce stresses at the face of the beam-column joint and the internal stresses in the joint panel as shown in Figure 4-7.
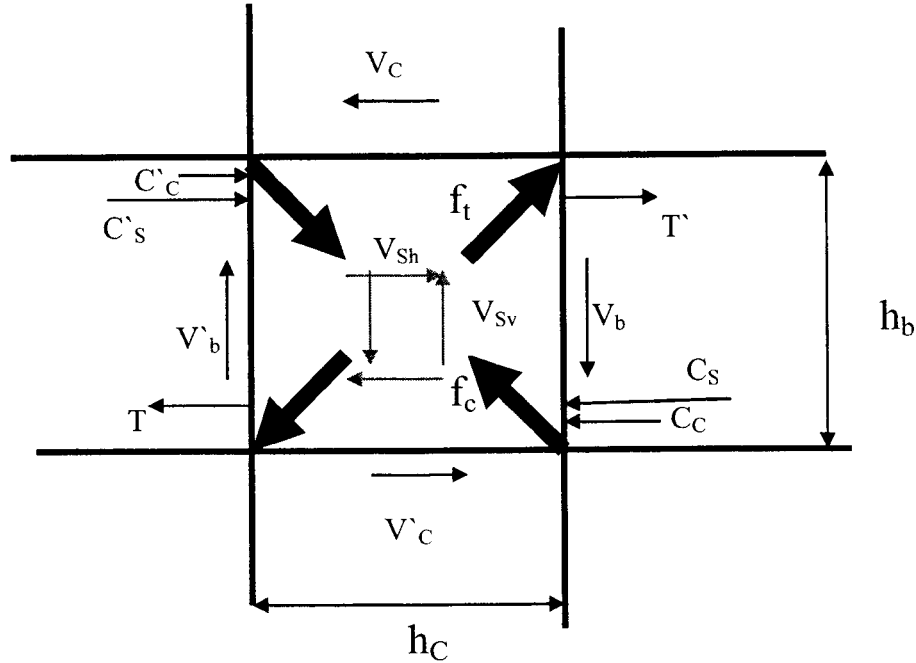
Figure 4-7 Equilibrium condition for an internal joint

As a result of the action of the stress resultant on the joint core, internal diagonal tensile and compressive stresses f_t, and f_c are produced. These internal diagonal stresses tend to cause diagonal cracking of the core concrete, and if this phenomenon is not restricted by a system of shear resistance, the failure of joint core occurs along a corner-to-corner diagonal plane.

As was seen before the internal horizontal shear in the column at the mid-section depth

is: $V_{jh} = T + T` - V_C$ same as: (4-3)

It seems sufficiently accurate to obtain the internal vertical shear as:

$V_{Sv} = V_{Sh} * (h_b / h_c);$ (4-9)

Where h_b & h_c are the beam and column depths, respectively.

57

Considering the shear deformations of joint cores in (Figure 4-8), and assuming the existence of uniform bond, the development of shear stresses applied to the boundaries of a joint core can be transferred by means of a diagonal compression field. In comparison to the tensile strains in the reinforcement, the concrete diagonal compression strains are generally negligible. Hence, there is a tendency for the joint core to deform and dilate as seismic actions continue. This implies that both vertical and horizontal reinforcement passing through the joint core must become longer; as one of the main reasons of debonding in the joint.
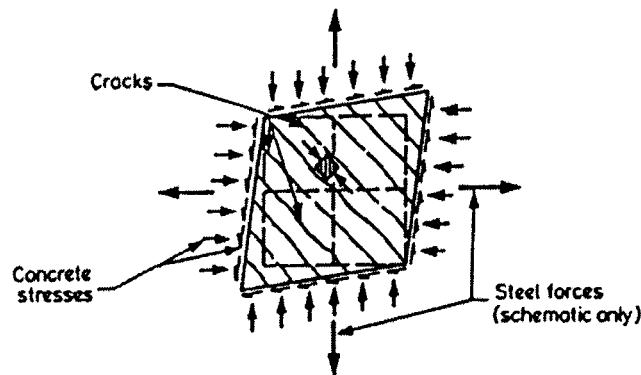
Figure 4-8 Shear deformations in a diagonally cracked joint core

The truss mechanism consists of the contribution to the shear resistance of the vertical and horizontal reinforcement inside the joint core. Horizontal and vertical forces transferred by bond from the beam and column longitudinal bars are transmitted to the core concrete mainly outside the shaded area of Figure 4-6. Despite extensive cracking in the joint core, a diagonal compression field with a resultant force D_S can be sustained to transmit the bond forces, if adequate transverse forces normal to the boundaries are provided through the presence of the joint core reinforcement. The truss mechanism generating this compression field involves the participation of horizontal reinforcement (normally in the form of joint hoops), vertical reinforcement (normally in the form of column intermediate bars), and numerous concrete struts. The contribution of this mechanism is sometimes referred to as the "shear carried by the shear reinforcement". If the beam-column connection contains horizontal reinforcement, additional load paths instead of the main diagonal strut can carry the diagonal compression alone. This will mobilize more concrete to resist the compression force. Therefore the compression stress, which causes the crushing of the diagonal concrete, is somehow alleviated.
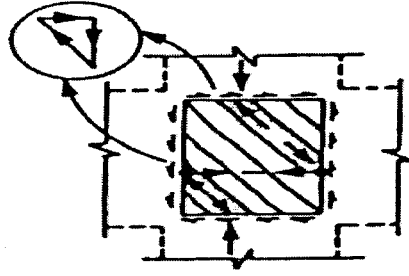
Figure 4-9 Diagonal compression field

To prevent diagonal tension to cause shear failure along the corner-to-corner diagonal failure plane, both horizontal and vertical shear reinforcement are required to enable the truss mechanism to be mobilized. Such reinforcement is usually provided in terms of joint hoops, and column longitudinal bars, respectively.

As it is evident in Figures 4-8, and 4-9, the level of column axial (compressive) force has an important effect in the value of the results of shear tension sustained by joint hoops. With axial compression in the column above the joint panel, the inclination of the strut will be steeper. In other word, if the amount of axial compression force exerted by the column to the joint panel is small, the amount of required horizontal joint reinforcement (hoops) increases. This is the reason why column axial stresses reduce the joint deformations, especially where there are not enough joint hoops. With column axial compression in the column transmitted through the joint, the inclination of the truss (α) as is shown in Figure 4-10, will be steeper, and less shear component is transferred through the diagonal compression strut. The increase in column axial load also increases the depth of the diagonal compression strut (Figure 4-10), resulting in the alleviation of the crushing compressive stress.

The following equation suggested by Paulay et al. 1992, shows the effect of the axial force on the depth of the flexural compression zone of the column.

$$C = (0.25 + 0.85 \ \frac{P_u}{f'_c A_g}) \ h_c \qquad (4-10)$$

Note: $T = \lambda_o\, f_y\, A_s$ accounts for overstrength in the tensile force in the upper bar.
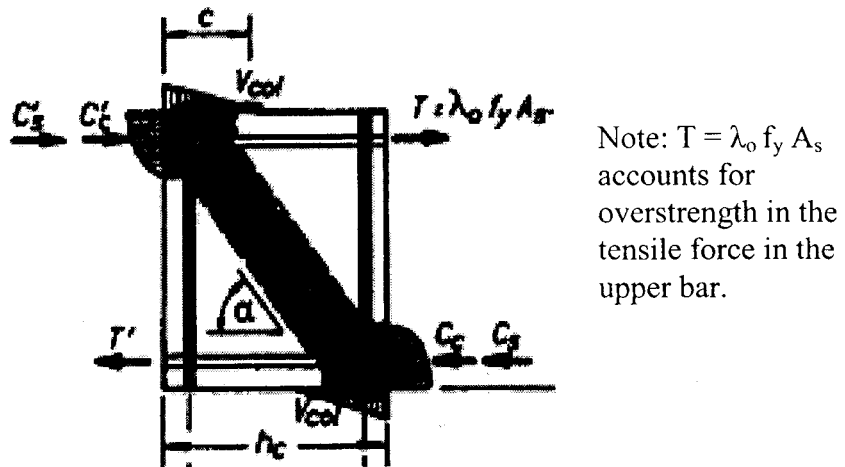
Figure 4-10 The main diagonal compression strut

The column axial force helps the clamping action in terms of providing more pressure, causing better bond condition between concrete and the reinforcement deformations. Reinforcement in the joint also has some confining effect in terms of exerting clamping action across splitting cracks. When the joint transverse reinforcement is insufficient, the joint hoops which transfer the tensile stresses start to yield and dilate, as the level of the force increases. The plastic deformation of the steel, which has already yielded, is not reversible. So in the next cycle of loading if the tensile strains imposed to the joints are smaller than the previous step, those hoops do not have their passive lateral confining effect due to dilation in the previous step. This phenomenon contributes to the stiffness degradation and disability of the joint to dissipate seismic energy at low shear force level after several load and displacement reversals.

The resistance of shear forces in a joint can be based on two described mechanisms. At lower levels of demand, where stresses are in elastic domain, the concrete is not cracked and the stress in reinforcement is below the yield stress. In this condition the joint can be considered as a shear panel, transferring forces through a series of compression struts and tensile ties. Unless the axial compression load on the column is large, or the beam plastic hinges are away from the joint panel, the truss mechanism may resist the majority of V_{sh} and V_{sv} (Figure 4-7), due to the large bond forces to be transferred within the joint.

As the loads increase, the concrete begins to crack and reinforcement begins to yield, causing degradation of the bond, resulting in greater tendency of the stresses to be anchored to opposite corners of the joint panel in both ends of the main compressive strut. So if bond deterioration happens in the early stages of loading, the truss mechanism is less likely to be mobilized. In the beam-column joint without transverse reinforcement the extensive diagonal cracking in tension leads to diagonal compression failure of the joint. Thus, the maximum compressive strength of the main diagonal strut determines the shear strength of the joint. This, as will be referred to, is one of the main facts in developing the new model presented in this study.

4.3.2 External Joints

In the exterior beam-column joint, only one beam frames into the joint panel, so the moments and consequently the induced shear at the joint is generally less than the case of interior beam-column joints, which are confined by more beams and have better condition of the joint core confinement. In this case the horizontal joint shear force is:

$$V_{jh} = T - V_{col} \qquad (4\text{-}11)$$

Where the value of T (tension force in the bars) is either $f_s A_s$, or $\lambda f_y A_s$ (λ is the reinforcement over-strength factor), depending on the condition of stress in steel bars. The internal forces in the joint panel are shown in figure 4-11-a.

The compression strut and truss mechanism are applicable to exterior joints. Since there is no beam on the other side of the joint, the hooks in the ends of both top and bottom beam bar, contributes to formation of the compression strut. A diagonal strut similar to that of interior joints in Figure 4-6, will develop between the bend of the hooked top tension beam bars and the lower right hand corner of the joint (Figure 4-11-b).The anchorage forces of the bars' end hooks; the bond stresses from the straight portion of the top bars, and the vertical forces introduced by the column above the joint will combine and form a diagonal compression force within the joint panel.

(a) Stress resultant   (b) Crack pattern
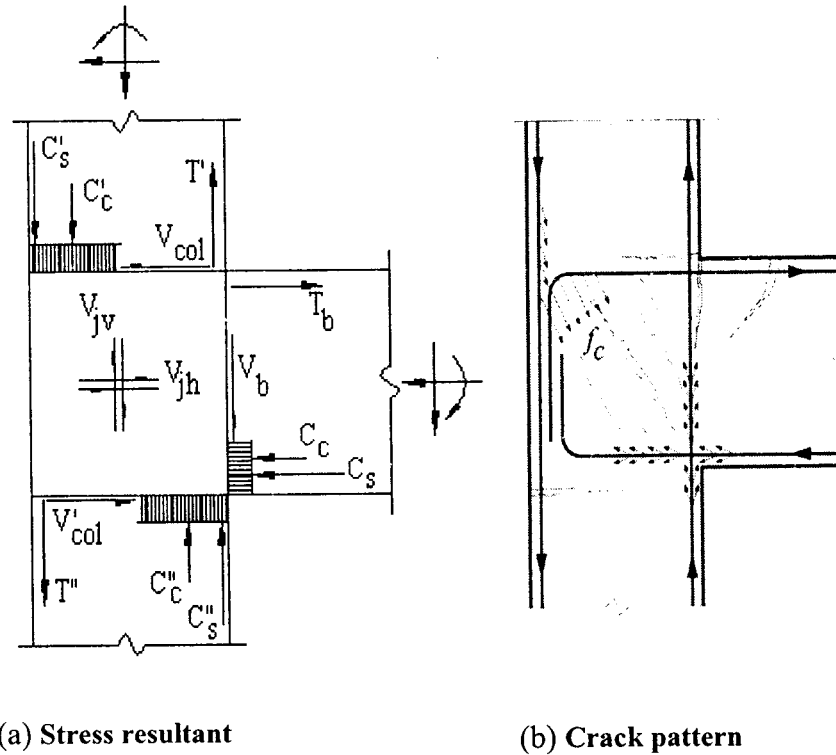
Figure 4 -11 Applied load and crack pattern in an exterior joint
(El-Amoury, 2003)

4.4 Shiohara Model (Shiohara, 1998)

In this model, which is particularly applicable to the interior beam-column joint, joint shear is assumed to be transferred through a diagonal strut like the traditional strut model, because existence of diagonal strut is supported by tests and analyses. However, cause of joint shear deformation should not be crush of diagonal strut due to compressive force in strut; the joint shear failure accounts for lower strength than calculated based on the flexural strength of beams or columns and also reduction of stiffness due to premature failure of joint shear panel accompanied with diagonal cracks and local crushing of concrete. In this model the shear deformation of the joint is attributed to rotational movement of four segments around contact points. These segments are produced by 45-degree cracks, which divide the panel into 4 triangular segments as shown in Figures 4-12, and 4-13.
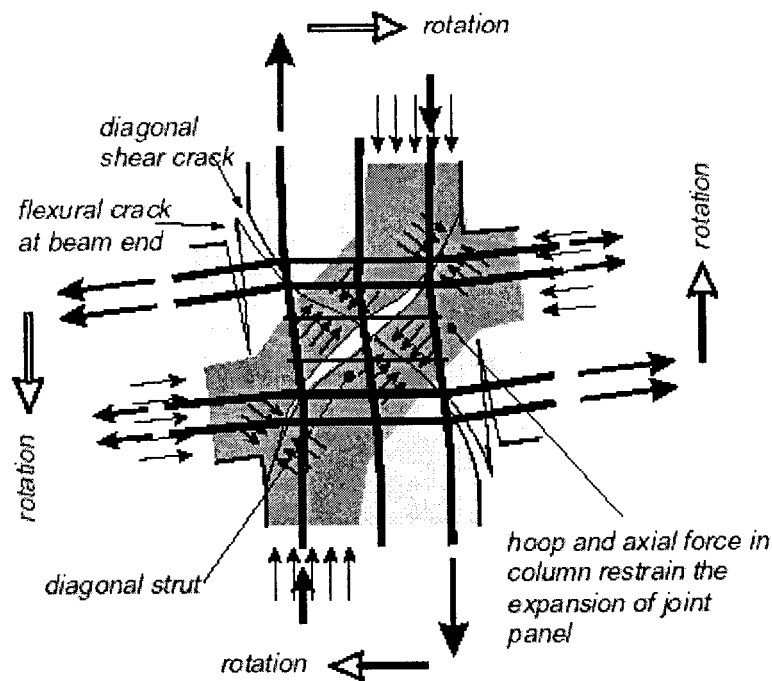
Figure 4-12 Joint failure mechanism and stress condition

By using this model, the moment resisting system of beam-to-column joint is investigated. In order to resist to the relative movements at the boundary of the segments, internal stress arises in longitudinal steel, joint hoops and concrete to resist the rotation of the segments. The location and distribution of boundary stress in concrete with consideration of compatibility of displacement and strain due to rotation of the segments is assumed as shown in Figure 4–13. It is assumed that the diagonal cracks exist with inclination of 45 degree, only normal stress is transmitted across the concrete cracks, and also there is no dowel force resisted by reinforcements.
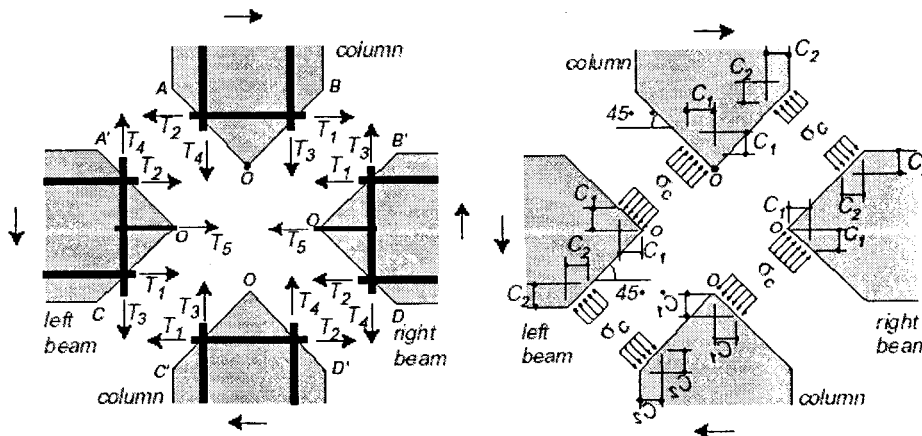
Figure 4-13 Internal stresses within the joint

Shear deformation concentrates at the boundaries, which consist of diagonal cracks and flexural cracks formed by shear or flexural stress as are depicted in Figure 4-14. Shear deformation of the joint is accompanied by expansion of joint panel (Figure 4-14(a)), so it is apparent that the axial force in column and the transverse reinforcement in joint are effective for reducing the deformation of joint panel. Total story drift consists of joint shear deformation and beam deformation. If sufficient amount of hoops are provided, the opening of the diagonal cracks is restrained, and the percentage of beam deformation in the total story drift increase, and the failure mode becomes beam reinforcement yielding.

(a) joint deformation mode   *(b) beam end deformation mode*
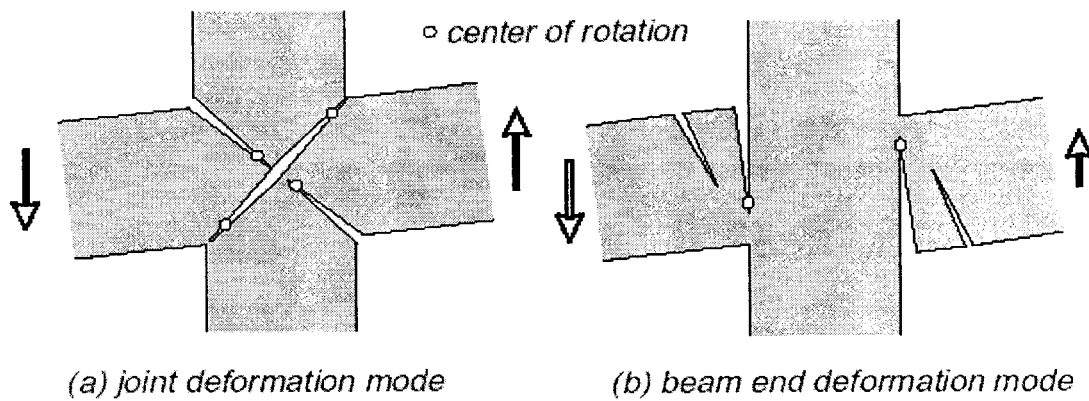
Figure 4-14 Joint failure mechanism models

4.4.1 Experimental Evidence

Joint shear stresses of twenty-one specimens subjected to cyclic loading were evaluated using Equation (4-1) and plotted against story drift angle in Figures 4-15, and 4-16.
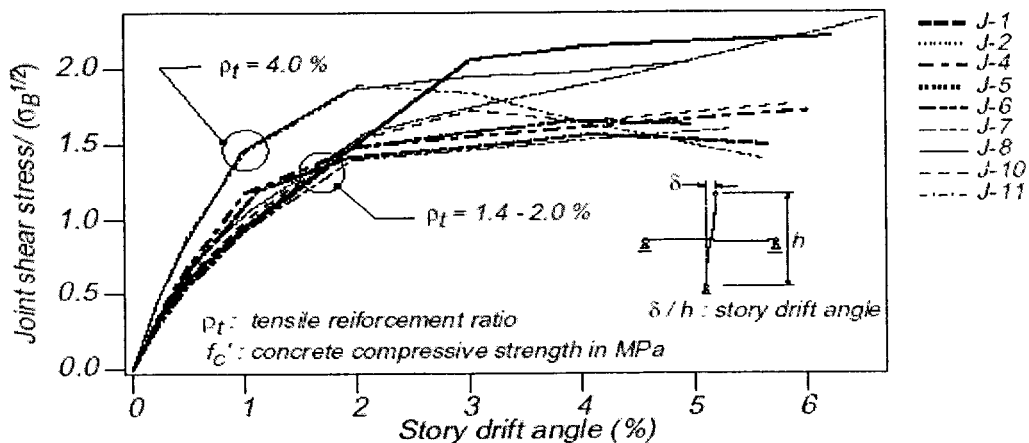
Figure 4-15 Relation of story shear vs. joint shear evaluated with equation (4-1) at load peaks (Shiohara, 1998)

64
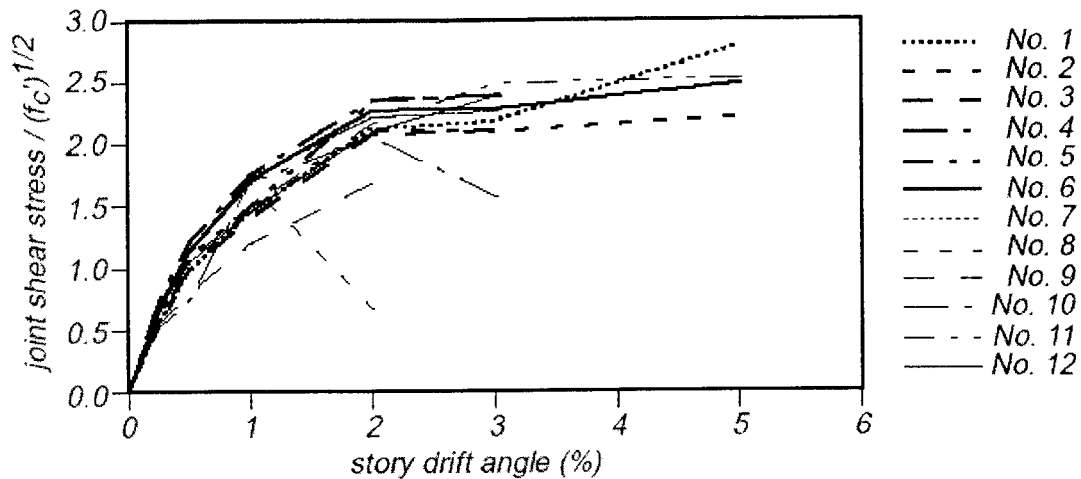
Figure 4-16 Relation of story shear vs. joint shear evaluated with equation (4-1) at load peaks (Shiohara, 1998)

Joint shear stress is calculated considering the effective joint sectional area to be the product of column depth and effective joint width. Joint shear stresses are normalized with square root of concrete compressive strength. It is shown, that constant joint shear was kept except that of specimen J-11, No. 8 and No.11. If compressive failure of diagonal strut occurs, joint shear should reach maximum first, then joint failure starts with decrease of joint shear. But joint shear increased for several specimens such as J-2, J-5, J-8 No.1, No.2 and No.6. In the most specimens, joint shear degradation was not observed while the appearance during the tests showed apparent joint shear failure. Therefore, it is concluded that the joint shear failure and the degradation of story shear are not results of the degradation of joint shear stress. This evidence is in contradiction with the hypothesis that the joint failure occurs when joint shear reaches its joint shear capacity after beam flexural yield as it is assumed in compressive strut model. The data also showed that the joint shear strength increases with increase of the amount of beam longitudinal reinforcement as well as the concrete compressive strength, while the amount of joint hoops showed not to have a significant effect.

To show that the decrease of the distance between stress resultants (degradation of moment resistance) in the beam at column face is the cause of story shear degradation at high story drifts, the values of the distance of stress resultants, normalized by effective depth (J_b), versus the story drift angles of the frame are obtained for the first nine specimens. They were calculated using the fact that the beam moment is product of force

65

in longitudinal reinforcement and the lever arm. The forces in the longitudinal reinforcement were obtained using strain history and the nonlinear relation between stress and strain for steel. It can be observed from Figure 4-17, that in all specimens the ratio of distance of stress resultant normalized with the effective depth decreases as the story drift increases.
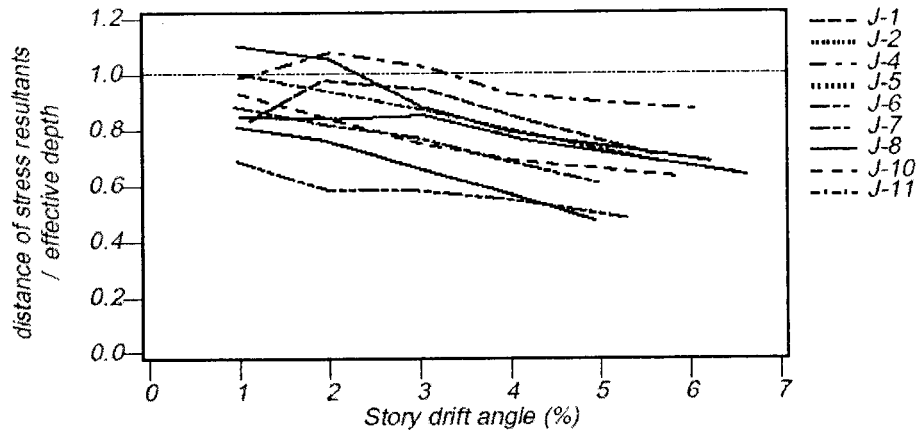
Figure 4-17 Transition of the moment lever arm length in beam at critical section calculated from observed moment and stress in reinforcing steel

Decrease of distance between locations of stress resultants were partly because the location of compressive stress resultants shifted to the center of beam. The reason is the change of stress in compressive reinforcement from compression to tension; due to poor bond condition within the joint panel as is shown in Figure 4-18, causing the location of stress resultant of compression shift towards the mid-height of the section.

(a) good bond   (b) poor bond
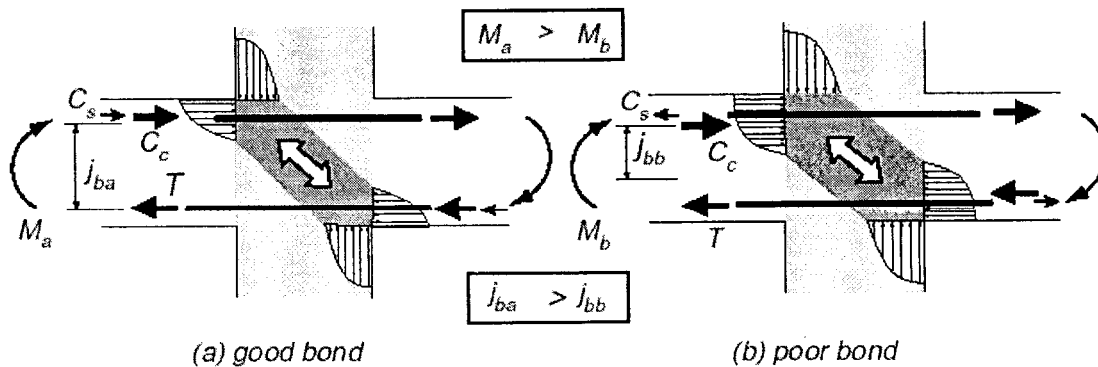
Figure 4-18 Effect of poor bond on moment resistance of beam-to-column joint

66

This may be the reason why some design methods that set limit value for the induced joint shear and also for the diameter ratio of the reinforcing bar passing through the joint panel have been successful. The mentioned recommendations cause the bond stress to be kept lower, resulting in sufficient anchorage capacity. Although the mechanism described above are in contradiction, but the recommendations stemming from each mechanism are almost similar.

Both models accept that the axial force in the column and the transverse reinforcement are effective for decreasing the joint shear deformation, in the first model as was explained; they help the strut and truss mechanisms to be more effective in transferring the shear stresses through the joint panel, and also the effects of confinement provided by the lateral reinforcement and the confinement due to the presence of axial force above the joint panel are significant in decreasing the shear deformation. In the second model they resist the relative movements at the boundary of the segments and the rotation of the segments (Figure 4-14(a)). The increase in horizontal reinforcement in the joint is also beneficial in terms of increasing the moment capacity of the joint relative to the induced moments at beams ends, which yield in flexure.

Another issue is the recommendation about the diameter of the bars passing through the joint. Both models agree that the higher diameter of the bar is detrimental to the shear capacity of the joint. The increase in the diameter of the bar causes the bond between the bar and the concrete become poorer. In the struts and ties model, the debonding of the reinforcement in the joint is the end of the truss mechanism to carry shear stresses, and the start to rely on the compression strut, which eventually leads to the failure of the joint in shear. It also increases the interstory drift of the structure, resulting in P-Delta effect to become more significant. In the shiohara's model the debonding of the bar is the most significant reason for the change of stress in compressive reinforcement from compression to tension, causing the location of stress resultant of compression shift towards the mid-height of the section.

Chapter 5

FIBER ELEMENT

5.1 General

The numerical analysis of the structures subjected to seismic force is a complex task. The need for rather accurate analytical models, which guarantee a sufficient safety level, is apparent. In recent years, analytical models and numerical techniques with large precision have been developed. These range from macro-scale of simplified elements to micro-scale of analysis of finite element methods. While refined finite element method is a wiser choice for detail study of small parts of the structure, it becomes computationally prohibitive when studying the nonlinear behavior of the whole structure subjected to dynamic loading of an earthquake. Frame models (macro-scale model) are the only economical solution for studying the' non-linear behavior of the whole structure with several hundred members but are not able to capture local behavior of the selected parts of the structure like beam-column joint.

The fiber model corresponds to a large level of discretization, where each structural member is modeled by single element, but the stress-strain history of a large number of points, for both steel and concrete, is evaluated during the analysis at several cross-sections inside the element (Spacone et al., 1996). The fiber model allows for accurate modeling of the cross –section geometry. The area of the cross section, the material, and spacing of cross-sections can be varied along the member to represent the nonlinear behavior of the critical regions more accurately. In fiber model, the beam-column element is divided into a discrete number of cross sections (segments). These are located at the control points of the numerical integration scheme that are used in the element formulation. The model assumes constant fiber properties over each segment length, based on the properties of the monitored slice at the center of each segment. The application of the above concept in fiber element in the program DRAIN-2DX is shown in Figure 5-1.

Regardless of the high memory demand and increasing computational cost, the accuracy of the model increases with the number of segments, and the number of fibers in each cross section. The non-linear behavior of the element is monitored at these control sections, which are in turn discretized into longitudinal fibers of plane concrete and

reinforcing steel. The non-linear behavior of the section is then captured from the integration of the non-linear stress-strain relationship of the fibers. This feature permits the modeling of any type of structural element with irregular cross-sections and different sectional areas as was seen in Chapter-3 for the case of the circular column, or with different material behavior models, as long as the assumption of plane sections remaining plane and normal to the longitudinal axis is not objected.

In the case of reinforced concrete this fact also implies a perfect bond between concrete and the reinforcing steel, that is the bond slip is assumed to be zero and full composite action is assumed for composite steel-concrete members. As was indicated, the non-linear behavior of the reinforced concrete element derives from the stress-strain relationship models of concrete and steel. Thus, the validity of the analytical results depends highly on the accuracy of the constituent material models.

5.2 Application of Fiber Model in Current Study

For the current study, which deals with the shear behavior of the exterior beam-column joints, the micro-scale modeling of the beam-column connection in terms of fiber model using DRAIN-2DX (Fiber Element) is adopted in which the region is considered as discretized, shared section of both beam and column, and the behavior is studied in detail.
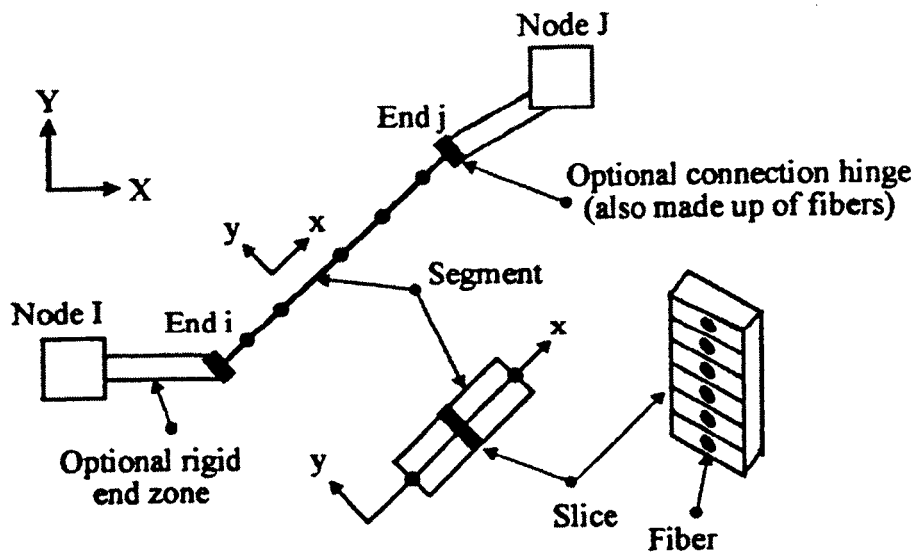
Figure 5-1 Element model (DRAIN-2DX)

69

Since there is no consideration of bond-slip in this study, there are only two rather simple material models required; one for reinforcing steel and one for plane concrete with consideration of confinement effect of the transverse reinforcement.

The element formulation requirement simplifies the material model to uni-axial behavior model, which has been thoroughly studied with several well-established models to date. Three-dimensional effects on material behavior can be included into the uni-axial model by appropriate modification of the parameters that define the monotonic envelope. This is important in the case of reinforced concrete which confining effect of transverse reinforcement and strain hardening of the concrete have important roles on the stress-strain behavior and so on the response of the structure.

Investigations have concluded that a crude concrete model suffices to accurately predict experimental results. This might be true in case of monotonic loading and cyclic loading that is restricted to small inelastic excursions. It is not true, however, in the case of severe cyclic loading. The strength deterioration of R/C members under large deformation reversals depends largely on the capacity of confined concrete to sustain stresses in the strain range beyond maximum strength. This requires the use of a refine concrete model. Even though many accurate and rather complete models have been published to date, the Kent-Park (1971) model for concrete in compression and Vebo-Gali (1977) model for concrete in tension are selected for the current study because they can be adopted in the fiber model program (DRAIN-2DX) and have the power to account for the confinement effect of transverse reinforcement by modifying the strain softening slope in the monotonic envelope, and also the power to include the tensile behavior of the concrete. The model offers a good compromise between simplicity and accuracy and remains as an excellent choice for the hysteretic behavior of concrete.

In fiber model formulation, the stress-strain models should be explicit function of strain. The fiber strains are determined from section deformation. The stress determination only involves a function evaluation based on the current fiber stress and strain and the given strain increment. This reduces the computational effort considerably relative to material models that are not explicit functions of strain, such as well-known Ramberg-Osgood model for steel.

70

The formulation of the beam element is based on the assumption of linear geometry. Plane sections remain plane and normal to the longitudinal axis during the element deformation history. This hypothesis is acceptable for small deformations of elements composed of homogeneous materials, but it does not properly account for phenomena, which are characteristic of reinforced concrete elements, such as cracking and debonding of the bars. The cracking and tension-stiffening phenomenon can be included in the model by appropriate modification of the stress-strain relationship of the constituent material, although these effects can be neglected in studies related to hysteretic behavior under large inelastic reversals.

5.3 Reference Axis

An important issue in nonlinear analysis of structure is the reference axis, which is not necessarily the centroidal axis' of the section and is moving along the depth of the section (Hoseini-Tabatabaii M., 2000). From the assumption that plane sections remain plane and normal to the longitudinal axis of the element, all stress and strains are parallel to this axis. This is based on the hypothesis that the axis passing from the geometric centroids of all defined sections coincides with the reference axis of the element. Otherwise the element should be divided into sub-elements with axes that connect the centroids of the selected sections.

As was mentioned above, for cases of nonlinear behavior of the materials, the assumption of the centriodal axis to be the reference axis is not accurate. The modulus of elasticity is also not constant throughout the whole section. A numerical solution is suggested for value of Y (Distance of the reference axis from top of the cross section) as:

$$Y = \frac{\sum y_{ic} E_{ic} A_{ic} + \sum y_{iS} E_{iS} A_{iS}}{\sum E_{ic} A_{ic} + \sum E_{iS} A_{iS}} \qquad (5\text{-}1)$$

Where: A_i = Area of fiber section i

E_i = Modulus of elasticity of the fiber section i

Y_i = Distance of the centroid of the fiber section i from the top of the cross section

DRAIN-2DX supports the mentioned feature and each fiber is identified by its cross-section area, distance from a reference axis, and its modulus of elasticity, which is determined from specifications of stress-strain relationship of the fiber material.

71

The examples below show the fact described above that each material fiber is considered separately in terms of the cross section area, centroid axis, and modulus of elasticity in the formulation of the element and equation (5-1) is automatically satisfied. As will be discussed in this chapter, the small number of fibers has resulted in inaccurate values for moment of inertia of each fiber with reference to longitudinal reference axis of the element.

5.3.1 Example

In the following examples shown in Figure 5-2, and Figure 5-3, the cross-sections are comprised of 4 fibers with properties depicted in the corresponding figure. It is apparent from the output data that each fiber is treated separately with the reference axis as the centroidal axis of the fiber and the material properties, which are defined by the stress-strain relationships of each material comprising the fiber.

Section #1
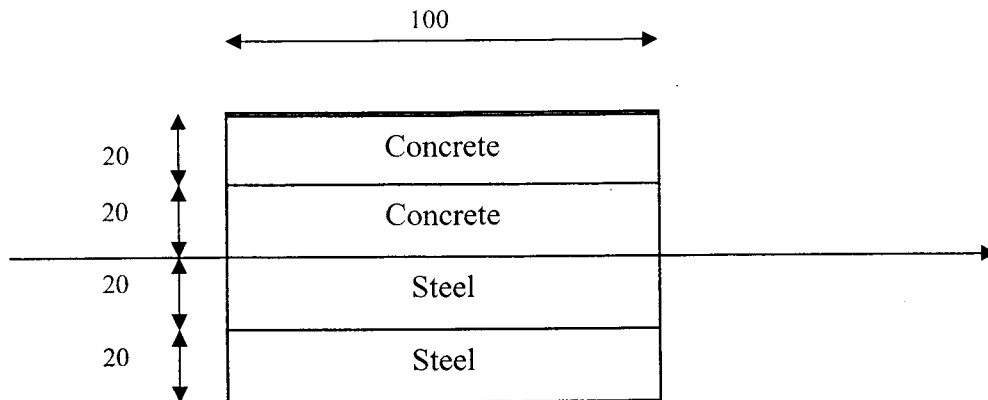
Figure 5-2 Section #1

Fiber Section   No. 1

No. of Fibers	Fiber Coord	Fiber Area	Matl Type
4			
	1.000E+01	2.000E+03	C01
	3.000E+01	2.000E+03	C01
	-1.000E+01	2.000E+03	S01
	-3.000E+01	2.000E+03	S01

Concrete Section   Area = 4.000E+03, ybar = 2.000E+01   I = 4.000E+05

Steel Section   Area = 4.000E+03,   ybar = -2.000E+01   I = 4.000E+05

Concrete Material Types

Type No.	Comprn Points	Tensn Points	Unloading Factor	Overshoot Tolerance	Stress Value	Strain Value	Stress Type	Tangent Modulus
1	3	2	0.000E+00	1.000E-03				
					1.7900E-02	6.3000E-04	comprn	2.8413E+01
					3.5800E-02	2.0000E-03	comprn	1.3066E+01
					7.2000E-03	3.5000E-02	comprn	-8.6667E-01
					3.3000E-03	1.5700E-04	tensn	2.1019E+01
					1.0000E-04	1.4530E-03	tensn	-2.4691E+00

Steel Material Types

Type No.	No. of Points	Overshoot Tolerance	Stress Value	Strain Value	Tangent Modulus
1	2	1.000E-04			
			4.7500E-01	2.5000E-03	1.9000E+02
			6.2000E-01	1.0000E-01	1.4872E+00

Section #2

Figure 5-3 Section #2

Fiber Section No. 2

No. of Fibers	Fiber Coord	Fiber Area	Matl Type
4			
	1.000E+01	2.000E+03	C01
	3.000E+01	2.000E+03	C01
	-1.000E+01	3.000E+03	C01
	-3.000E+01	4.000E+03	C01

Concrete Section   Area = 1.100E+04,   ybar = -6.364E+00   I = 5.455E+06

Concrete Material Types

Type No.	Comprn Points	Tensn Points	Unloading Factor	Overshoot Tolerance	Stress Value	Strain Value	Stress Type	Tangent Modulus
1	3	2	0.000E+00	1.000E-03				
					1.7900E-02	6.3000E-04	comprn	2.8413E+01
					3.5800E-02	2.0000E-03	comprn	1.3066E+01
					7.2000E-03	3.5000E-02	comprn	-8.6667E-01
					3.3000E-03	1.5700E-04	tensn	2.1019E+01
					1.0000E-04	1.4530E-03	tensn	-2.4691E+00

Steel Material Types

Type No.	No. of Points	Overshoot Tolerance	Stress Value	Strain Value	Tangent Modulus
1	2	1.000E-04			
			4.7500E-01	2.5000E-03	1.9000E+02
			6.2000E-01	1.0000E-01	1.4872E+00

5.4   Effect of the Number of Fibers in the Cross-Section

As written in the DRAIN-2DX guidelines, there are no limits specified for the number of fibers in the cross section or the number of segments in an element. There are however, limits on the maximum memory and disk storage than can be occupied by the data for anyone element. There is also a minimum of 2 fibers for a section. If these limits are exceeded, an error message will be printed in the .ECH file, and the program will not execute. The limits are set for a maximum of roughly 200 total fibers in any element.

74

These limits can be increased, if necessary, by changing the value of blank COMMON length (NTSTP) in PARAMETER (NTSTP=50000) statement in MAIN.FOR subroutine in the main directory. It may be appropriate to specify a large number of fibers for a small analysis model consisting of one or two elements. However, if several such elements are specified as part of a large model, the execution time may be long.

Although the large number of fibers increases the accuracy and also the execution time, there must be a compromise between accuracy and time of execution. For this reason the results of analysis of a rectangular section moment of inertia (I) with different number of fibers are compared to the calculated value obtained by the equation:

$I = b*h^3/12$

(For a rectangular section with b = h = 400 mm, $I = 400^4/12 = 2.1333$ E9 mm^4).

Following are the result of the analysis of the same section with different number of fibers in the cross section (slice).

Note: the number of fibers and the value of the moment of inertia (I) are underlined.

Fiber Section Type No. 1

No. of Fibers	Shear GA	Shear Modulus	Fiber Coord	Fiber Area	Matl Type
2					
			1.000E+02	8.000E+04	C01
			-1.000E+02	8.000E+04	C01

Concrete Section   Area = 1.600E+05, ybar = 0.000E+00 I = 1.600E+09

Fiber Section Type No. 2

No. of Fibers	Shear GA	Shear Modulus	Fiber Coord	Fiber Area	Matl Type
4					
			5.000E+01	4.000E+04	C01
			1.500E+02	4.000E+04	C01
			-5.000E+01	4.000E+04	C01
			-1.500E+02	4.000E+04	C01

Concrete Section   Area = 1.600E+05, ybar = 0.000E+00 I = 2.000E+09

Fiber Section Type No. 3

No. of Fibers	Shear GA	Shear Modulus	Fiber Coord	Fiber Area	Matl Type
10					
			2.000E+01	1.600E+04	C01
			6.000E+01	1.600E+04	C01
			1.000E+02	1.600E+04	C01
			1.400E+02	1.600E+04	C01
			1.800E+02	1.600E+04	C01
			-2.000E+01	1.600E+04	C01
			-6.000E+01	1.600E+04	C01
			-1.000E+02	1.600E+04	C01
			-1.400E+02	1.600E+04	C01
			-1.800E+02	1.600E+04	C01

Concrete Section   Area = 1.600E+05, ybar = 0.000E+00 $I = 2.112E+09$

*Note: in the following, because of the large size of the output data; the Fiber Coord, Fiber Area and material Type sections are omitted, and only the results are included.

Fiber Section Type No. 4

No. of Fibers	Shear GA	Shear Modulus	Fiber Coord	Fiber Area	Matl Type
20					

Concrete Section   Area = 1.600E+05, ybar = 0.000E+00 $I = 2.128E+09$

Fiber Section Type No. 5

No. of Fibers	Shear GA	Shear Modulus	Fiber Coord	Fiber Area	Matl Type
40					

Concrete Section   Area = 1.600E+05, ybar = 0.000E+00 $I = 2.132E+09$

76

Fiber Section Type No. 6

No. of	Shear	Shear	Fiber	Fiber	Matl
Fibers	GA	Modulus	Coord	Area	Type
80					

Concrete Section   Area = 1.600E+05, ybar = 0.000E+00 I = 2.133E+09

The above data for the moment of inertia of the cross section obtained from the output data of the DRAIN-2DX program are plotted versus the theoretical value for the moment of inertia of the cross section in Figure 5-4.
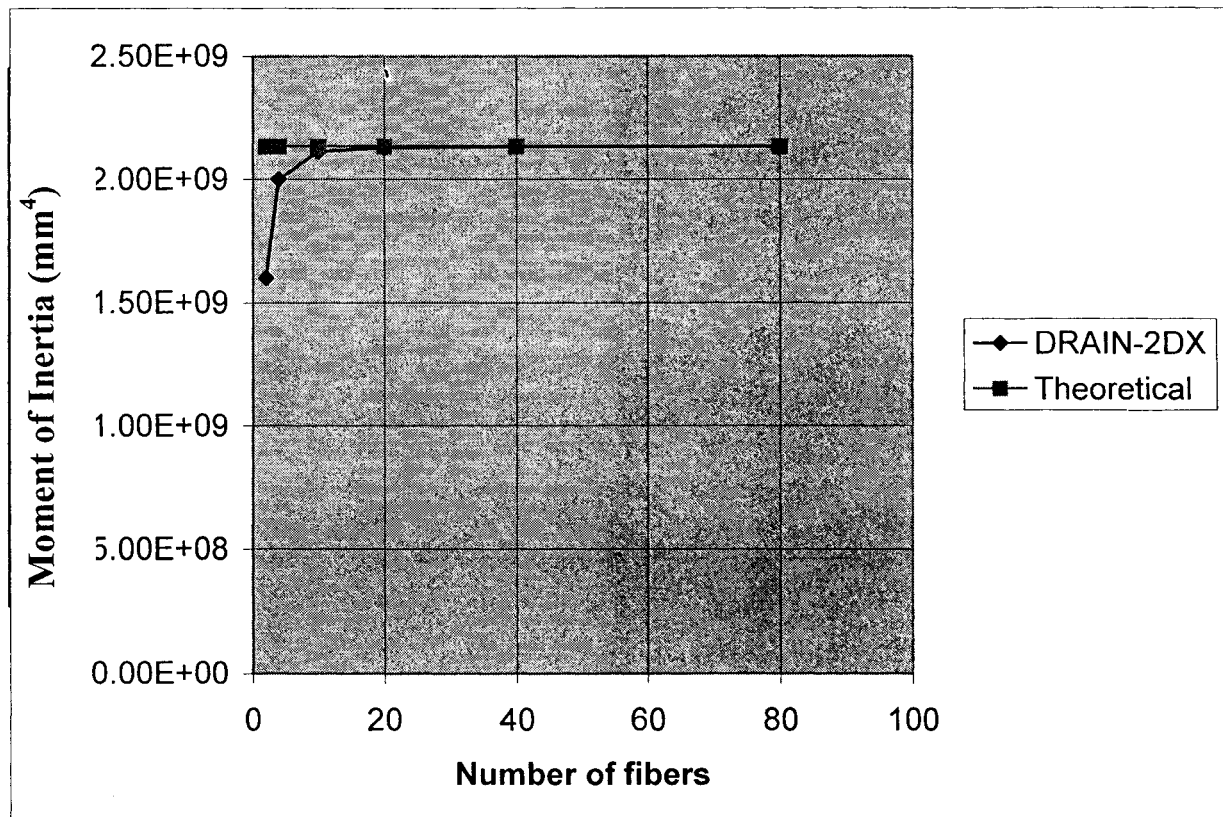
Figure 5-4 Comparison between the moments of inertia
for section with different numbers of fiber

It can be observed from Figure 5-4 that for the number of fibers of more that 40 there is a negligible difference between the analytical value obtained from DRAIN-2DX, and the theoretical value of the moment of inertia. For smaller number fibers, the

difference in the results may lead to inaccuracy in the entire analysis of the structure. For example the analytical value of the moment of inertia of the section using only 2 fibers for the section is 1.6E9, which has a difference ratio of around 40% with the real value (2.133E9). Thus, the result of the entire analysis based on selection of two fibers for the cross-section, is not accurate. Throughout this research, wherever the section in under bending moments and the value of the moment of inertia of the cross-section has an important role, the number of fibers is selected to be 40.

Chapter 6
A PROPOSED MODEL FOR EXTERNAL JOINT SHEAR MECHANISM

6.1 General

A model is proposed to simulate the behavior of the external beam-column joints in shear. The model is based on the fact that the shear resistance mechanism in the joint core without transverse reinforcement relies on the diagonal concrete strut, and the shear resistance capacity of the joint as was discussed in section 4.3.1(the strut and ties model), is determined by the compression strength of the concrete strut within the joint. The other fact is that the stress and strain in all the beam and column sections are changing non-linearly during the application of the loading, which as was discussed especially in section 4-4 (Shiohara model), causes the stress resultant to move, and the depth of the compression zone on the faces of the joint to change.

The proposed model is based on the fiber concept and is implemented in the well-known nonlinear program DRAIN-2DX. In this model, the external beam-column joint sub-assemblage shown in Figure 6-1 is regarded as two separate elements as is shown in Figure 6-2. The beam and the column have been discretized into fibers in order to capture the stresses and strains within any cross-section within the length of the elements. The beam and column are formulated in the program as fiber elements with dimensions and material properties defined by the fibers' properties and parameters in each element by user. That means each point on the fibers of the element section is regarded as a part of the element and follows the formulations defining the relationships between stresses and strains within the element.
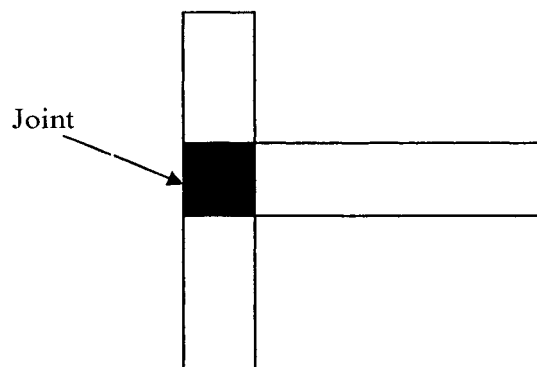
Figure 6-1 The external beam column joint
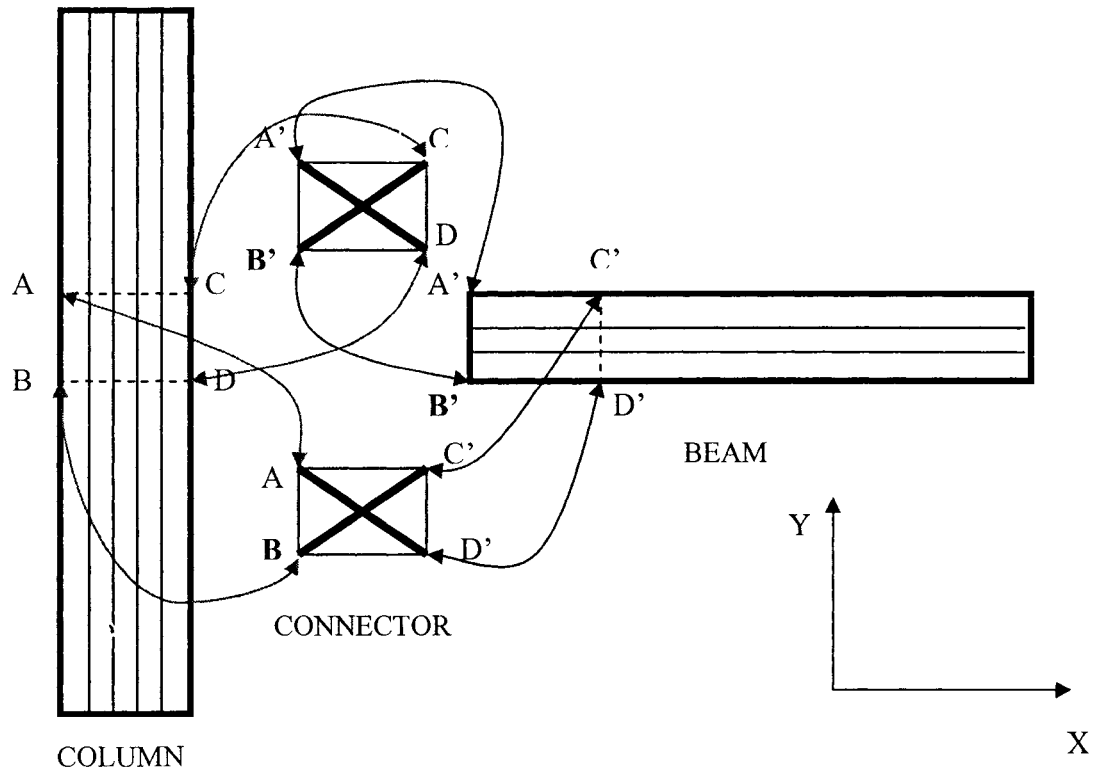
Figure 6-2 Configuration of the proposed model

In order to simulate the connection of the beam and the column within the joint zone the assumptions are:

As shown in Figure 6-2, the vertical plane for the column, and vertical plane for the beam, which define the midsections of the beam and column, are representatives of the behavior (stresses and strains) throughout the beam and column. In other word it is assumed that the two-dimensional model is a representative of the three-dimensional model. The rectangle A'B'C'D' at the end of the beam in the region, which the beam frames into the column, and the same size rectangle ABCD in the middle of the column, which the beam is connected to the column, are the parts that are regarded as the beam-column joint. For simulating the real behavior of the joint, it is assumed that the joint is comprised of two identical connectors A'B'CD, and ABC'D' which are connected to the corresponding nodes on the beam and column, and enforce the deformation of the beam-end and deformation of the mid-column to be the same within the joint zone.

80

6.2 Mechanism of Shear Resistance in the Proposed Model

In the beam-column sub-assemblage shown in Figure 6-3(a), the downward load is applied on the beam tip. If the beam is considered to be separate from the column, this load causes the beam to slide down. In Figure 6-3(b), the connector is attached from the left lateral side to column's left lateral side on nodes A, and B. This connector is attached from the right lateral side to beam on nodes C, and D. As it is evident, the end of the beam is free to move (Figure 6-3(b)). Simultaneously an identical connector, which is shown in Figure 6-3(c), prevents the movement of the beam's end. In Figure 6-3(c) the connector is attached from the left lateral side to beam's end on nodes A, and B. This connector is attached from the right lateral side to column's right lateral side on nodes C, and D. The load on the beam tip causes the connector to deform in order to maintain the integrity of the beam and column within the joint panel. The two diagonal struts in each connector are the only mechanism of preventing the excessive shear deformation in the connectors. As it is shown in Figure 6-3(a), in the case of downward load on the beam tip, the diagonal struts, one in Figure 6-3(b), and one in Figure 6-3(c), in the direction of AD will be in compression and the other two diagonal struts in the direction of BC will be in tension (as one of each pairs of struts is shown in the Figure 6-3(a) by black line for compression, and a gray line for tension)

(a)

(b)

(c)

Note: The mechanism in (a) is decomposed into two simultaneous mechanism in (b) and (c)
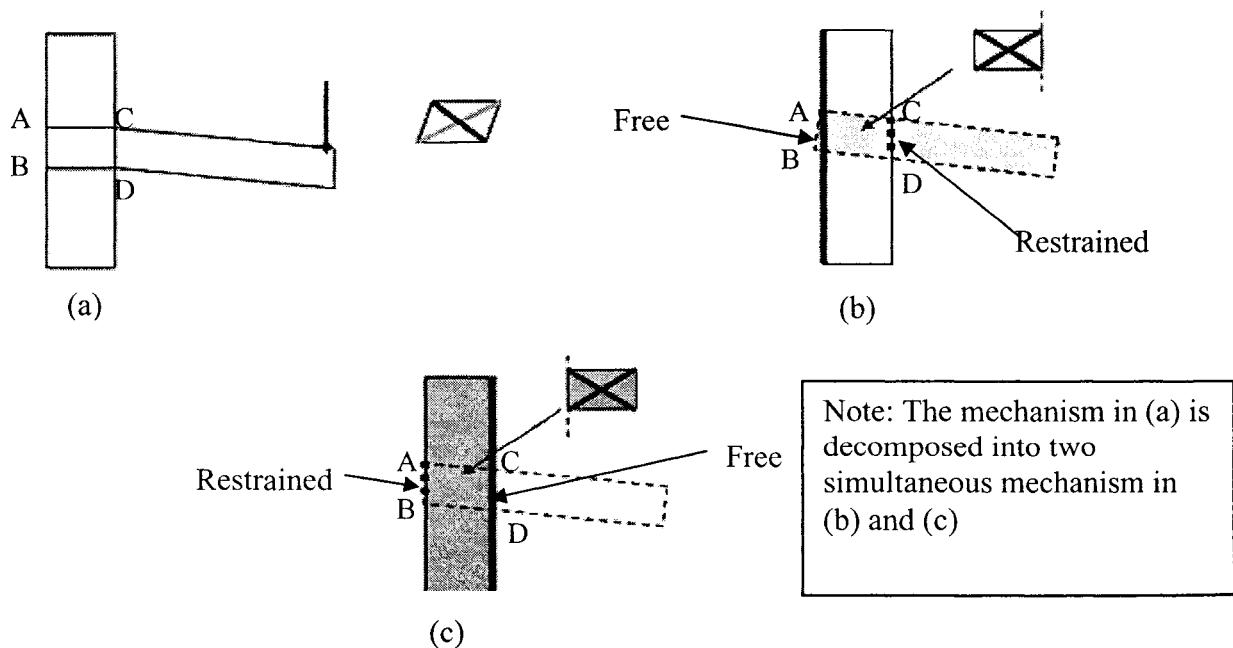
Figure 6-3 The mechanism of shear resistance in the case of downward load on the beam tip

The same description is applicable for describing the mechanism when an upward load is applied on the beam's tip as shown in Figure 6-4, except that there are changes in the direction relative to the case of the downward load on the beam's tip.
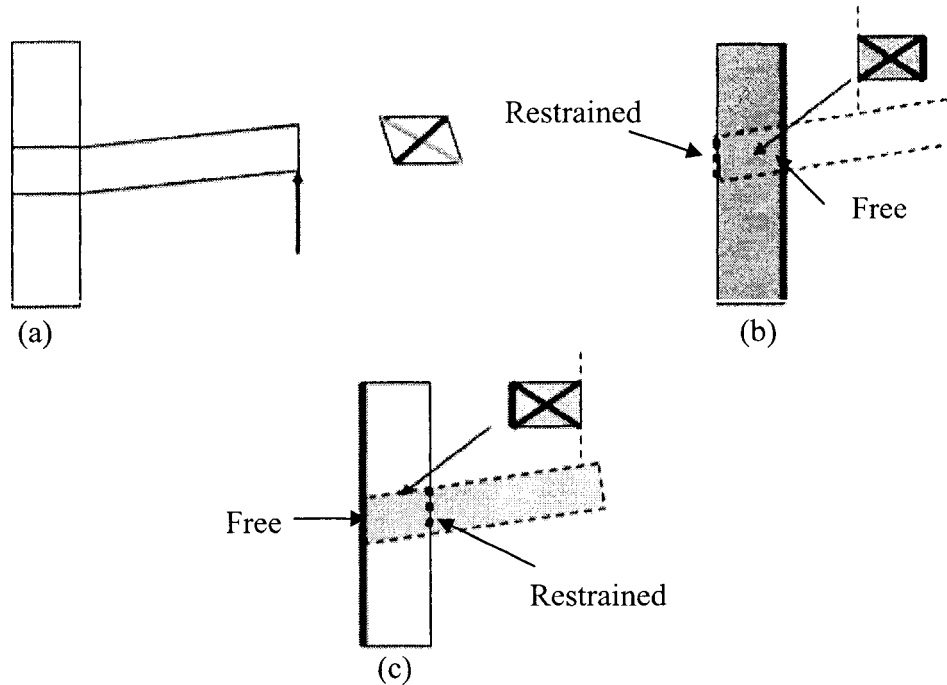
Figure 6-4 The mechanism of shear resistance in the case of upward load on the beam tip

The two connectors, which have the role of shear resistance mechanism in the joint, are each comprised of four very stiff beam elements without any deformations (A'B', A'C, CD, B'D in Figure 6-2). These beams are pinned to each other's end, making a rectangle with depth and with the same as those of the joint region. For each connector, two diagonal concrete struts shown as the dashed lines, are connected to those pins, and resist the shear deformation of the connectors as shown in Figure 6-5(a). Because the concrete struts can only take axial compression, as will be discussed later in section 6.4, the properties of concrete in the struts are modified in tension

6-3 The Connectors

The two identical connectors have important roles in this model. As was discussed and depicted in Figure (6-2), each connector is connected from one lateral side to two nodes with same (X) coordinates on the joint region of the beam's end, and from the other

lateral side to two nodes with same (X) coordinates on the joint region in the column's middle part.

Stiff
beams

(a) The connector after the deformation   (b) Shear deformation of the joint
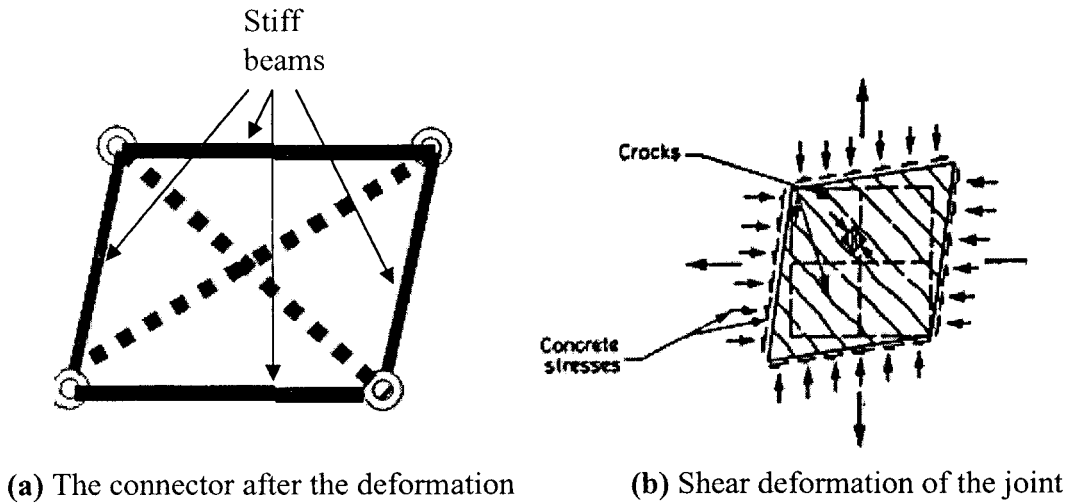
Figure 6-5 Shear deformation in the beam-column joint

Each connector is comprised of 4 identical very stiff beams (without any deflection and deformation) that are pinned to each other's end. In DRAIN-2DX this is done by using four Element #2 (Plastic hinge beam-column element) with very high arbitrary values of 'Young modulus' and 'Yield moment', knowing that the element does not take axial deformation. The values of 'Young modulus' and 'Yield moment' of these four beams are considered to be 1.10^{12} N/mm^2, and 1.10^{12} N.mm, respectively. The four beam elements ends are then connected to each other using four Element #4 (Simple connection element) with very high arbitrary values of 'Initial stiffness' and 'Yield force' in the translational direction, making them free to rotate in the XY plane. The values of 'Initial stiffness' and 'Yield force' were considered to be 5.10^{11} N/mm, and 1.10^{12} N, respectively. The system can simulate the shear deformation as shown in Figure 6-5(b).

In order to prevent the excessive deformation of each identical connector, two diagonal concrete struts with the same property as the concrete of the beam and column are connected to the pins. Again four connection elements similar to those mentioned above are used to connect these struts to the pins.

Some models have used springs for simulating the behavior of the struts, but the author believes that using concrete strut is the best choice for modeling the nonlinear behavior of the diagonal concrete struts.

83

6-4 Determination of the Properties of the Diagonal Struts

As was discussed before, the joint resistance capacity is determined by the compression strength of the diagonal struts. For determination of the cross-section of the diagonal struts the procedure is as follows.

The peak strength capacity of the beam-column assemblage must be determined. This is done by a quasi-static force-control cyclic loading until the structure is unstable. The peak force can also be determined by consideration of the over-strength of the reinforcement and the section's yield moment. In the current study, because there was no specification for over-strength factor, or the strain hardening ratio of the steel, the peak loads are taken from the result of each experiment, otherwise the yield force of the section, which can be easily determined, multiplied by an over-strength factor (1.05-1.10) is a very good estimate for the ultimate load.

The peak load is applied to the beams end while axial load is applied on the column. For all the four diagonal connectors an arbitrary cross-section is assumed (For example 6000 mm^2). The analysis done by the program determines the value of the diagonal struts' axial loads, which confirms that two diagonal struts are in compression. This axial load is independent of the properties of the material, but is dependant on the elements' sizes and loads (including the axial load on the column). The cross section of the all four identical diagonal struts is calculated by dividing the largest value for strut's axial compression force between the two compression struts, by the value of the compressive strength of the concrete, f'_c.

The other two struts are in tension. The properties of diagonal struts in tension should be modified in the concrete model in the program for strut's concrete properties, other wise the concrete will in tension and the analysis will be terminated. Generally for concrete in tension, the stress-strain curve corresponds to the relations between values of tensile stress and rather small values of strains. The modifications for the diagonal strut, relates very large values of strains for the same values of tensile stresses. For better description of the methodology, the procedures for the example Test#6 in Chapter-7, which will be discussed later, are described as follows.

An external beam-column joint with the concrete having maximum compression strength equal to 40.1 N/mm^2, is subjected to an axial load on the column, and a cyclic

loading on the beam tip (Figure 6-6). Other specification of the test is described in sections 7-2, and 7-3. The beam is shown in Figure 6-6 as the element between nodes 6, and 7 (Node 6 coordinates should correspond to the coordinates of the center of the joint panel). The column length is divided into two parts. The lower part is between node 1 (foundation) to node 3, which is assumed to be in the center of the joint panel. The upper part is between node 4, which has identical coordinates as nodes 3, and 5 (the top of column, where the axial load is applied). Nodes 3 and 4 are slaved to each other from all degrees of freedom. This makes the column a single element extended between nodes 1, and 5.

For connecting the beam to the column, four nodes with coordinates of the corners of the joint panel (Nodes 8, 9, 10, and11) are slaved to node 3. Similarly, four nodes with coordinates of the joint panel corners (nodes 12, 13, 14, and 15) are slaved to node 6 on the beam's end. The two mentioned connectors attach lines 12-15 to 9-10, and 8-11 to 13-14.
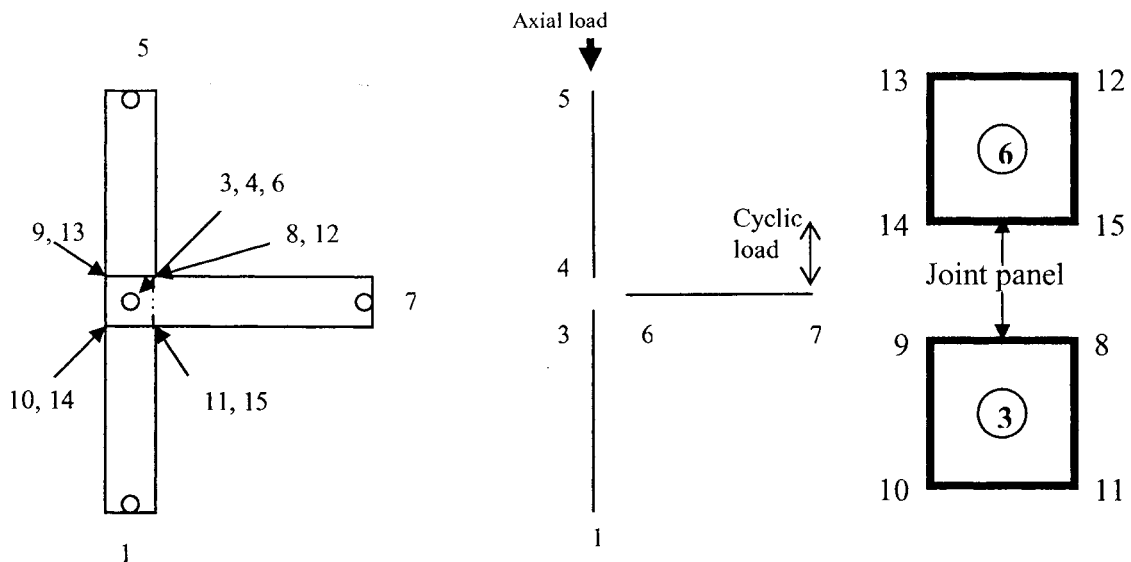
Figure 6-6 Configuration of the exterior beam column joint in the proposed model

The values for stress-strain relationship for concrete for specimen Test#6 are calculated based on the Kent-Park (1971) model for compression, and Vebo-Gali (1977) model for tension. These values are shown in Table 6.1 and Figure 6-7.

Table 6-1 Concrete material for beam & column for Test #6

	STRESS (N/mm^2)	STRAIN
1st point for compression	20.0	.00067
2nd point for compression	40.1	.002
3rd point for compression	8.02	.017
1st point for tension	3.534	.00016
2nd point for tension	0.1	.00145
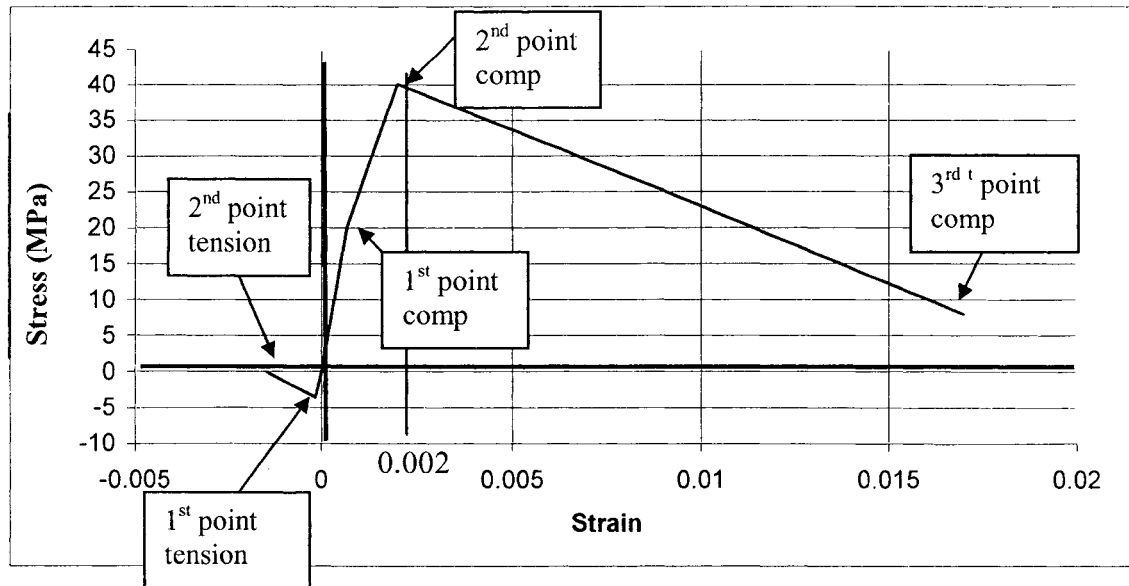
Figure 6-7 Stress-strain relationships for concrete in beam & column

The modification for the diagonal strut is shown in Table 6-2. After the modification the strains are assumed to take very large values for the same values for tensile stresses, which is illustrated in Figures 6-8, and 6-9 (The tensile stresses and strains are shown by negative values in those figures). Modification of the properties in tension should prevent the concrete to fail in tension. According to the model for tension, the small values of strain for the tensile stresses (Table 6-1), causes the concrete to fail in larger tensile strains during the application of the cyclic loads. The modification relates the same stresses to the strain many times larger than the actual tensile strain, and is shown in Table 6-2.

86

Table 6-2 Concrete material for diagonal struts for Test #6

	STRESS (N/mm^2)	STRAIN
1st point for compression	40.1	.002
2nd point for compression	8.02	.017
1st point for tension	3.534	1. ** (modified for tension)
2nd point for tension	0.1	2. ** (modified for tension)
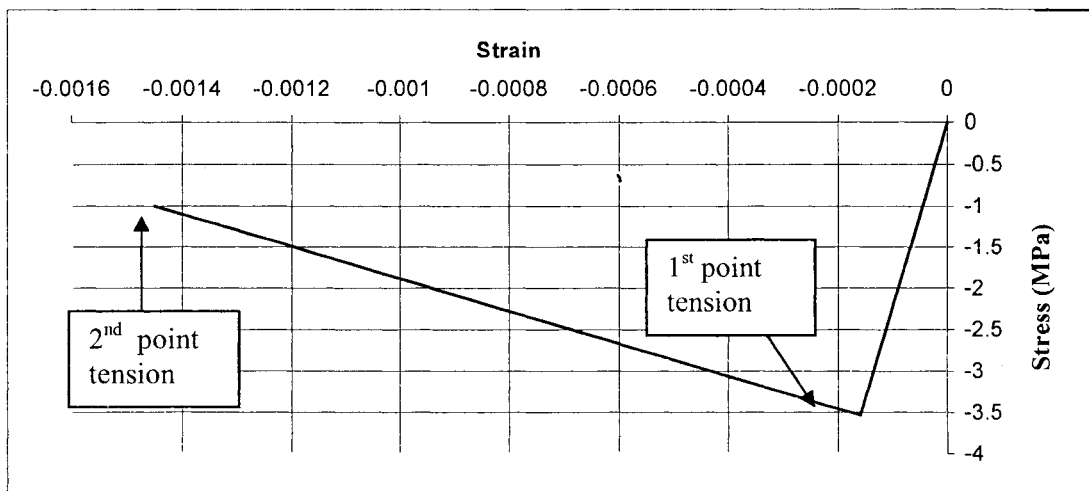
Figure 6-8 Stress-strain relationships for concrete in tension for diagonal struts before modification
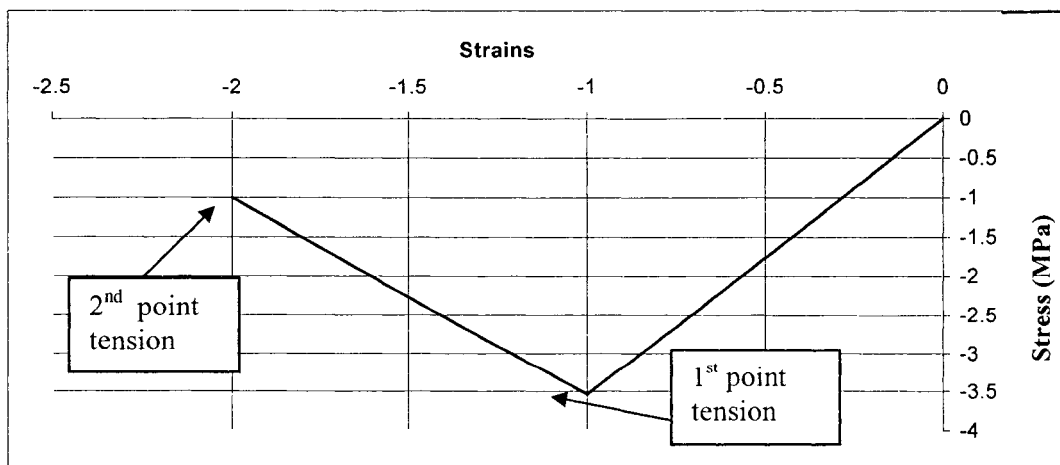
Figure 6-9 Stress-strain relationships for concrete in tension for diagonal struts after modification

The properties of the concrete in the strut should be the same as the properties of the concrete in the beam or the column in the Table 6-1. The properties in compression are the same and specified only by two points (determining the point for cracking of the concrete causes many complications in the execution of the program), but the properties in tension as was discussed should be modified by having two rather large strain 1, and 2; corresponding to the tensile stresses 3.534, and 0.1 kN/mm^2, respectively. The above modification causes the struts in tension to take small values of tensile strength during large tensile strain demand.

During the analysis of the sub-assemblage as will be discussed in Chapter-7, it is seen that the model is able to predict the non-linear response of the beam-column very well, except after the peak load, where there is a sudden drop in the strength of the beam-column assemblage. This is not comparable with the experimental results. This phenomenon is illustrated in Figure 6-10. The lateral load drastically drops after the maximum strength of 275 kN. This corresponds to the strain of 1.77% in which the strength drops to 49 kN. This is not the simulation of the experimental behavior of the beam-column joint under cyclic loading, which is shown in Figure 6-11. According to the experimental data as will be discussed in section 7.5.2, the peak lateral load sustained by the specimen was 267 kN at strain of 1.77%.
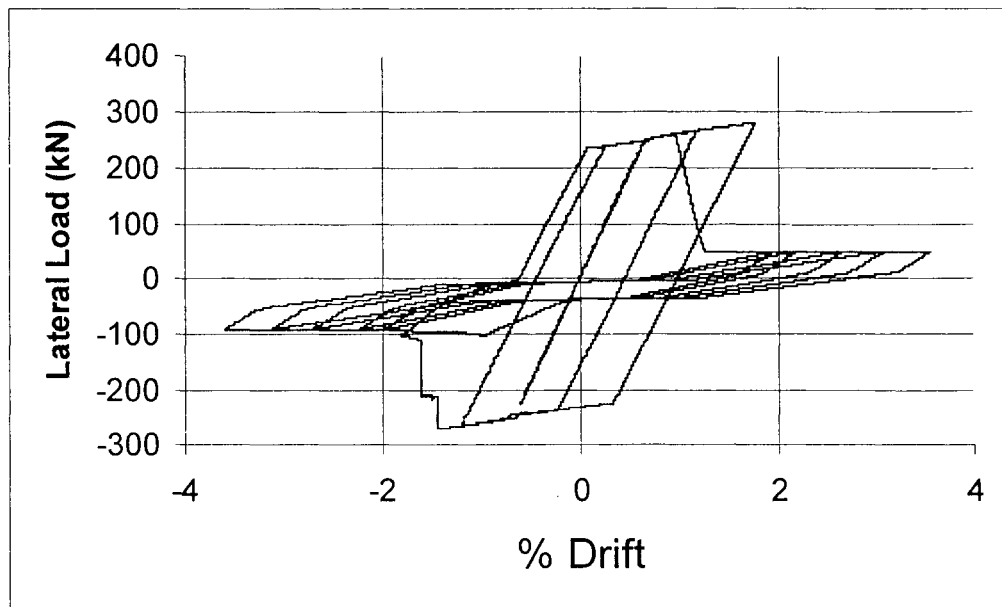
Figure 6-10 Predicted load-drift curves by the proposed model for the case of same properties for beam, column and struts in specimen Test #6

88
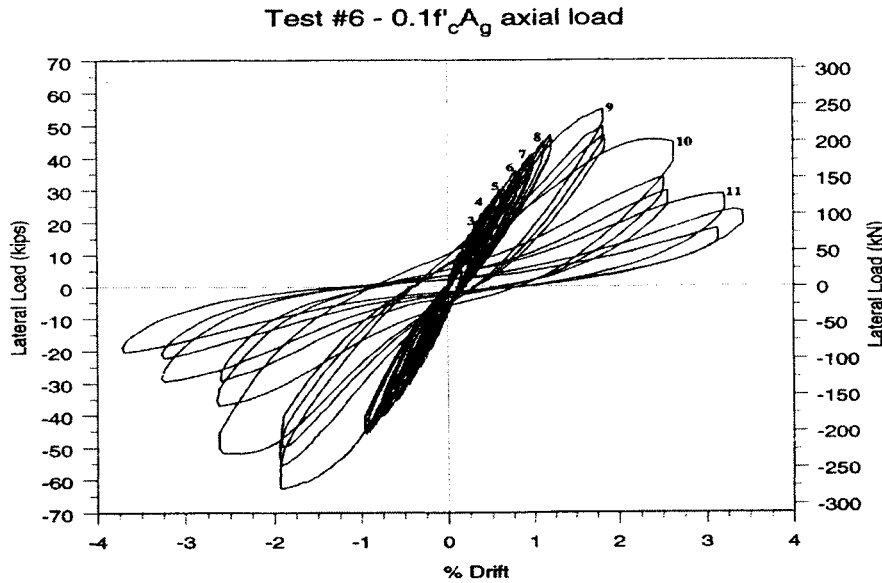
Figure 6-11 Experimental behavior of specimen Test #6 under cyclic loading

Further analyses were carried out to enhance the results of the analytical model. After several analyses and determination of the effect of each parameter on the results and the shape of the lateral load-drift curve, it was concluded that by using two different properties for the stress-strain relationship of the concrete of the diagonal struts, significant improvements in the results were observed. The diagonal strut's concrete is then divided into two concrete properties with different strain softening ratio for the descending branch in compression, namely Type-1, and Type-2. The concrete properties before the peak strength, f'c are identical, but after the peak compressive strength point, the stress-strain relationship curve has two different descending slopes. This may be due to the high confinement pressure on the diagonal struts in the joint panel. For better understanding the behavior of the concrete strut, the stress-strain relationships for the concrete in the beam, column, and the strut for the specimen Test#6, are shown in the Figures 6-12 through 6-14. As is shown in Figure 6-12, the concrete strength in compression increases with increase in strain up to maximum stress of 40.1 MPa corresponding to the strain of 0.002. After the maximum strength is reached, then the concrete strength decreases with increase of strain, up to the maximum strain of the 0.017, where the compressive strength falls to 8.02 MPa.

After this point the concrete is assumed to have the same strength even with increase in the strain (Part CD in the Kent & Park model, shown in Figure 2-8). As was discussed, the stress-strain relationship for the struts in compression up to the point of maximum compression strength, is the same as the concrete in the column or beam, but for the concrete in the strut after the maximum strength, which occurs the strain of 0.002, the rate of strains-softening should be modified to give comparable results to the experimental evidences.
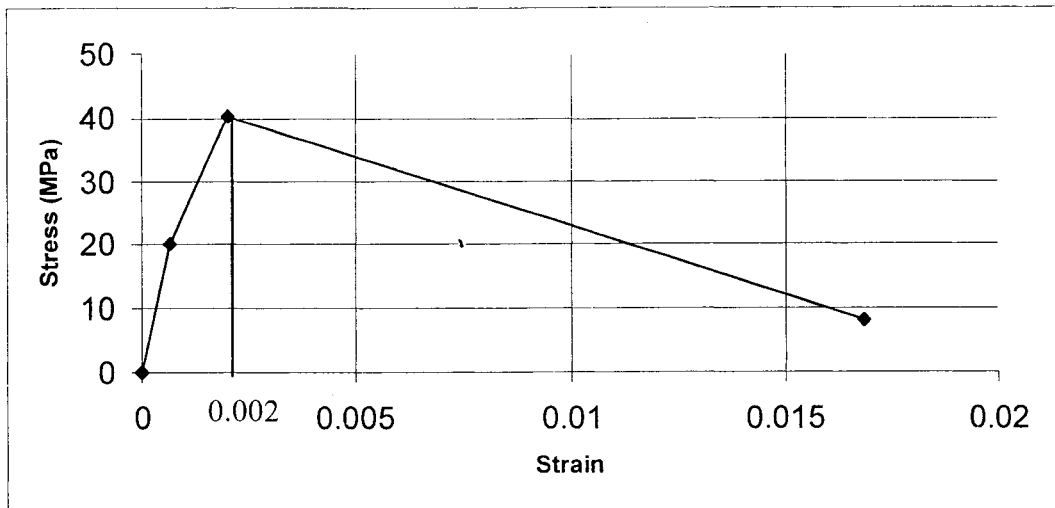
Figure 6-12 Stress-strain curve for beam, and column concrete in compression

The Type-1 concrete in the compression strut has the maximum strain of 0.03, at the stress of 8.02 MPa, equal to 20% f'c. The stress-strain curve is shown in Figure 6-13.
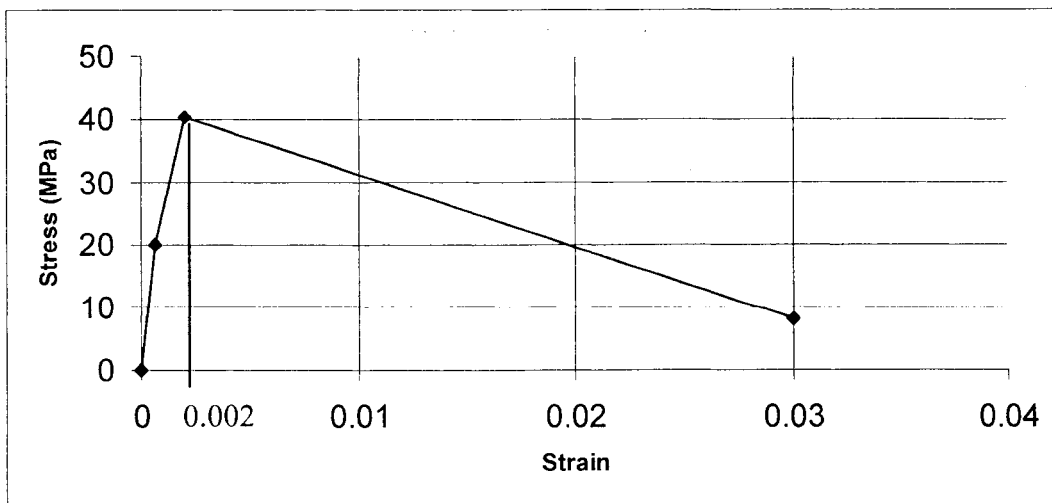
Figure 6-13 Stress-strain relationships for concrete in compression in strut Type-1

90

The Type-2 concrete in the compression strut has the maximum strain of 0.05, at the stress of 16.04 MPa, equal to 40% f'c. The stress-strain curve is shown in Figure 6-14.
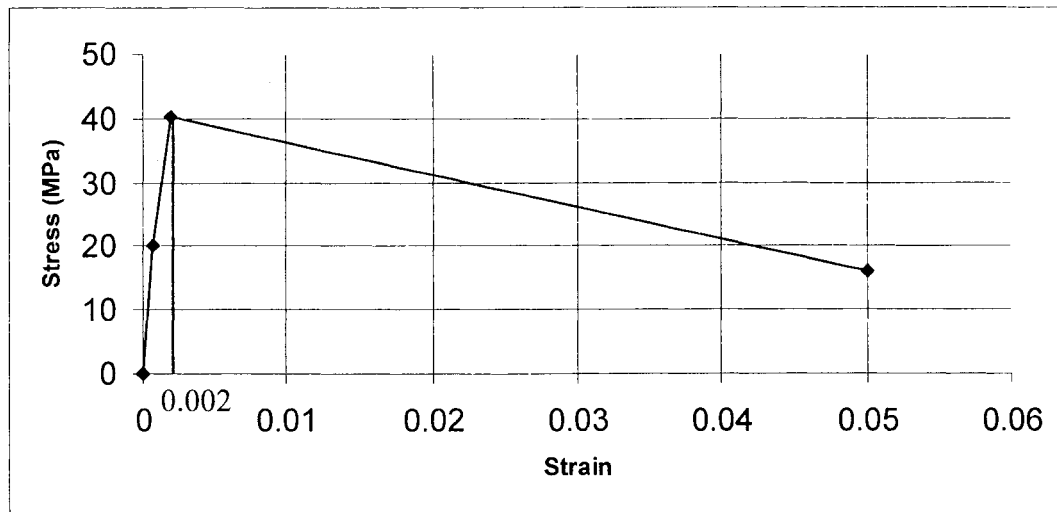
Figure 6-14 Stress-strain relationships for concrete in compression in strut Type-2

Both concrete materials are modified in tension in order not to allow the strut section to take larger tensile stress than the concrete tensile strength. The modification as was discussed is shown again in Figure 6-15.
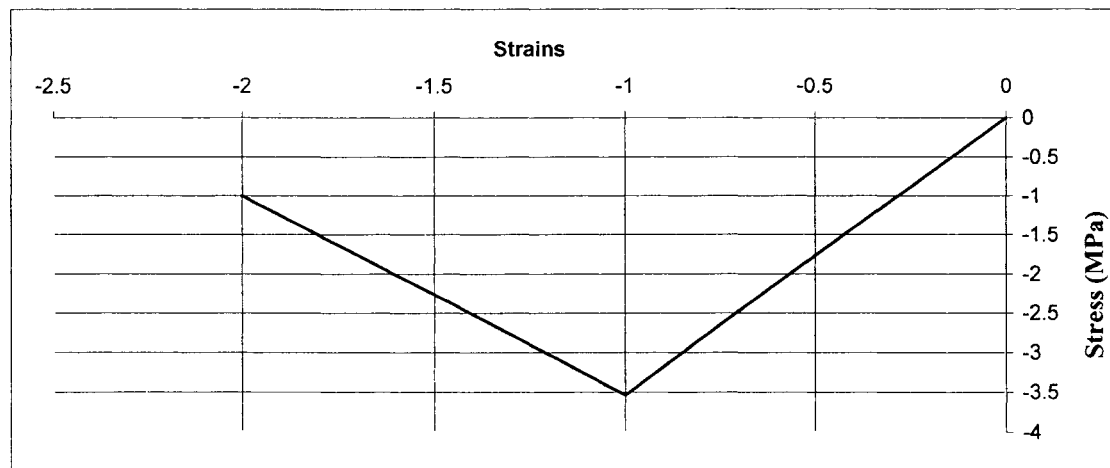
Figure 6-15 Stress-strain relationships for concrete in tension in strut, Type-1 & Type-2

The second important issue in this model is the ratio of each concrete type cross-section area in the strut. If the concrete cross-section in the strut is equally divided to Type-1 to Type-2, it was observed that despite the accuracy of the result, some improvement in the shape of the load-drift curve could be maintained.

The cross-section area of the strut is calculated by dividing the axial compression stress in the strut by the maximum strength of the concrete. The analysis of the different beam-column joints showed that the ratio of concrete cross-section area of Type-2 to Type-1 equal to: [1.15-1.20] for column with axial load of $0.1(f_c A_g)$, and [1.05-1.10] for column axial with axial load of $0.25(f_c A_g)$ gave comparable results to experimental evidences (f_c is the maximum compressive strength of the concrete and A_g is the gross cross-section of the column).

Presence of the beam and column longitudinal reinforcement in the joint panel, and its effect on the joint shear capacity is accounted for by using 2 slender steel sections within the strut with sectional area equal to 0.3% of the strut cross section area. To illustrate the determination of the cross-section areas of each type of concrete, the procedure for the example Test #6 of Chapter-7 is as follows.

The larges value of axial compressive force in all of the struts during the application of the section ultimate load on the beam (Extracted from output data):   204.5 kN

Note: Knowing the ultimate load from the values of the experimental data, the axial compressive force in the strut can be calculated by obtaining a load on the beam end tip and corresponding axial load induced in the struts within any segment in the analysis from the output file. By dividing the beam end force to the corresponding strut axial force, the factor is obtained for the induced axial load in the strut, corresponding to a unit load applied on the beam's end tip. By multiplying the following factor and the ultimate force the axial compressive force in the strut is obtained.

Note: The units are: kN, and mm.

Approximate Area of strut cross section = P/ f'_c= 204.5 / 0.0401 = 5098 mm^2

Corresponding steel area = 0.003* 5098= 15 mm^2

Stress carried by reinforcement in the strut = A_s f'_y =15* 0.45 =6.75 kN

Stress carried by concrete in the strut = 204.5- 6.75 = 197.7 kN

Area of strut cross section = 197.7 / 0.0401 = 4930 mm^2

Ratio of concrete of Type-2 to Type-1 is selected equal to: 1.17

Area of Type-1 = 4930 / (1+1.17) = 2270 mm^2

Area of Type-2 = 2270 * 1.17 = 2656 mm^2

Each strut is divided to 10 fibers, 4 fibers for concrete Type-1, 4 fibers for concrete Type-2, and 2 fibers for steel reinforcement.

Area of each fiber Type-1 = 2270 / 4 = 567.5 mm^2

Area of each fiber Type-2 = 2656 / 4 = 665 mm^2

Area of each steel reinforcement fiber = 4930 * 0.003 = 14 mm^2

Distance from the reference axis of the strut cross section (mm)	Cross section area (mm^2)	Material type
2.5	665.	Strut concrete Type-2
7.5	665.	Strut concrete Type-2
12.5	567.5.	Strut concrete Type-1
17.5	567.5	Strut concrete Type-1
2	7.0	Beam reinforcement
-2	8.0	Column reinforcement
-2.5	665.	Strut concrete Type-2
-7.5	665.	Strut concrete Type-2
-12.5	567.5	Strut concrete Type-1
-17.5	567.5	Strut concrete Type-1

It is necessary to mention that the factors mentioned above are taken from the indicated range; for example 1.17 from the rage [1.15-1.20], gives the best comparable results.
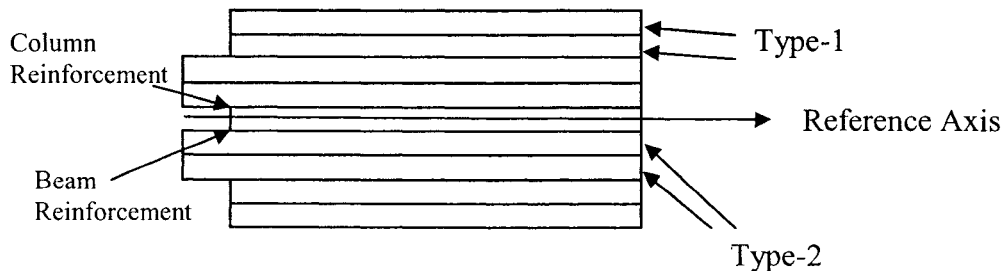
Figure 6-16 Diagonal strut cross-section

In Figure 6-17 the modified result is compared with the mentioned result and also the experimental result.
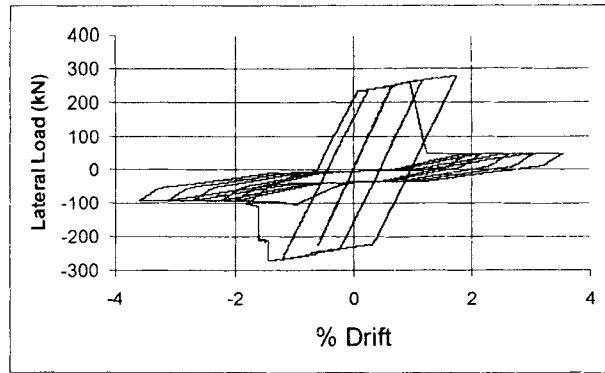
(a) Before modification
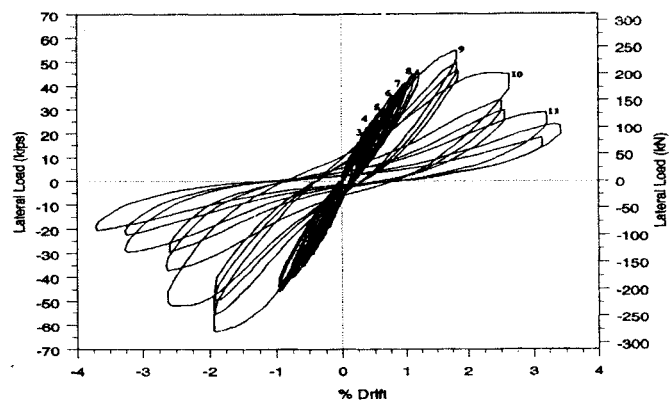
(b) Experiment
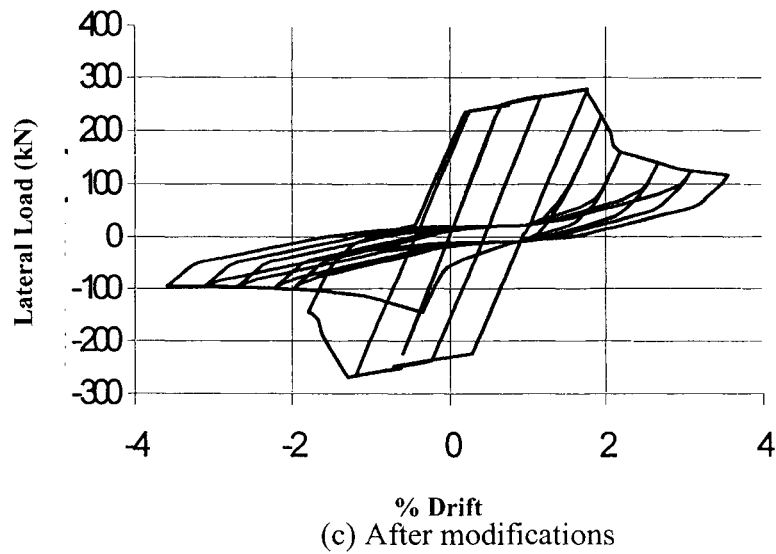
(c) After modifications

Figure 6-17 The effect of modification

As will be discussed in the next chapter, the above-mentioned approach yields comparable results with experimental values.

Chapter 7

MODELING THE SHEAR BEHAVIOR OF
EXTERIOR BEAM-COLUMN JOINTS

7.1 General

The experiment, and experimental results presented in this chapter are from the research performed at the University of Utah, and was supported in part by the Pacific Earthquake Engineering Research Center under the title "Performance-Based Evaluation of Exterior Reinforced Concrete Building Joints for Seismic Excitation" [Clyde et al., 2000].

Four half-scale RC exterior joints were tested to investigate their behavior in a shear-critical failure mode. The joints were subjected to quasi-static cyclic loading, and their performance was examined for lateral load capacity, ductility, drift, and other performance criteria.

7.1.1 Specimens and Experimental Setup

As is typical of building frames in the structures that were built prior to 1970's, reinforced concrete structures have limited ductility and several performance deficiencies that prevent them from meeting the current seismic design criteria.

The beam-to-column connections targeted in this research suffer from lack of confining reinforcement in the joints. A typical exterior beam-column joint in a reinforced concrete frame built in 1964 is shown in Figure 7-1. For the test specimens, the overall dimensions of the original joint were reduced by half. The longitudinal reinforcement in the beam was increased to prevent early degradation of the beam. There is no transverse reinforcement within the joint core this will ensure the shear mode of failure in the joint, to prevail. The specimen dimensions and reinforcements for the test are shown in Figure 7-1.

The properties of reinforcement, which is the same for all specimens, and the properties of concrete in all four specimens are listed in the Tables 7-1, and 7-2, respectively.
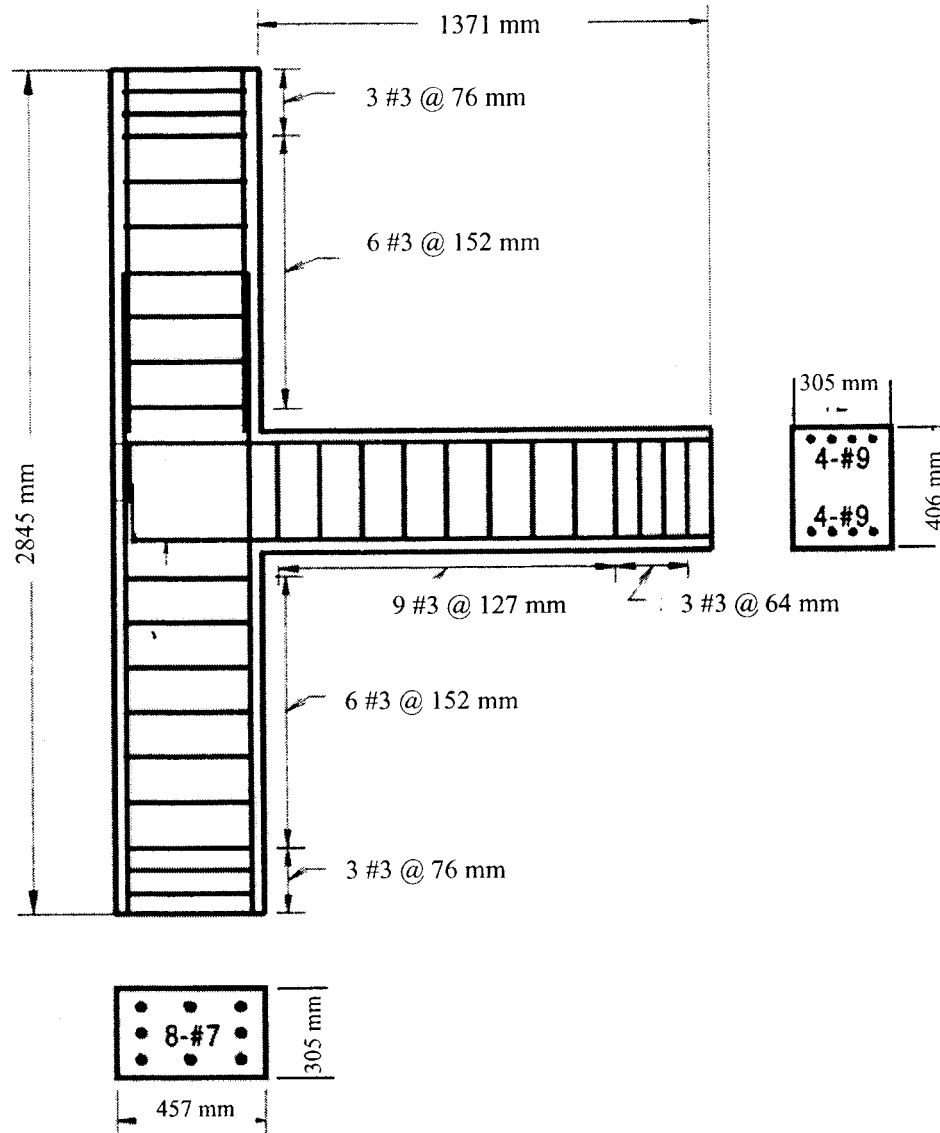
Figure 7-1 Specimen dimension and reinforcement details

Table 7-1 Steel reinforcement strength

Reinforcement Type	Bar Size	F_u ksi (MPa)	F_y ksi (MPa)
beam longitudinal	9	108.2 (746.0)	65.9 (454.4)
column longitudinal	7	107.6 (741.9)	68.1 (469.5)
stirrups/ties	3	94.9 (654.3)	62.0 (427.5)

F_y: Yield strength of reinforcement
F_u: Ultimate strength of reinforcement

Table 7-2 Concrete strength of the specimens

Test No.	f'c Psi (MPa)
2	6700 (46.2)
4	5940 (41.0)
5	5370 (37.0)
6	5823 (40.1)

f'c: maximum concrete compressive strength

7.2 Specification of Elements

7.2.1 Beam

The beam is 12 inch (305 mm) wide and 16 inch (406 mm) deep. It is symmetrically reinforced with 4-#9 bars for both the positive and negative reinforcement; the steel ratio is 2.47% at both top and bottom. Each longitudinal bar has a 7.5 inch (191mm) hook bent at 90°. The bottom beam reinforcement is bent up into a hook at the joint, and the top reinforcement is bent down into a hook at the joint. The hooks overlap approximately 2 in. (51 mm) and are tied together, one inside the other as shown in Figure 7-1.

The transverse reinforcement is a #3 bar closed stirrup with 140° bend and 2.5 inch (63.5 mm) extension on both ends as shown in Figure 7-2. The stirrups are spaced at 5 inch (127 mm) along the beam except within 8 inch (203 mm) of the beam end, where the spacing is reduced by half to 2.5 inch (63.5 mm). The closer spacing was intended to give adequate strength in the beam tip, where the cyclic force was applied during the test. The original half-scale model required a reinforcement ratio 0.76% in the top and 0.48% in the bottom. The decision to increase the beam longitudinal reinforcement was based on the objective to study joint shear failure at high drift levels and not beam flexural degradation. The 2.47% of longitudinal steel present in both the top and bottom of the beam meant that the design joint core shear forces developed would be relatively high.
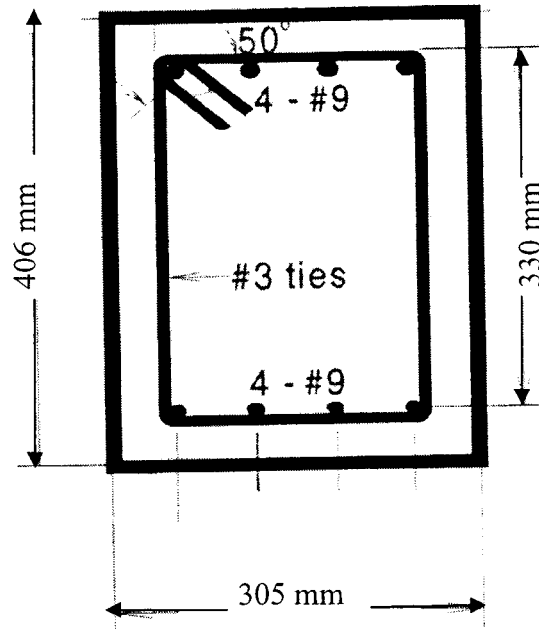
Figure 7-2 Beam cross-section

7-2-2 Column

The column is 12 inch (305 mm) wide and 18 inch (457 mm) deep. It is reinforced with 8-#7 bars evenly distributed around the perimeter of the column, thus having a steel ratio of 2.54%. The longitudinal reinforcement in the bottom column extends continuously up through the joint and 21 inch (533 mm) into the top column, as shown in Figure 7-1. The top column longitudinal reinforcement is spliced over the 21 inch (533 mm) length and extends to the upper end of the column, or a distance $24d_b$, which is insufficient by current standards.

The transverse reinforcement in the column consists of #3 bar closed stirrups with 140° bends and 2.5 inch (63.5 cm) extensions on both ends; this is shown in Figure 7-3. The stirrups are spaced at 6 inch (152 mm) along the height of the column, except within the joint region where there is no transverse reinforcement. The spacing is decreased to 3 inch (76 mm) at the upper and lower ends of the column, where the column was supported during the test.

98

457 mm

305 mm

50°

#3 ties

8 - #7
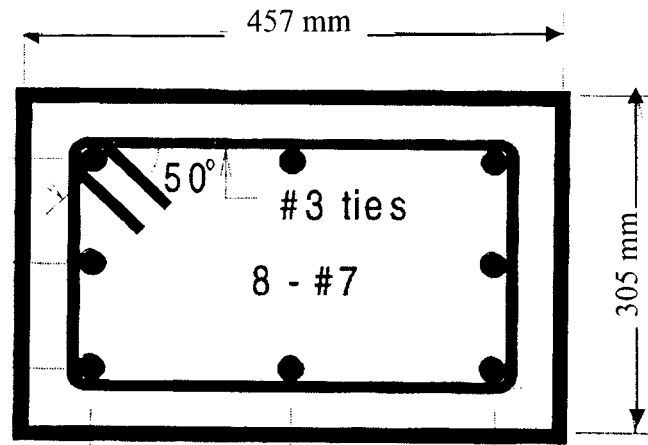
Figure 7-3 Column cross section

7-3 The Test Procedures

The column was mounted horizontally as is shown in Figure 7-4, and an axial load equal to $0.1f'_cA_g$ (f'_c is the maximum compressive strength of the concrete and A_g is the gross cross-section of the column) for two of the specimens (specimen #2 & specimen #6), and $0.25\ A_g\ f'_c$ for the other two specimens (specimen #4 & specimen #5), was applied using a small hydraulic cylinder. The compressive axial load was transferred to the column portion of the specimen through four threaded rods. The compressive axial load was set to an initial value and was then left to change at will, as the beam was subjected to load reversals. The lateral load was applied cyclically, in a quasi-static fashion, at the end of the beam through a loading collar.
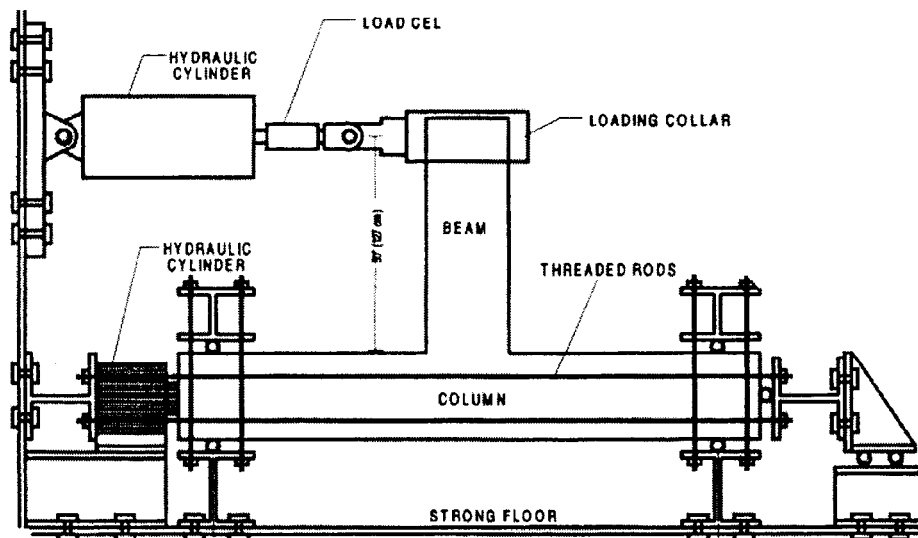
Figure 7-4 Test setup

The first portion of the test was load-controlled, which is shown in Figure 7-5. The lateral load was increased in 5 kip (22.2 kN) increments. At every load step, three cycles were performed, each cycle containing a push and pull segment. After the first yielding of the reinforcement, the testing was carried out using displacement control. Three cycles were performed at each displacement step, and the displacement was increased as a fraction of the initial yield displacement. The test continued until the lateral load dropped below 50% of its peak value. The displacement control loading is shown in Figure 7-6.
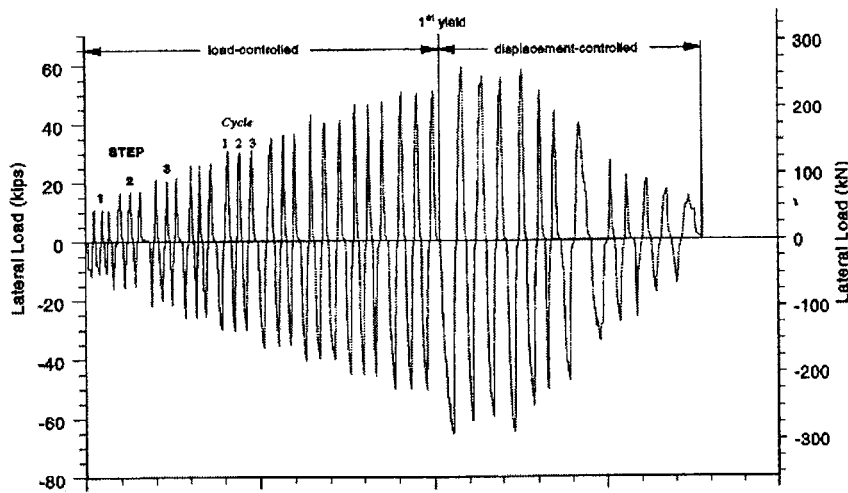
Figure 7-5 Load-control patterns
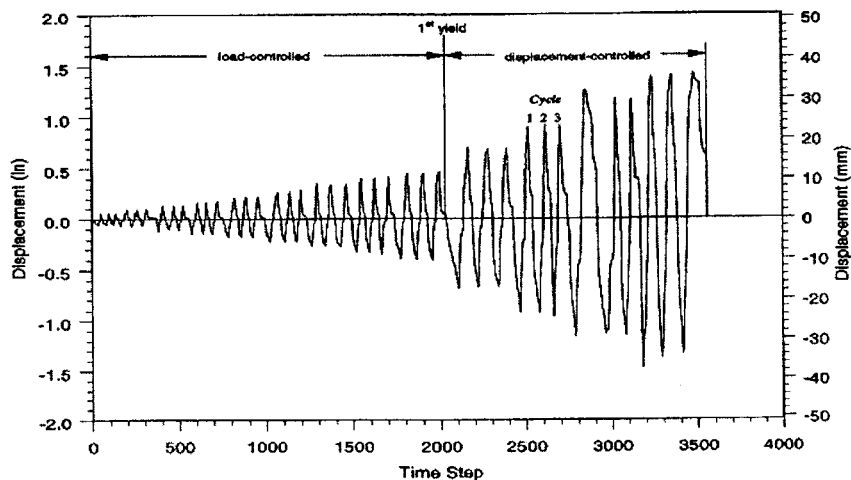
Figure 7-6 Displacement-control patterns

100

7.4 Modeling the Experiment

7.4.1 IDARC2D

In IDARC-2D, there is no option of exact simulation of the experimental test, because there is no option of applying the quasi-static load vertically and no choice of applying the column axial load horizontally. So as an approximation of the real behavior of the system, the following procedures were followed. The input data for specimen Test #6 are attached in Appendix (A).

As shown in Figure 7-7, the system was mounted horizontally and two rather strong and rigid columns with large cross sections were used with "End moment release" option to simulate the two supports at both ends of the column. The column properties were plugged in the beam input section, and the beam properties were plugged in the column input section of the program, although IDARC-2D takes column and beam as two different macro-model elements.
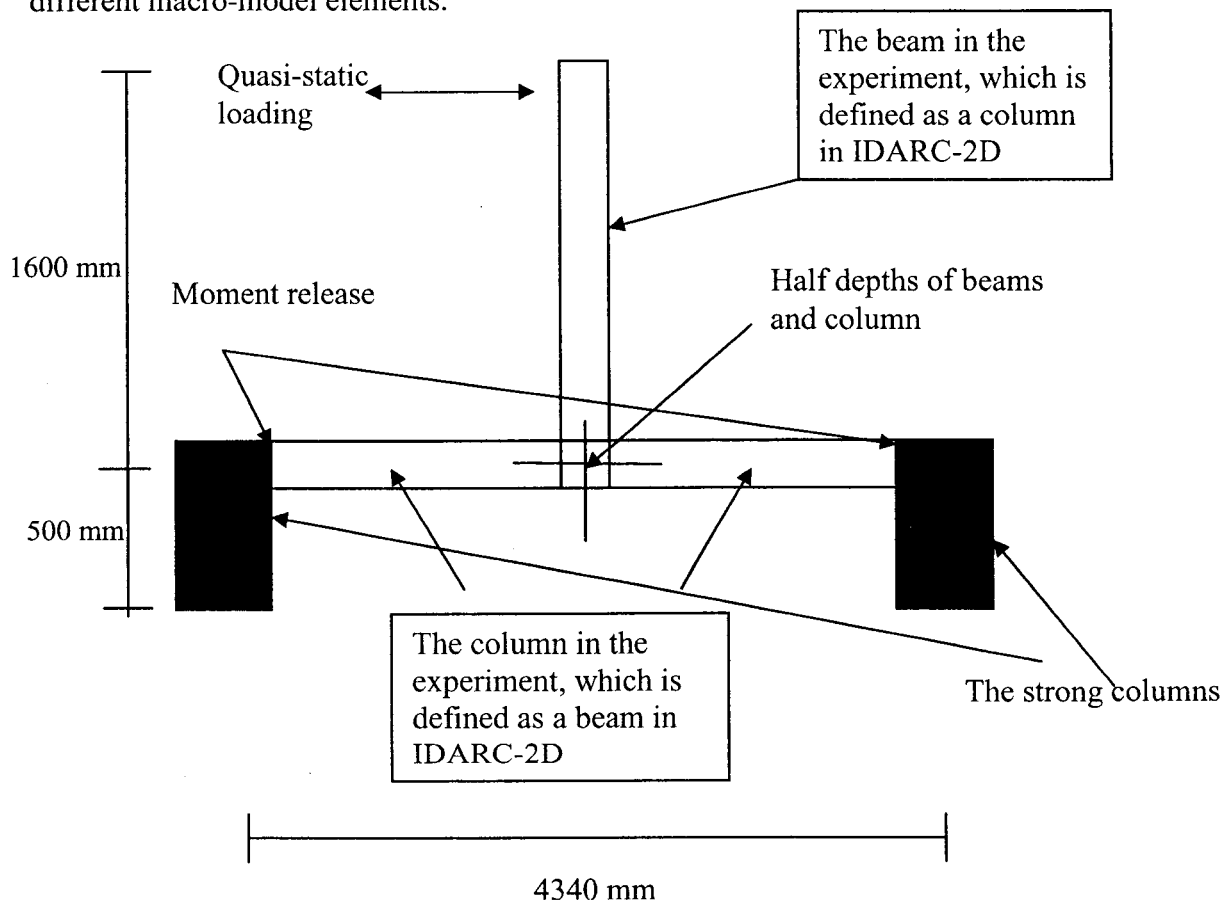
Figure 7-7 Simulation of the test specimen in IDARC-2D

7.4.1.1 Rigid Zone in IDARC2D

In Figures 7-8, the input details for column's rigid zones in IDARC2D, is illustrated. The length of the rigid zone is defined by value of RAMC2 (Rigid Arm at column's top) and RAMC1 (Rigid Arm at column's bottom). As it is shown in the Figure 7-8, the value can range according to rigidity of the connection, between zero, and half-depth (rigid connection) of the framing beam in the top or the bottom of the column.

Note: AMLC is the parameter defining the clear length of the column, plus the length of two rigid arms.
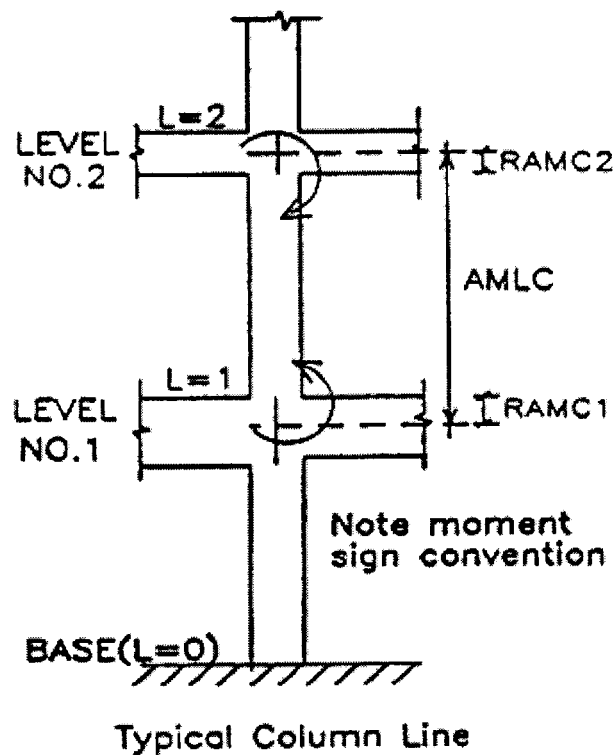
Figure 7-8 Input details for column's rigid zone in IDARC2D

In Figure 7-9, the input details for beam's rigid zones in IDARC2D, is illustrated. The length of the rigid zone is defined by value of RAMB2 (Rigid Arm at beam's right end) and RAMB1 (Rigid Arm at beam's left end). As it is shown in the Figure 7-9, the value can range according to rigidity of the connection, between zero, and half-depth (rigid connection) of the framing column in the right end or the left end of the beam.

Note: AMLB is the parameter defining the clear length of the beam, plus the length of two rigid arms.

102
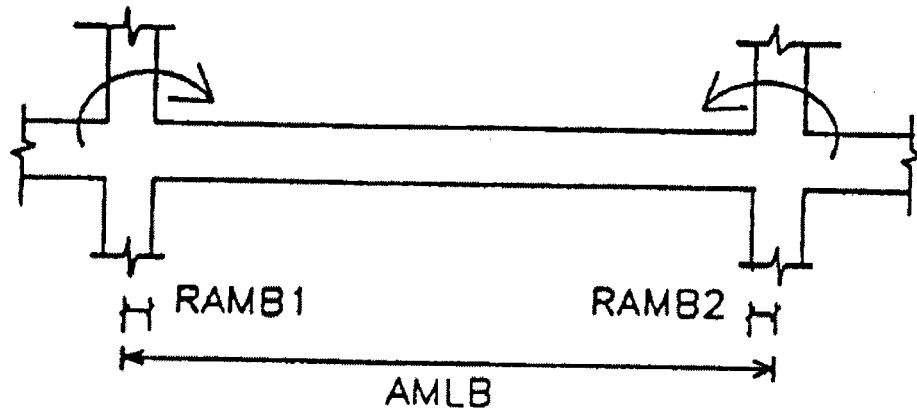
Figure 7-9 Input details for beams in IDARC2D

In the exterior beam-column joint example, according the mentioned guidelines of the program, for defining the rigid zone, as it is shown in Figure 7-7, half depth of the joint panel was defined as rigid zone length at the column's bottom, where it is connected to the beams. The beam is divided into two equal beams with end rigid zones equal to half of the depth of the joint where they are connected to the column.

In the experimental test, the connections of the column to the restrains at top and bottom were simulated by connecting the beams' ends to two very stiff columns with large cross sections. To allow the beams' ends to rotate, moment releases in the columns were defined in the input data of the program (Note: if the moment releases are defined for the beams ends rather than the column ends the results are significantly inaccurate).

Similar to the experiment, the analysis is first performed in load-control quasi-static mode. The yield loads of the sections calculated using IDARC-2D, and DRAIN-2DX as will be discussed for each specimen, are different from the experimental values for all the four specimens; however, in this study, for comparison, the values of the experimental results are taken.

IDARC-2D is unable to perform load-control mode and displacement control mode, in a single analysis, therefore after the load-control mode, where the section was in linear elastic state, the displacement-control loading begins. This is the part in the analysis where the hysteretic loop and ductility behavior of the system are defined. The program needs the hysteretic parameters to be defined to perform the analysis. In other word, the hysteretic rules control the relation between the stresses and strain during the

103

load application. This is the part where the joint behavior can be modeled in terms of degrading parameter for stiffness and strength and state of bond behavior of the connection. This is one of the main weak-points of such programs, because without the knowledge of the accurate values of those parameters, it is impossible to get accurate results from the analysis. In the example of the bridge pier in Chapter-3, it was evident that those values should refer to a section with very small values of stiffness degradation, strength deterioration and bond slip, the reason is that the column's connection to the foundation had large volume of longitudinal and transverse reinforcement, which helped the mechanism of the shear resistance of the connection to be fully mobilized, and postponed the degrading phenomenon like debonding of the reinforcement and concrete. In the current example, the joint has failure mode in shear resistance, so the accurate hysteretic rule parameters in terms of stiffness degradation and strength deterioration are the only way to define the degradation in stiffness and strength of the system. In this part of the study, the objective is experimental calibration of the hysteretic behavior of the test specimens. The calibration of the hysteretic rule parameters governing the behavior of the system has been achieved by reproducing the experimental results of the test.

In the following, the results of experimental test for each specimen are described. Then the results of the analytical models using IDARC-2D and DRAIN-2DX (the proposed model) adopted in this study are shown and compared. In IDARC-2D a vertex-oriented model for the hysteretic rules was adopted using different parameters for stiffness degradation, strength deterioration and bond slip. Like the experiment, each cycle was performed three times. In DRAIN-2DX, because of the large size of the output data (20 MB in case of one cycle of loading through the analysis), each cycle was performed once as a representative for the stable loops in the hysteretic loops. The values of hysteretic parameters in IDARC-2D for each specimen are described below. The Figure 3-4 from Chapter-3 can be used for better illustration of the degrading parameters in these examples, using the following symbols for the parameters shown in Table 7-3. It is again noted that the only way to account for the axial load on the column was the values of the hysteretic parameters, knowing that more axial force, and more maximum strength of concrete, reduces the ductility.

HC:	Stiffness degrading parameter
HBD:	Strength degrading parameter (ductility based)
HBE:	Strength degrading parameter (energy-controlled)
HS:	Slip or crack closing parameter

Table 7-3 Typical ranges of values for hysteretic parameters

HC	0.1	Severe degradation
	2.0	Nominal degradation
	10.0	Negligible degradation
HBD	0.0	No degradation
	0.1	Nominal deterioration
	0.4	Severe deterioration
HBE	0.0	No degradation
	0.1	Nominal deterioration
	0.4	Severe deterioration
HS	0.1	Extremely pinched loops
	0.5	Nominal pinching
	1.0	No pinching

7.4.2 DRAIN-2DX

In the DRAIN-2DX, modeling of each test the procedure is the same as discussed in the description of the model in Chapter-4. The only difference is the cross-sections of the struts, which are fully described, after each load-drift curve in the following examples.

7.5 Analytical Modeling and Results of the Tested Specimens

The procedure for the experimental test is discussed in section 7.3 of this chapter. In the following, the description of the experimental evidence taken from the reference, and the analytical modeling, first using IDARC2D, and then using DRAIN-2DX for each of the four specimens is sequentially presented.

105

7.5.1 Specimen Tests #2

7.5.1.1 Experimental Results

The specimen #2 was loaded with 0.1f'cAg. The first yielding occurred in a bottom, longitudinal bar in load step four. The lateral load at yielding was 20.9 kips (93 kN) at a lateral displacement of 0.31 inch (7.8 mm). Only hairline cracking was apparent at this point during the test. Measurable flexural cracks in the beam and shear cracks in the joint appeared during the seventh load step corresponding to a lateral load of approximately 40 kips (178 kN). The joint ultimately failed at a displacement of 1.94 in. (49 mm) corresponding to a drift of 2.95%, and the load had dropped to 30.1 kips (134 kN). The peak lateral load sustained by the specimen was 60.1 kips (267 kN), and at drift of 1.77%. Figure 7-10, shows the experimental load-drift curve for Test #2.
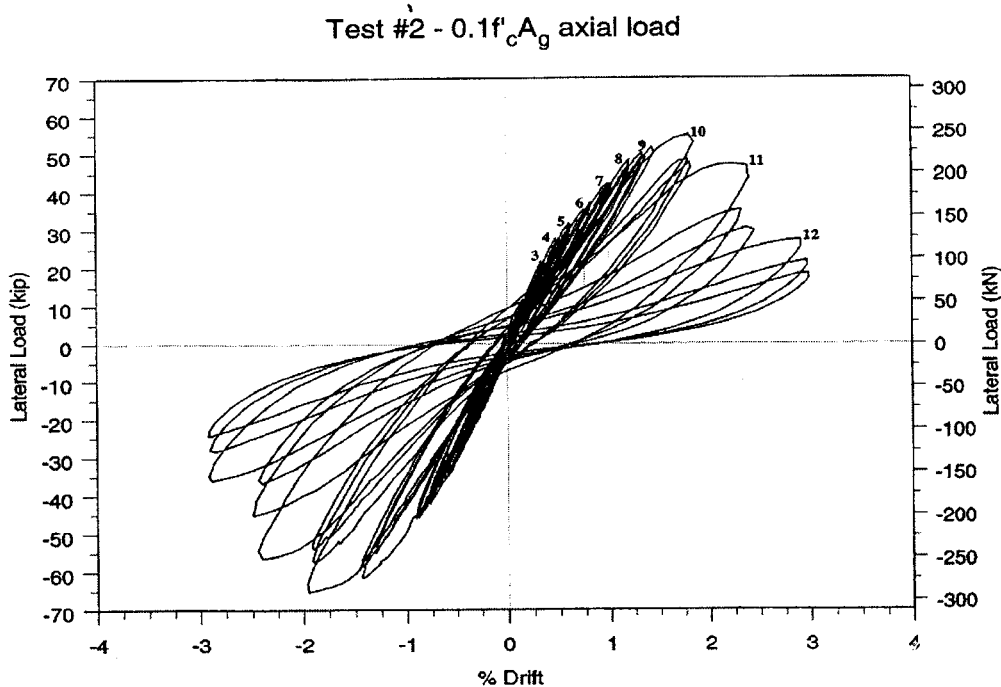
Figure 7-10 Test #2 load-drift curve (Experimental)

7-5-1-2 Modeling in IDARC2D

In the following the different input sections for specimen Test #2 for modeling in IDARC2D is described. For the other specimens all the input sections are the same (which will not be repeated), except the concrete properties section and the hysteretic rules section which is different for all four specimens.

FLOOR ELEVATIONS

500,2100

In Figure 7-7, the length of the strong column up to the mid-depth of the beam is taken as 500 mm. The distance from the top of the main column to the ground is 1600, so in IDARC2D, the elevation is shown as 500+1600= 2100mm.

CONCRETE PROPERTIES

1, 0.0462 ,32 , 0, 0.0, 0.0, 0.0

2, 0.1,47,0,0,0,0

In the input section above 1 refers to the section properties type, which is 1 for the main column, in which the concrete compressive strength (28 days) is taken as 46.2 kN/mm^2, and Modulus of elasticity of concrete is taken as 32000 kN/mm^2. The rest of the parameters are taken as default; that means Strain at maximum stress of concrete will be 2%, Stress at tension cracking will be 0.12*46.2= 5.54 kN/mm^2, Ultimate strain in compression (EPSU), and Parameter defining the slope of the falling branch (ZF), are internally calculated by the program according to the previously described model of Kent and Park.

$$ZF = \frac{0.5}{\epsilon_{50u} + \epsilon_{50h} - 0.002}$$

Where;

$$\epsilon_{50u} = \frac{3+0.002\, f'_c}{f'_c - 1000}$$

$$\epsilon_{50h} = \frac{3}{4} \rho_s \sqrt{\frac{b''}{S_h}}$$

For the second concrete property, which refers to the strong columns the concrete compressive strength (28 days) is taken as 100 kN/mm^2, and Modulus of elasticity of concrete is taken as 470000 KN/mm^2. The default values are obtained using the aforementioned equations.

REINFORCEMENT PROPERTIES

1, 0.454, 0.746, 0, 0, 0

2, 0.47, 0.742, 0, 0, 0

In the input section above 1 refers to the reinforcement properties of the beam, Yield strength of longitudinal reinforcement is equal to 454 kN/mm^2, Ultimate strength of longitudinal reinforcement is taken as 746 kN/mm^2, Modulus of elasticity of longitudinal reinforcement is 2×10^5 kN/mm^2. The rest of the parameters are taken as default; that means: Modulus of strain hardening is: ESH = (ES / 60), which is equal to 2×10^5 /60 = 3333.3 kN/mm^2, and the Strain at start of hardening will be 3.0%.

In the second line in the input section above 2 refers to the reinforcement properties of the columns (the main column, and the strong columns), Yield strength of longitudinal reinforcement is equal to 470 kN/mm^2, Ultimate strength of longitudinal reinforcement is taken as 742 kN/mm^2, Modulus of elasticity of longitudinal reinforcement is 2×105 kN/mm2. The rest of the parameters are taken as default; that means: Modulus of strain hardening is: ESH = (ES / 60), which is equal to 2×105 /60 = 3333.3 kN/mm^2, and the Strain at start of hardening will be 3.0%.

COLUMN DIMENSIONS

1   **Main column**

1,1,1,0,1600, 228, 0

   1, 406, 305   ,43 ,2560 ,9.5,127,0.5

   1, 406, 305   ,43 ,2560 ,9.5,127,0.5

1   **Strong columns**

2,2,1,0,500 , 0, 228

   1, 1500, 1500, 50, 2560, 11.3, 50, 1

   1, 1500, 1500, 50, 2560, 11.3, 50, 1

In the first input section above, 1 in the first line refers to the section shape, which is rectangular, The 1, 1, 1, 0, refer to the column type set number, concrete type number, steel type number, and axial load, respectively. The length of the main column is taken as 1600 mm; rigid arm at the bottom is taken as the mid-depth of the framing beams which is 228 mm. The rigid arm at the top is taken as zero because the column's top is free. The 1, in the beginning of the 3rd, and 4th lines refers to the only hysteretic rule number.

The depth and width of the column are the same throughout the length of the column and are 457 mm, and 305 mm, respectively. The cover concrete is defined to have 43 mm thickness. The cross-section area of the longitudinal reinforcement is 2560

mm^2. The hoop bar diameter and spacing are 9.5 mm, and 127 mm, respectively. The 0.5 in the end of the line refers to effectiveness of column confinement, as shown in Figure 7-11.

Minimal Confinement   Nominal Confinement   Well Confined
CEFF = 0.5   CEFF = 0.66   CEFF = 1.0
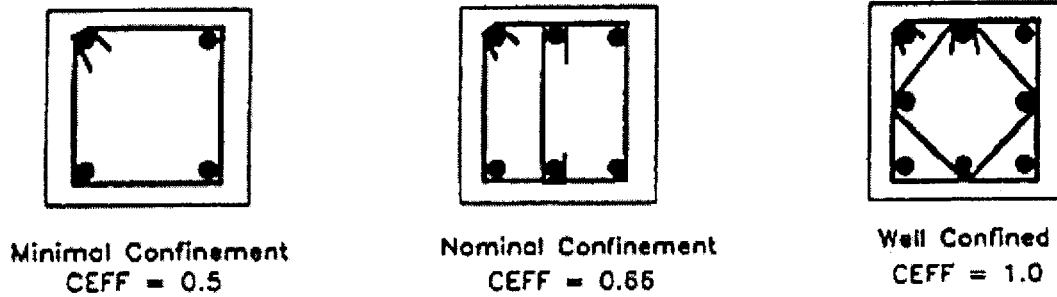
Figure 7-11 Effectiveness of confinement for typical hoop arrangements in IDARC2D

For defining the arbitrary specifications of the strong columns, the length is defined to be 500 mm with rigid arm equal to 228 mm on the top. The depth, and width of the column are the same throughout the length of the column and are 1500 mm. The cover concrete is defined to have 50 mm thickness. The cross-section area of the longitudinal reinforcement is 2560 mm^2. The hoop bar diameter and spacing are 11.3 mm, and 50 mm, respectively. The 1 in the end of the line refers to effectiveness of column confinement, as shown in Figure 7-11. The above specifications make the column very rigid and stiff.

BEAM DIMENSIONS

1,1,2, 2170,750, 203

    1, 457.0, 305.0 ,305.0, 0, 43, 1161, 1161, 9.5, 150

    1, 457.0, 305.0 ,305.0, 0, 43, 1161, 1161, 9.5, 150

1,1,2, 2170, 203, 750

    1, 457.0, 305.0 ,305.0, 0, 43, 1161, 1161, 9.5, 150

    1, 457.0, 305.0 ,305.0, 0, 43, 1161, 1161, 9.5, 150

In the first input section above, 1 in the first line refers to the beam type set number, which is 1, The 1, 2, refer to the concrete type number, and steel type number, respectively. The length of the beam is taken as 2170 mm. The rigid arm at the end, where it is connected to the strong column is the mid-depth of the strong column, and is equal to 750 mm. The rigid arm at the other end, where it is connected to the main

column is the mid-depth of the main column, and is equal to 203 mm. The 1, in the beginning of the 3rd, and 4th lines refers to the only hysteretic rule number.

The depth and width of the beam are the same throughout the length of the beam and are 406 mm, and 305 mm, respectively. The cover concrete is defined to have 43 mm thickness. The cross-section area of the longitudinal reinforcement is 1161 mm^2. The hoop bar diameter and spacing are 9.5 mm, and 150 mm, respectively.

The second part in the beam dimension specification refers to the other beam which is opposite of the first one, and has identical specifications.

MOMENT RELEASES

1,1,2,2

2,1,3,2

(In the above moment releases section, 1, and 2 in the beginning of the first and second lines refer to moment releases ID number. The next 1 indicates that column element is chosen for moment release. 2, and 3 refers to the strong columns, which were numbered as column #2, and column #3. The last value in the both lines is 2, which indicates that the moment release is performed at the top of the column.

HYSTERETIC MODELING RULES

This is the section, which is different for each specimen. The values should refer to section with no pinching, but severe degradation in strength and stiffness. For each test, the exact values that are shown in the hysteretic rule table (Table 7-4 in this case), are obtained by a trail and error process, to get the best comparable results to the experiment.

Table 7-4 Input properties for Test #2

f'c (N/mm^2)	Ec (N/mm^2)	HC	HBD	HBE	HS
46.2	32000	1	0.52	0.94	1

After execution of the program, the lateral load-drift curve, which is shown in Figure 7-12, is obtained. The result data show that the maximum lateral load sustained by the specimen was 272 kN, and at drift of 0.6%, corresponding to the yielding point of the reinforcement. The maximum load is comparable to the value of experiment but the

110

corresponding drift is different. At the end of the test, the load had dropped to 135 kN, at the drift of 2.95%, which is identical to the experiment.
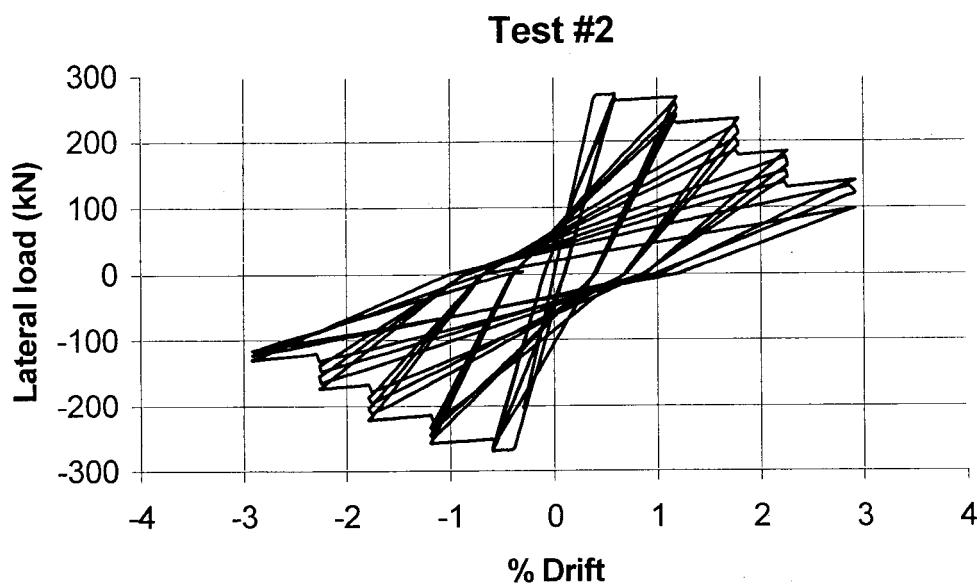
Figure 7-12 Load-drift curve (IDARC-2D)

7.5.1.3 Modeling in DRAIN-2DX

The procedure for modeling the test in DRAIN-2DX is the same for all four specimens. In test#2, the mentioned parameters in section 6-4 are defined as shown in Tables 7-5 through 7-8. The areas of the concrete types in the diagonal struts are calculated, as discussed in section 6.4. After the execution of the program the curve in Figure 7-13 is obtained.

Table 7-5 Concrete material for column for Test #2

	STRESS (N/mm²)	STRAIN
1st point for compression	23.1	.000722
2nd point for compression	46.2	.002
3rd point for compression	9.24	.016
1st point for tension	3.8	.00016
2nd point for tension	0.1	.00146

111

Table 7-6 Concrete materials for beam for Test #2

	STRESS (N/mm^2)	STRAIN
1st point for compression	23.1	.000722
2nd point for compression	46.2	.002
3rd point for compression	9.24	.016
1st point for tension	3.8	.00016
2nd point for tension	0.1	.00146

Table 7-7 Concrete material Type-1 for diagonal struts for Test #2

	STRESS (N/mm^2)	STRAIN
1st point for compression	46.2	.002
2nd point for compression	9.24	.030
1st point for tension	1	1. ** (modified for tension)
2nd point for tension	0.1	2. ** (modified for tension)

Table 7-8 Concrete material Type-2 for diagonal struts for Test #2

	STRESS (N/mm^2)	STRAIN
1st point for compression	46.2	.002
2nd point for compression	19	.050
1st point for tension	1	1. ** (modified for tension)
2nd point for tension	0.1	2. ** (modified for tension)

112

Distance from the reference axis of the strut cross section (mm)	Cross section area (mm²)	Material type
2.5	585	Strut concrete Type-2
7.5	585	Strut concrete Type-2
12.5	485	Strut concrete Type-1
17.5	490	Strut concrete Type-1
2	6.0	Beam reinforcement
-2	7.0	Column reinforcement
-2.5	585	Strut concrete Type-2
-7.5	585	Strut concrete Type-2
-12.5	485	Strut concrete Type-1
-17.5	490	Strut concrete Type-1

$$\frac{\text{Cross-Section Type-2}}{\text{Cross-Section Type-1}} = 1.2 \text{ (which is in the range [1.15-1.2]). } \textit{See page 92}$$

The curve in Figure 7-13, shows that the maximum load sustained by the specimen is 280 kN, at the drift of 1.77%. These values are comparable to the experimental values of 267 kN, and 1.77%. By the end of the test, the analytical value shows the lateral load of 115 kN corresponding to the drift of 2.95%, which is almost identical to the values of experimental hysteretic loop in the second repetition of the last load step.
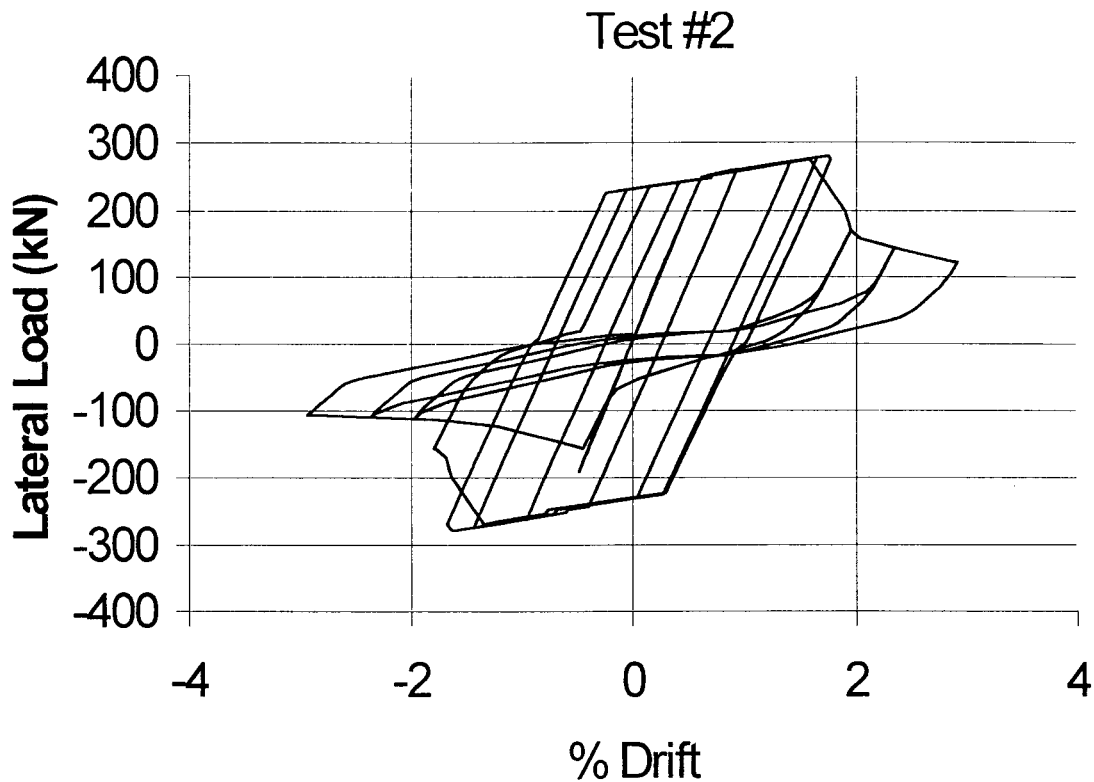
Figure 7-13 Load-Drift curve (Proposed model, DRAIN-2DX)

7.5.2 Specimen Tests #6

7.5.2.1 Experimental Results

The specimen #6 was loaded with $0.1f'_cA_g$. The first yielding occurred in a bottom, longitudinal bar in load step five. The lateral load at yielding was 29.0 kips (129 kN) at a lateral displacement of 0.38 in. (9.7 mm). Hairline flexural cracking was apparent at this point during the test. Measurable flexural cracks in the beam and shear cracks in the joint appeared during the seventh load step corresponding to a lateral load of approximately 35 kips (156 kN). The joint ultimately failed at a displacement of 2.35 in. (60 mm) corresponding to a drift of 3.57%, and the load had dropped to 29 kips (129 kN). The peak lateral load sustained by the specimen was 59.0 kips (262 kN), and at drift of 1.77%. Figure 7-14, shows the experimental result for lateral load-drift curve of the specimen #6

114
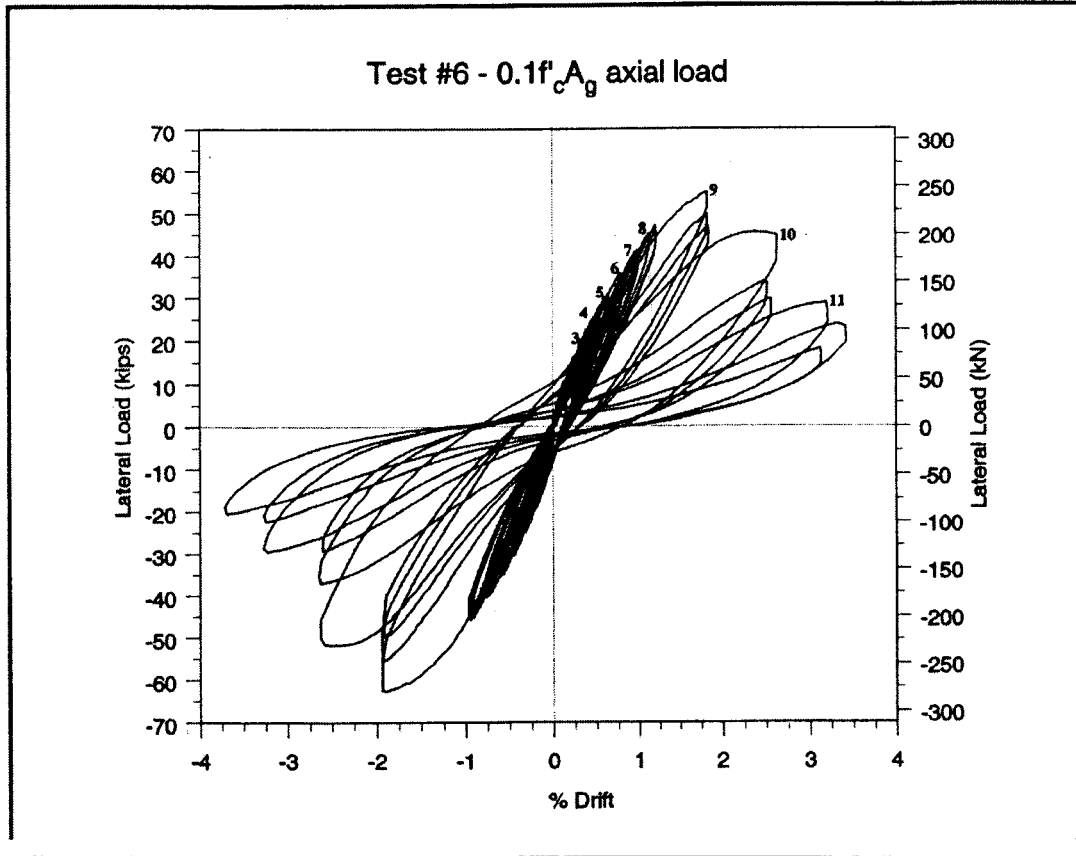
Figure 7-14 Test #6 load-drift curve (Experimental)

7.5.2.2 Modeling in IDARC2D

The procedure for test #6 is similar to Test #2, the only difference are the values shown in Table 7-9.

Table 7-9 Input properties for Test #6

f'c (N/mm²)	Ec (N/mm²)	HC	HBD	HBE	HS
40.1	30000	1	0.52	0.92	1

After execution of the program, the lateral load-drift curve, which is shown in Figure 7-15, is obtained. The result data show that the maximum lateral load sustained by the specimen was 271, and at drift of 0.6%, corresponding to the yielding point of the reinforcement. The maximum load is comparable to the value of experiment (262 kN),

but the corresponding drift (1.77%), is different. At the end of the test, the load had dropped to 134 kN, at the drift of 3.57%, which is similar to the experimental values of 129kN, and 3.57%, respectively.
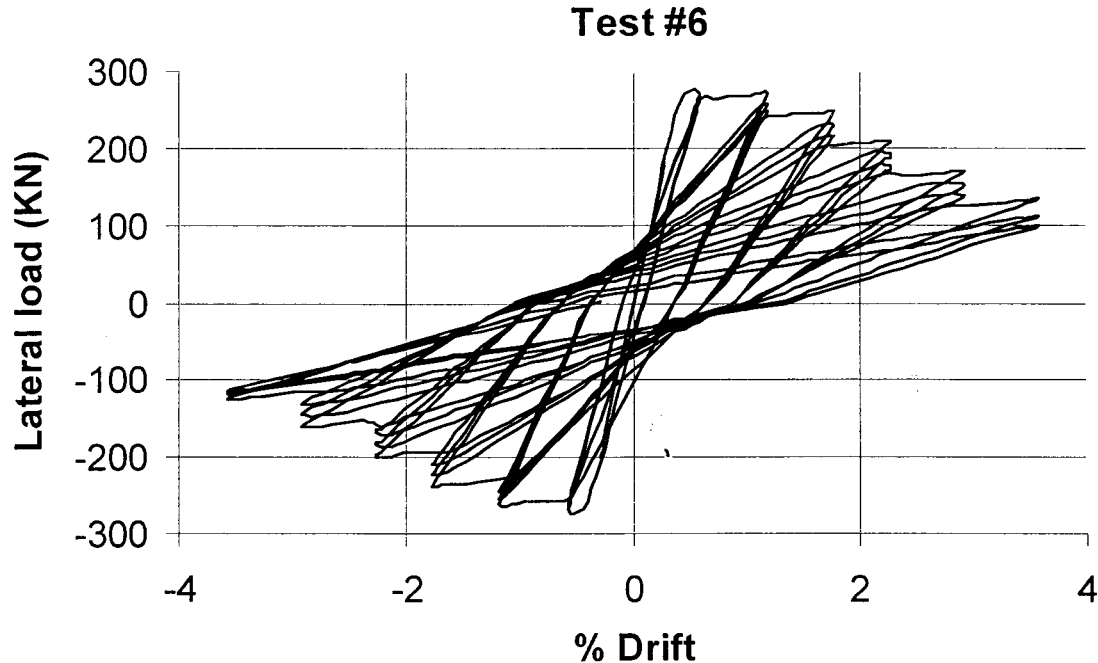
Figure 7-15 Load-drift curve (IDARC-2D)

7.5.2.3 Modeling in DRAIN-2DX

The procedure for modeling the test in DRAIN-2DX is the same for all four specimens. In test#6, the mentioned parameters in section 6.4 are defined as shown in Tables 7-10 through 7-13. The areas of the concrete types in the diagonal struts are calculated, as discussed in section 6-4. After the execution of the program the curve in Figure 7-16 is obtained.

Table 7-10 Concrete material for column for Test #6

	STRESS (N/mm^2)	STRAIN
1st point for compression	20.0	.00067
2nd point for compression	40.1	.002
3rd point for compression	8.02	.017
1st point for tension	3.534	.00016
2nd point for tension	0.1	.00145

116

Table 7-11 Concrete material for beam for Test #6

	STRESS (N/mm^2)	STRAIN
1st point for compression	20.0	.00067
2nd point for compression	40.1	.002
3rd point for compression	8.02	.017
1st point for tension	3.534	.00016
2nd point for tension	0.1	.00145

Table 7-12 Concrete material Type-2 for diagonal struts for Test #6

	STRESS (N/mm^2)	STRAIN
1st point for compression	40.1	.002
2nd point for compression	8	.030
1st point for tension	1	1. ** (modified for tension)
2nd point for tension	0.1	2. ** (modified for tension)

Table 7-13 Concrete material Type-2 for diagonal struts for Test #6

	STRESS (N/mm^2)	STRAIN
1st point for compression	40.1	.002
2nd point for compression	16	.05
1st point for tension	1	1. ** (modified for tension)
2nd point for tension	0.1	2. ** (modified for tension)

Distance from the reference axis of the strut cross section (mm)	Cross section area (mm^2)	Material type
2.5	665.	Strut concrete Type-2
7.5	665.	Strut concrete Type-2
12.5	567.5	Strut concrete Type-1
17.5	567.5	Strut concrete Type-1
2	7.0	Beam reinforcement
-2	8.0	Column reinforcement
-2.5	665.	Strut concrete Type-2
-7.5	665.	Strut concrete Type-2
-12.5	567.5	Strut concrete Type-1
-17.5	567.5	Strut concrete Type-1

$$\frac{\text{Cross-Section Type-2}}{\text{Cross-Section Type-1}} = 1.17 \text{ (which is in the range [1.15-1.2])}. \textit{ See page 92}$$

The curve in the Figure 7-16, shows that the maximum load sustained by the specimen is 278 kN, at the drift of 1.77%. These values are comparable to the experimental values of 262 kN, and 1.77%. By the end of the test, the analytical value shows the lateral load of 115 kN corresponding to the drift of 3.57%, which is almost identical to the values of experimental hysteretic loop in the second repetition of the last load step

Test #6
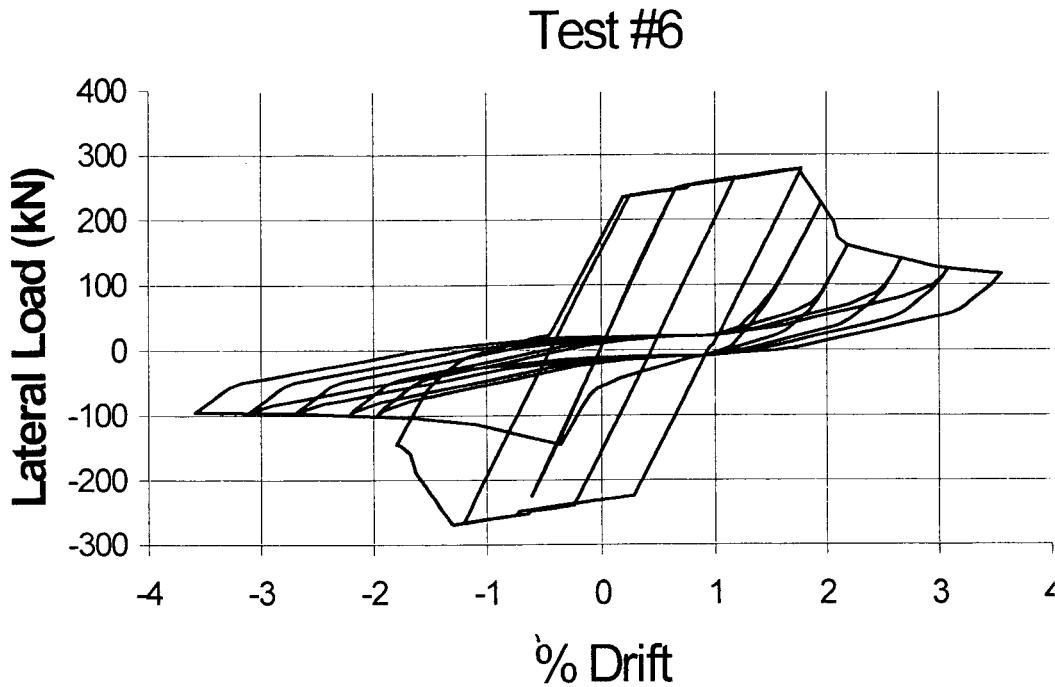
Figure 7-16 Load-Drift curve (Proposed model, DRAIN-2DX)

7.5.3   Specimen Tests #4

7.5.3.1 Experimental Results

The specimen #4 was loaded with $0.25f'_cA_g$. Hairline flexural cracking started in the second load step. The first yielding occurred in a top, longitudinal bar in load step nine. The lateral load at yielding was 50.7 kips (226 kN) at a lateral displacement of 0.45 in. (11.4 mm). Measurable flexural cracks in the beam and shear cracks in the joint appeared during the tenth load step corresponding to a lateral load of approximately 60kips (267 kN). The joint ultimately failed at a displacement of 1.45 in. (37 mm) corresponding to a drift of 3.57%, and the load had dropped to 23 kips (102 kN). The peak lateral load sustained by the specimen was 62.0 kips (276 kN). Figure 7-17 shows the experimental result for lateral load-drift curve of the specimen #4

119
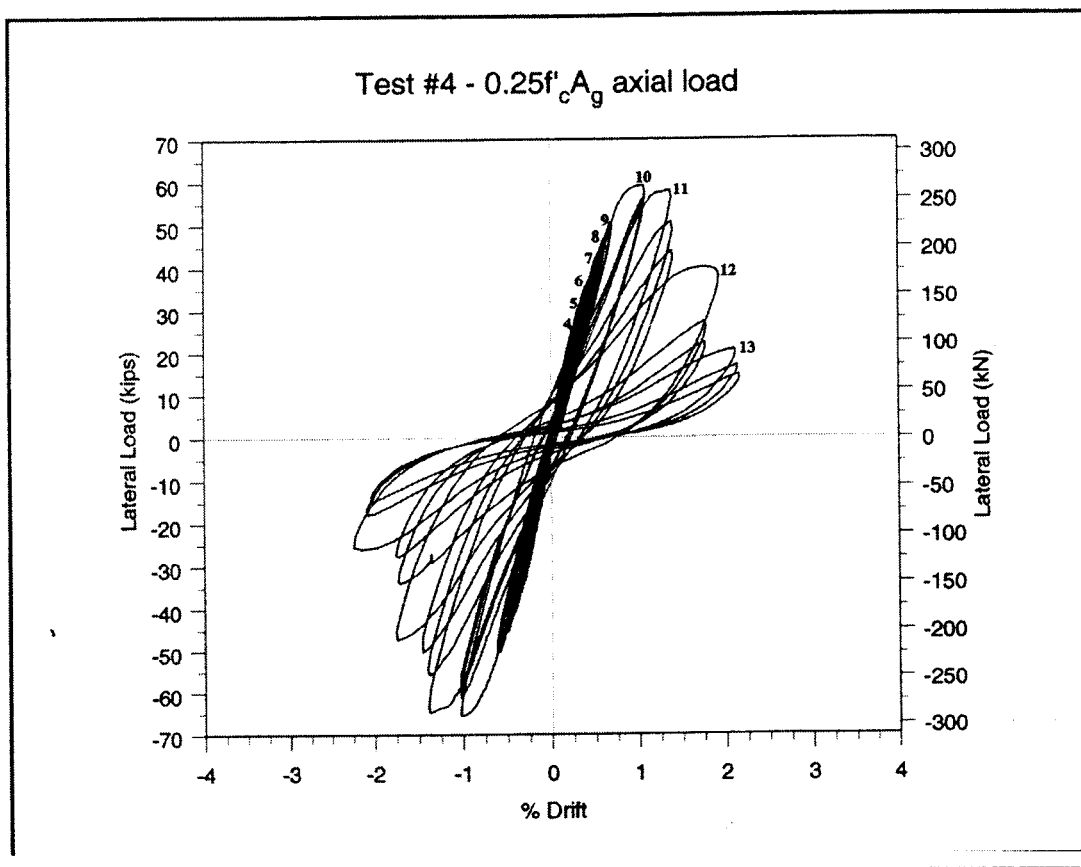
Figure 7-17 Test #4 load-drift curve (Experimental)

7.5.3.2 Modeling in IDARC2D

The procedure for test #6 is similar to Test #2, the only difference are the values shown in Table 7-14.

Table 7-14 Input properties for Test #4

f'c (N/mm²)	Ec (N/mm²)	HC	HBD	HBE	HS
41	30000	1	0.52	0.97	1

After execution of the program, the lateral load-drift curve, which is shown in Figure 7-18, is obtained. The result data show that the maximum lateral load sustained by the specimen was 269 kN, and at drift of 0.45%, corresponding to the yielding point of

120

the reinforcement. The maximum load is comparable to the value of experiment (276 kN), but the corresponding drift (1.15%), is different. At the end of the test, the load had dropped to 96 kN, at the drift of 2.2%, which similar to the experimental values of 102kN, and 2.2%, respectively.
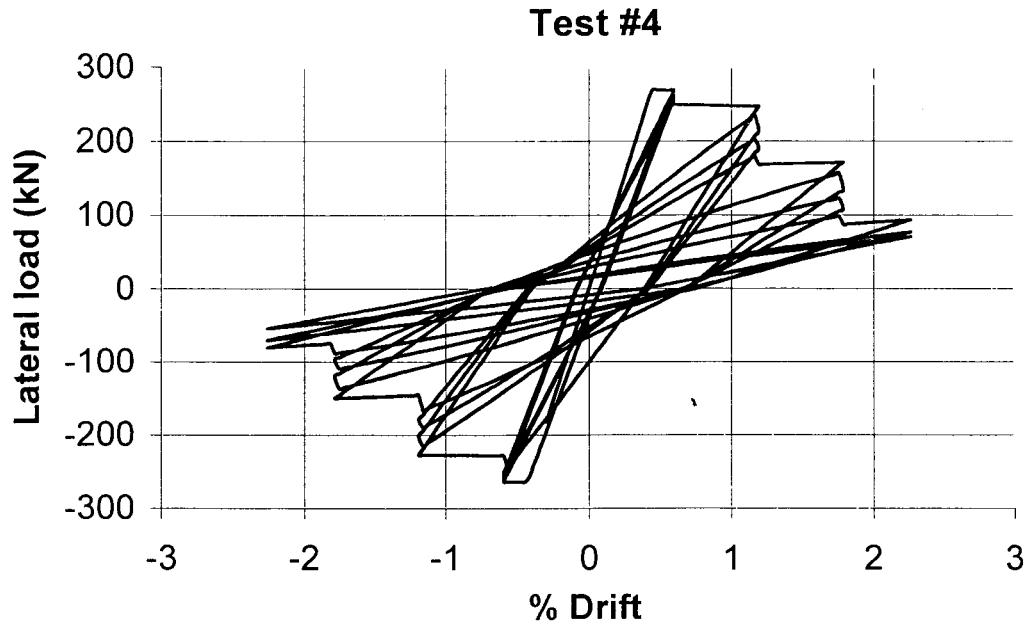

Figure 7-18 Load-drift curve (IDARC-2D)

7-5-3-3 Modeling in DRAIN-2DX

The procedure for modeling the test in DRAIN-2DX is the same for all four specimens. In test#4, the mentioned parameters in section 6-4 are defined as shown in Tables 7-15 through 7-18. The areas of the concrete types in the diagonal struts are calculated, as discussed in section 6-4. After the execution of the program the curve in Figure 7-19 is obtained.

Table 7-15 Concrete material for column for Test #4

	STRESS (N/mm^2)	STRAIN
1st point for compression	20.5	.000683
2nd point for compression	40.1	.002
3rd point for compression	8.2	.017
1st point for tension	3.57	.00016
2nd point for tension	0.1	.00147

121

Table 7-16 Concrete material for beam Test #4

	STRESS (N/mm^2)	STRAIN
1st point for compression	20.5	.000683
2nd point for compression	40.1	.002
3rd point for compression	8.2	.017
1st point for tension	3.57	.00016
2nd point for tension	0.1	.00147

Table 7-17 Concrete material Type-1 for diagonal struts for Test #4

	STRESS (N/mm^2)	STRAIN
1st point for compression	41	.002
2nd point for compression	8	.05
1st point for tension	1	1. ** (modified for tension)
2nd point for tension	0.1	2. ** (modified for tension)

Table 7-18 Concrete material Type-2 for diagonal struts for Test #4

	STRESS (N/mm^2)	STRAIN
1st point for compression	41	.002
2nd point for compression	17	.05
1st point for tension	1	1. ** (modified for tension)
2nd point for tension	0.1	2. ** (modified for tension)

Distance from the reference axis of the strut cross section (mm)	Cross section area (mm^2)	Material type
2.5	595	Strut concrete Type-2
7.5	595	Strut concrete Type-2
12.5	570.	Strut concrete Type-1
17.5	570	Strut concrete Type-1
2	7.0	Beam reinforcement
-2	7.0	Column reinforcement
-2.5	595	Strut concrete Type-2
-7.5	595	Strut concrete Type-2
-12.5	570	Strut concrete Type-1
-17.5	570	Strut concrete Type-1

$$\frac{\text{Cross-Section Type-2}}{\text{Cross-Section Type-1}} = 1.04 \text{ (which is in the range [1.05-1.10]). } See\ page\ 92$$

The curve in the Figure 7-19, shows that the maximum load sustained by the specimen is 267 kN, at the drift of 1.20%. These values are comparable to the experimental values of 276 kN, and 1.15%. By the end of the test, the analytical value shows the lateral load of 102 kN corresponding to the drift of 2.2%, which is almost identical to the values of experimental hysteretic loop in the first cycle of the last load step.

Test #4
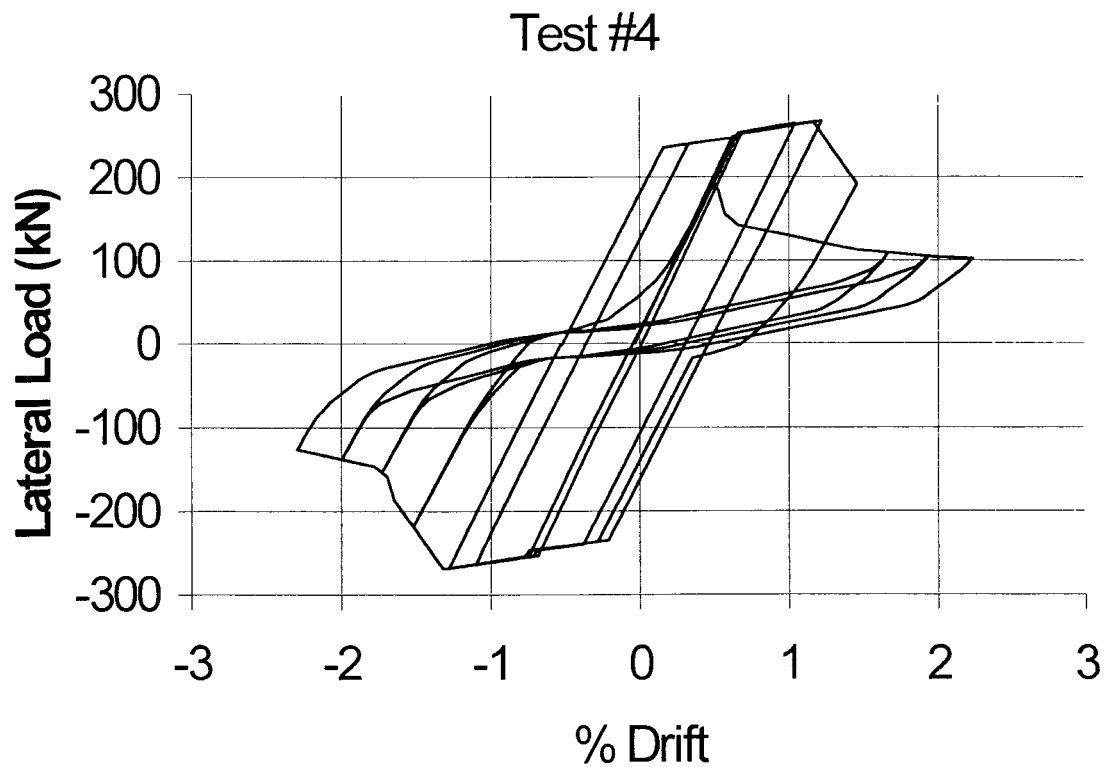
Figure 7-19 Load-Drift curve (Proposed model, DRAIN-2DX)

7.5.4   Specimen Tests #5

7-5-4-1 Experimental Results

The specimen #5 was loaded with $0.25f'_cA_g$. The first yielding occurred in a top, longitudinal bar in load step nine. The lateral load at yielding was 52.0 kips (231 kN) at a lateral displacement of 0.70 in. (17.8 mm). The joint ultimately failed at a displacement of 1.90 in. (48 mm) corresponding to a drift of 2.90%, and the lateral had dropped to 22 kips (98 kN). The peak lateral load sustained by the specimen was 60.0 kips (267 kN). Figure 7-20, shows the experimental result for lateral load-drift curve of the specimen #5

124
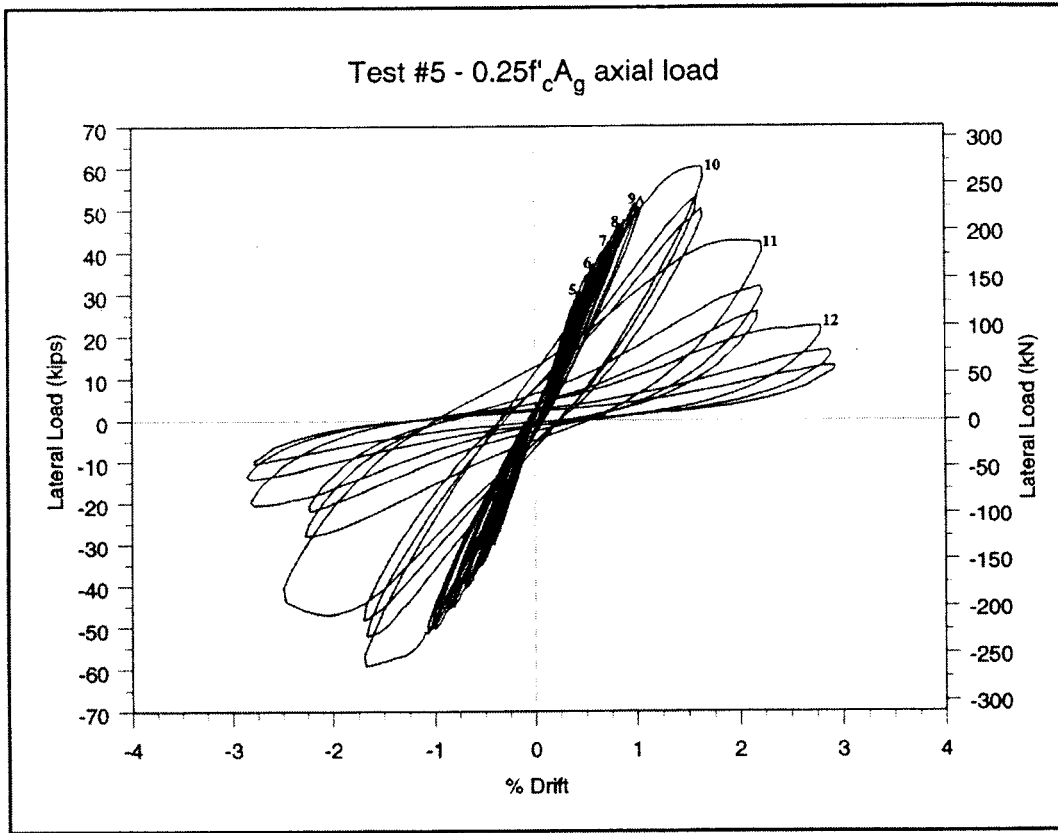
Figure 7-20 Test #5 load-drift curve (Experimental)

7-5-4-2 Modeling in IDARC2D

The procedure for test #5 is similar to Test #2, the only differences are the values shown in Table 7-19.

Table 7-19 Input properties for Test #5

f'c (N/mm^2)	Ec (N/mm^2)	HC	HBD	HBE	HS
37	28000	1	0.50	0.95	1

After execution of the program, the lateral load-drift curve, which is shown in Figure 7-21, is obtained. The result data show that the maximum lateral load sustained by the specimen was 268, and at drift of 0.6%, corresponding to the yielding point of the reinforcement. The maximum load is comparable to the value of experiment (267 kN),

125

but the corresponding drift (1.70%), is different. At the end of the test, the load had dropped to 100 kN, at the drift of 2.9%, which similar to the experimental values of 98 kN, and 2.9%, respectively.
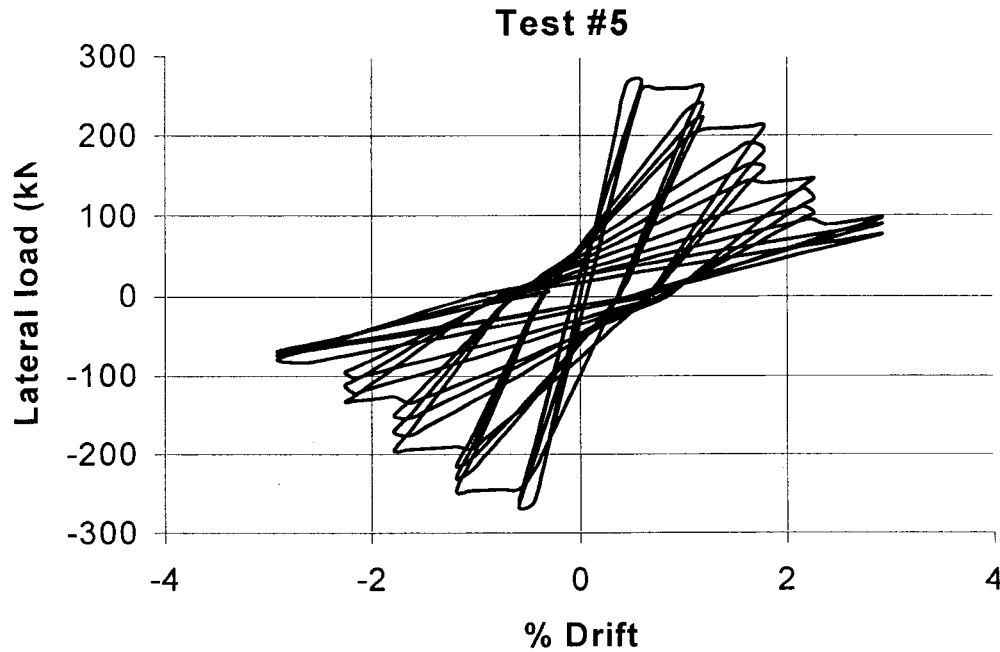

Figure 7-21 Load-drift curve (IDARC-2D)

7-5-4-3 Modeling in DRAIN-2DX

The procedure for modeling the test in DRAIN-2DX is the same for all four specimens. In test#4, the mentioned parameters in section 6-4 are defined as shown in Tables 7-20 through 7-23. The areas of the concrete types in the diagonal struts are calculated, as discussed in section 6-4. After the execution of the program the curve in Figure 7-22 is obtained.

Table 7-20 Concrete material for column for Test #5

	STRESS (N/mm^2)	STRAIN
1st point for compression	18.5	.00065
2nd point for compression	3.7	.002
3rd point for compression	7.4	.017
1st point for tension	3.4	.000158
2nd point for tension	0.1	.00146

126

Table 7-21 Concrete material for beam for Test #5

	STRESS (N/mm^2)	STRAIN
1st point for compression	18.5	.00065
2nd point for compression	37	.002
3rd point for compression	7.4	.017
1st point for tension	3.4	.000158
2nd point for tension	0.1	.00146

Table 7-22 Concrete material Type-1 for diagonal struts for Test #5

	STRESS (N/mm^2)	STRAIN
1st point for compression	37	.002
2nd point for compression	7.4	.05
1st point for tension	1	1. ** (modified for tension)
2nd point for tension	0.1	2. ** (modified for tension)

Table 7-23 Concrete material Type-2 for diagonal struts for Test #5

	STRESS (N/mm^2)	STRAIN
1st point for compression	37	.002
2nd point for compression	15	.05
1st point for tension	1	1. ** (modified for tension)
2nd point for tension	0.1	2. ** (modified for tension)

Distance from the reference axis of the strut cross section (mm)	Cross section area (mm^2)	Material type
2.5	665.	Strut concrete Type-2
7.5	665.	Strut concrete Type-2
12.5	640.	Strut concrete Type-1
17.5	640.	Strut concrete Type-1
2	7.0	Beam reinforcement
-2	8.0	Column reinforcement
-2.5	665.	Strut concrete Type-2
-7.5	665.	Strut concrete Type-2
-12.5	640.	Strut concrete Type-1
-17.5	640.	Strut concrete Type-1

$$\frac{\text{Cross-Section Type-2}}{\text{Cross-Section Type-1}} = 1.04 \text{ (which is in the range [1.05-1.10])}. \textit{ See page 95}$$

The curve in Figure 7-22 shows that the maximum load sustained by the specimen is 269 kN, at the drift of 1.40%. These values are comparable to the experimental values of 267 kN, and 1.70%. By the end of the test, the analytical value shows the lateral load of 98 kN corresponding to the drift of 2.9%, which is almost identical to the values of experimental hysteretic loop in the first cycle of the last load step.

Test #5
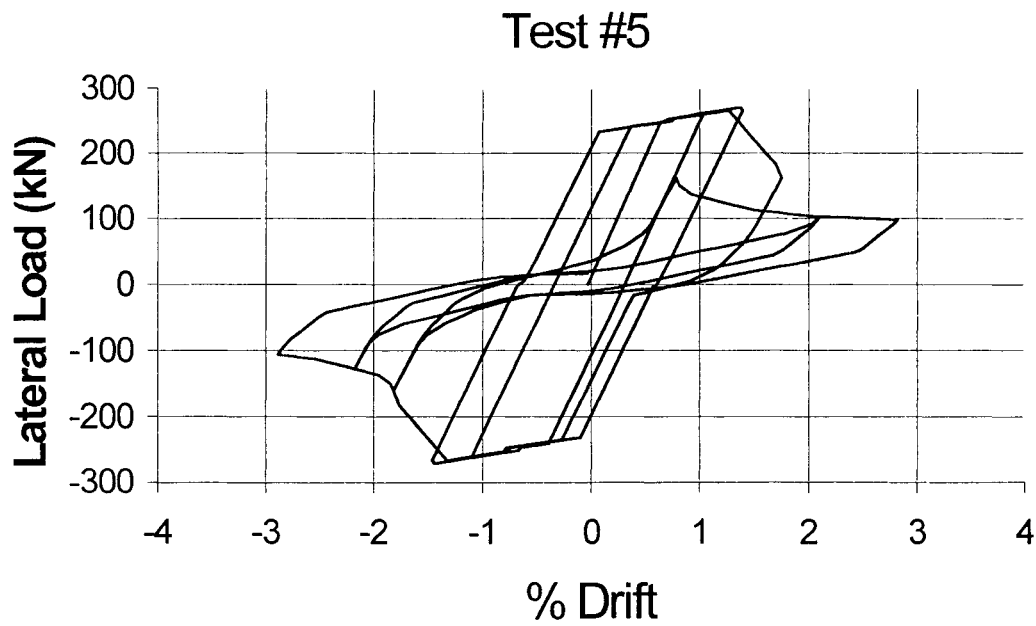
Figure 7-22 Load-Drift curve (Proposed model, DRAIN-2DX)

In Figures 7-23 through 7-26 the experimental result, and analytical results for each test, using IDARC2D, and DRAIN-2DX (the proposed model), are repeated for comparison.
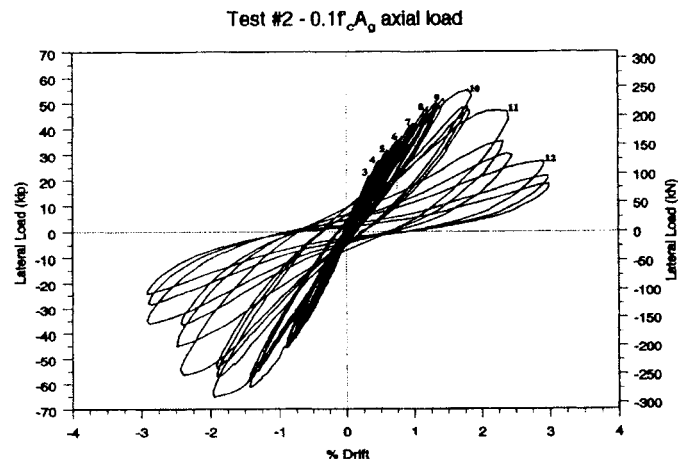
(a) Experiment
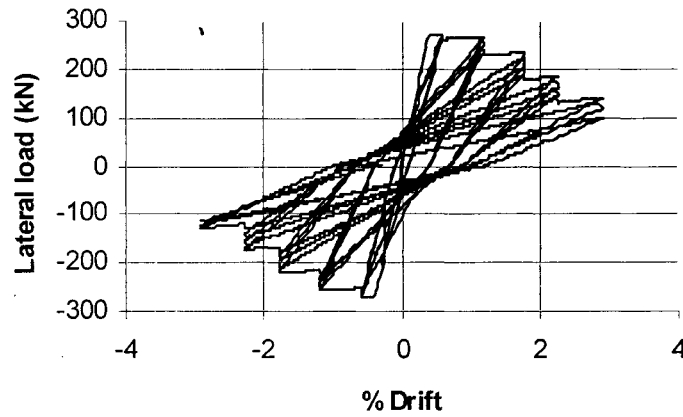
(b) IDARC2D
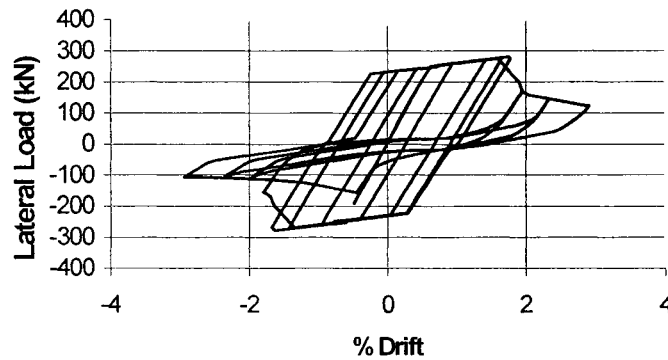
(c) DRAIN-2DX

Figure 7-24 Comparison of the experimental and analytical results (Test#2)
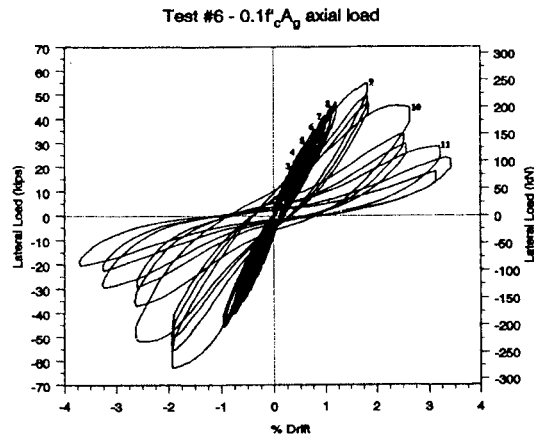
(a) Experiment
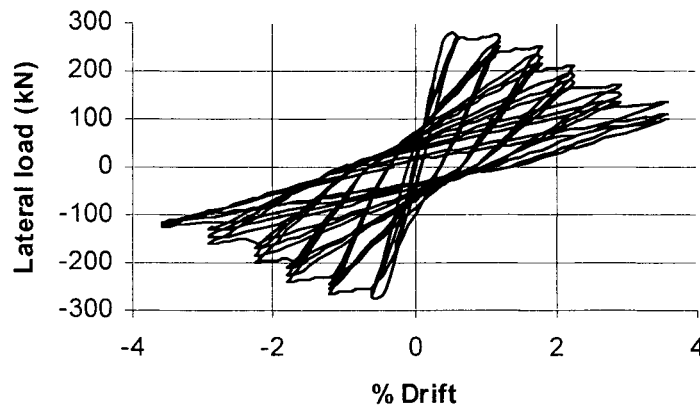
(b) IDARC2D
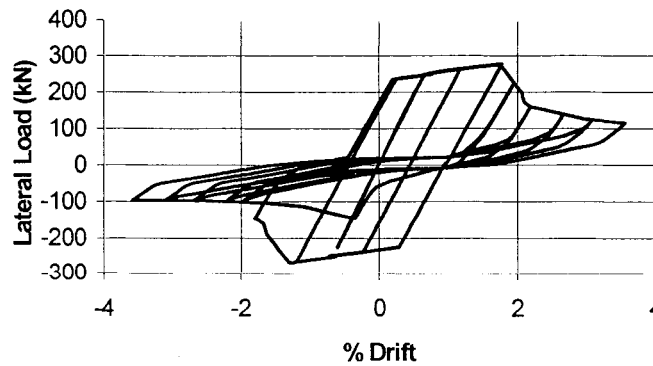
(c) DRAIN-2DX

Figure 7-25 Comparison of the experimental and analytical results (Test#6)

131

(a) Experiment

(b)IDARC2D
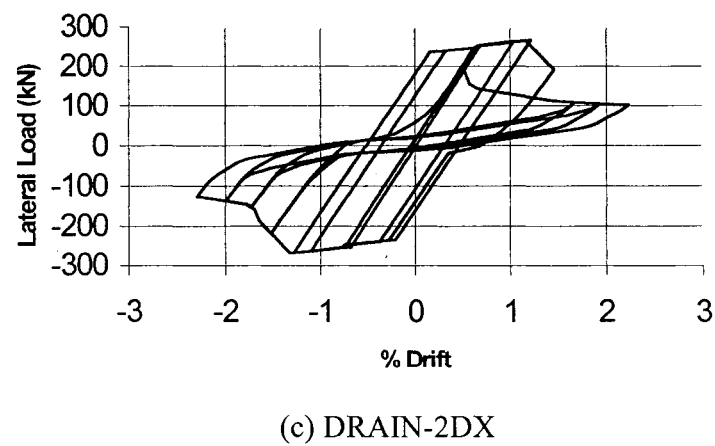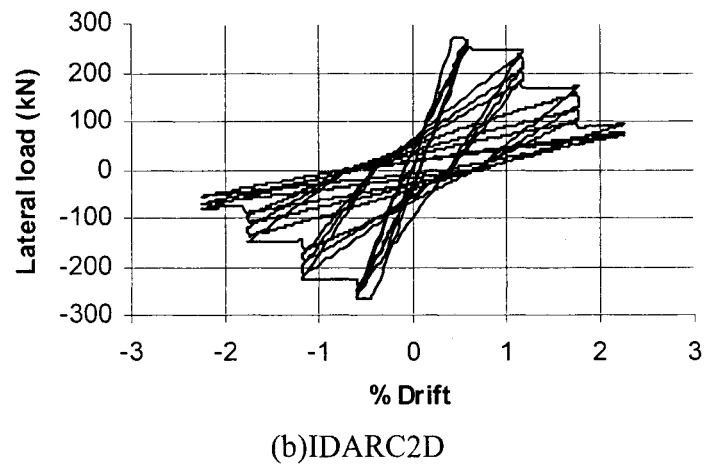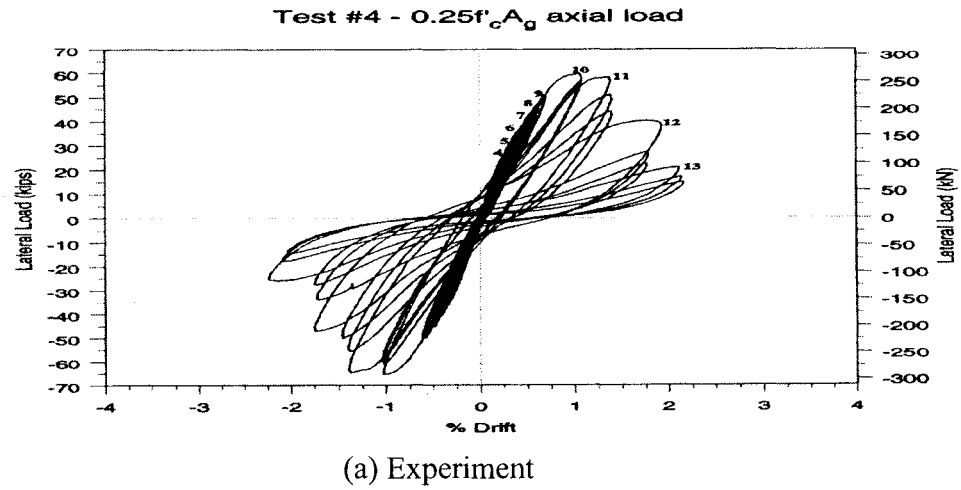
(c) DRAIN-2DX

Figure 7-26 Comparison of the experimental and analytical results (Test#4)

132
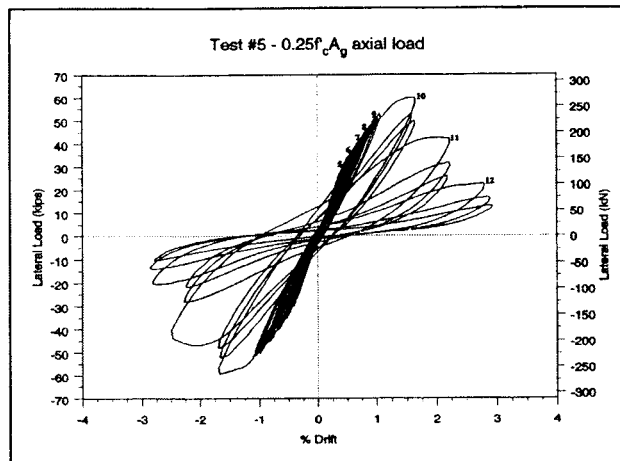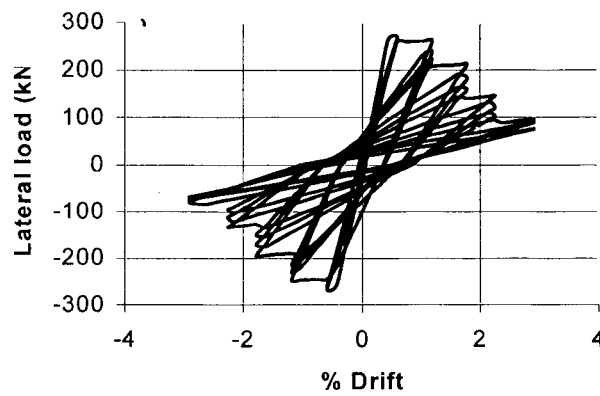
(a) Experiment

(b) IDARC2D
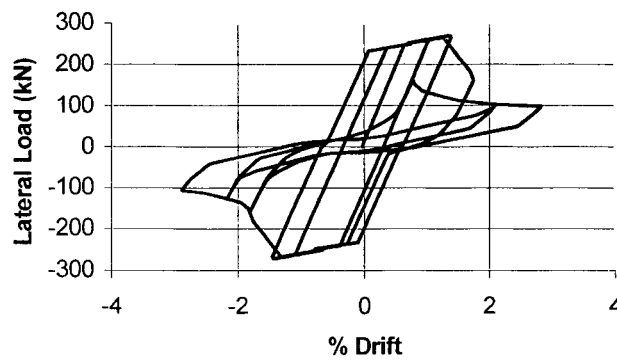
(c) DRAIN-2DX

Figure 7-27 Comparison of the experimental and analytical results (Test#5)

133

CHAPTER 8

SUMMARY, CONCLUSIONS, AND RECOMMENDATIONS

8.1 Summary

The objectives of this research were to discuss the behavior of reinforced concrete beam-column joints in shear, and to analytically evaluate the behavior of pre-seismic code designed exterior beam-column joint under application of cyclic loading. A new model for shear behavior of external beam-column joint was also proposed. The analytical modeling in this study was done, using two different well-known computer programs for nonlinear dynamic analysis of frame structures, DRAIN_2DX (element type 15), and IDARC2D. The advantages of using each one for the beam-column joints in the reinforced concrete structures are discussed.

The first phase of analytical modeling in this study was simulation of an experimental test on a circular reinforced concrete column, using the above-mentioned programs. The column was under the application of cyclic lateral displacement on the column's top while an axial load was applied on the column. This part also discussed the modeling of the circular cross-section with fiber elements. Both programs were able to predict the behavior of the experiment with very similar results.

The new model for exterior beam-column joints, proposed in this study, is based on the well-known "strut and ties model", and considering the changes in the location of the resultant of forces on the joint perimeter, during load reversals. This was implemented by using fiber concept in DRAIN-2DX program.

The second phase of the analytical modeling in this study was simulation of experimental tests on four external beam-column joints under application of cyclic lateral displacement on the beam's tip, while an axial load was present on the column's top.

The results of the analyses were compared to experimental evidences, and the advantages of using each program, was discussed.

8.2 Conclusions

Based on the results of the study described in this thesis, the following conclusions were made.

1- Reinforced beam-column joint with no shear reinforcement in the joint zone, experiences brittle joint shear failure during earthquake load reversals.

2- The shear behavior of the external joint could be modeled by application of the well-known "strut and ties model", and considering the changes in the location of the resultant of forces on the joint perimeter.

3- A new model was proposed to predict the behavior of external beam-column joint in shear. The model adopts the diagonal strut model (Park and Paulay) with consideration of the change in the location of the resultant of compression and tension forces on the joint panel perimeter, which was discussed in Shiohara's model. These concepts were implemented in the nonlinear analysis program DRAIN-2DX, using fiber elements.

4- A macro-model based model using IDARC2D, although had limited features in modeling the joint zone in terms of content of reinforcement, and also application of different directions of loading to the structure, was able to simulate the hysteretic behavior, and degrading shear resistance mechanism of the external joints. The simulation requires exact values of hysteretic rules parameter, which is difficult to determine in the case of the prediction of behavior of elements.

The main advantage of the program was simplicity, and the speed in the analysis, which is important in the case of analysis of structures with several members.

5- The proposed new model using fiber element, was able to predict very comparable results to the experiment, by following a unified method for all specimens, and without requirement of determining several unknown exact values for factors that rules the behavior. The main advantage was high ability in the prediction of the behavior of the elements. The only problem was complexity and time consumption of the model.

Finally it should be noted that the proposed new model, presented in this study was based on limited experimental data. To establish a general conclusion on the ability of the model, a comprehensive testing program for shear deficient external joints is needed.

8.3 Recommendations for Future Researches

Further research is needed in the following areas:

1- This study had focused on the behavior of shear deficient joints, neglecting the bar-slip phenomenon. The main assumption was adequate anchorage, and perfect bond between reinforcement and concrete. A comprehensive model is needed with simultaneous regards to both degrading phenomena.

2- A parametric study is needed with more comprehensive experimental data to determine the ability of the proposed model to assess the behavior of external joints under different conditions of axial loads on the column, and different reinforcement contents and configurations in the joint zone.

3- After determination of the behavior of the beam-column joint in terms of determination of the degrading parameters, using the proposed model in DRAIN-2DX, then the results can be used by macro-element based programs like IDARC2D for analysis of the frame structures with several members.

REFERENCES

ACI Committee 318. 1971. "Building Code Requirements for Reinforced Concrete (ACI 318-71)", American Concrete Institute, Detroit, pp. 78.

ACI 224.2R-92. 2001. "Cracking of Concrete Members in Direct Tension", ACI manual of concrete practice, American Concrete Institute, Farmington Hill, MI.

Allahabadi, R. Powell, G.H. 1988."DRAIN-2DX User Guide." Technical Report UCB/EERC 88/06, University of California, Berkeley.

Baker, A. L. L., Amarakone, A. M. N. 1964. "Inelastic Hyperstatic Frames Analysis", Proceedings of the International Symposium on the Flexural Mechanics of Reinforced Concrete, ASCE-ACI, Miami, November, pp. 85-142.

Bashur, F.K, Darwin, D. 1978. "Nonlinear Model for Reinforced Concrete Slabs". Journal of Structural Division, ASCE, Vol. 104, No. ST1, pp. 157-170.

Blume, J. A., Newmark, N. M., and Corning, L. H. 1961. "Design of Multistory Reinforced Concrete Buildings for Earthquake Motion", Portland Cement Association, Chicago, pp. 318.

Clyde, C., Pantelides, C. P., and Reaveley, L. D. 2000. "Performance-Based Evaluation of Exterior Reinforced Concrete Building Joints for Seismic Excitation", Pacific Earthquake Engineering Research center, University of Utah. PEER Report 2000/05.

Chan,W. L. 1995. "The Ultimate Strength and Deformation of Plastic Hinges in Reinforced Concrete Frameworks", Magazine of Concrete Research, Vol. 7, No. 21, pp. 121-132.

Cheok, G. S. and Stone, W. C. 1990. "Behavior of 1/6 Scale Model Bridge Columns Subjected to Inelastic Cyclic Loading", ACI Structural Journal, Vol. 87, No. 6, pp. 630-638.

Cusson, D., and Paultre, P. 1994. "High-Strength Concrete Columns Confined by Rectangular Ties", ASCE Journal of Structural Engineering, Vol. 120, No. 3, pp. 783-804.

D. C. Kent. 1969. "Inelastic behavior of reinforced concrete members with cyclic loading", Ph.D. Dissertation, University of Canterbury, Christchurch, New Zealand,

Dodd, L.L, Restrepo Posada, J.I. 1995. "A Model for Predicting the Cyclic Behavior of Reinforcing Steel", Journal of Structural Engineering, American Society of Civil Engineers, Vol. 121, No. 3, pp. 433-445.

El-Amoury, T. A. 2003. " Seismic Rehabilitation of Concrete Frame Beam-Column Joint" Ph.D. Dissertation, McMaster University, Hamilton, Canada

Evans, R.H., and Marathe, M.S. 1968. "Microcracking and Stress-Strain Curves for Concrete in Tension", Materials and Structures, Research and Testing (RILEM, Paris), V. 1, No. 1, pp. 61-64.

Gupta, A., and Krawinkler, H. 2000. "Estimation of Seismic Drift Demands for Frame Structures," International Journal for Earthquake Engineering and Structural Dynamics, Vol. 29, No. 10,

Hakuto, S., Park, R., Tanaka, H. 2000. "Seismic load test on interior and exterior beam-column joints with substandard reinforcing details" ACI structural journal. V.97, No.1

Hoseini-Tabatabaii M. 2000. "Nonlinear Analysis of 2-D Reinforced Concrete Frames Considering the Confining Effect of Transverse reinforcement," MS Thesis, Ferdowsi University, Mashhad-Iran.

Kent, D. C. 1969. " Inelastic behavior of reinforced concrete members with cyclic loading", Ph.D. Dissertation, University of Canterbury, Christchurch, New Zealand

Kent, D. C., Park, R. 1971. "Flexural Members with Confined Concrete", Journal of the Structural Division, ASCE, V. 97, No. ST7, pp. 1969-1990.

Kwak, H. G., Filippou, F. C. 1990. "Finite element analysis of reinforced concrete structures under monotonic loads". Report No. UCB/SEMM-90/14 Structural engineering mechanics and materials. Department of Civil Engineering, University of California, Berkeley, California.
www.ce.berkeley.edu/~filippou/Research/ Publications/Reports/semm9014.pdf

Laible, J.P., R.N. White, P. Gergely. 1977. "Experimental Investigation of Seismic Shear Transfer Across Cracks in Concrete Nuclear Containment Vessels." *ACI Special Publication* 539 (1977): 203-226

Mander, J.B., Priestley, M.J.N., Park, R. 1988. "Theoretical Stress-Strain model for Confined Concrete", Journal of Structural Engineering , ASCE, V.114, No.8, pp.1804-1826.

Mehta, P. K., P. J. M. Monteiro. 1993. "Concrete: Properties, Microstructure and Materials", The McGraw-Hill Companies, Inc., New York.

Ngo, D. Scordelis, A.C. 1967. "Finite Element Analysis of Reinforced Concrete Beams," Journal of ACI, Vol. 64, No. 3, pp. 152-163.

Paulay, T., Loeber P.J. 1977. "Shear Transfer By Aggregate Interlock." ACI Special Publication 421 (1977): 1-15.

Paulay, T., Priestly, M. J. N. 1992. "Seismic design of reinforced concrete and masonry building", New York: Willey.

Popovics, S. 1969. "A Review of Stress-Strain Relationships for Concrete". Journal of ACI, Vol. 66, No. 5, pp. 756-764.

Prakash, V., Powell, G.H., and Campbell, S. 1993. "DRAIN-2DX: Base Program Description, and User Guide. Version 1.10". University of California at Berkeley.

Reinhorn AM, Kunnath SK, Valles-Mattox R. 1996. "IDARC 2D Version 4.0: Users Manual", State University of New York at Buffalo: Department of Civil Engineering.

Roy, H. E. H., Sozen, M. A. 1964. "Ductility of Concrete", Proceedings of the International Symposium on the Flexural Mechanics of Reinforced Concrete", ASCE-ACI, Miami, pp. 213-224.

Sargin, M. 1971. "Stress-Strain Relationships for Concrete and the Analysis of Structural Concrete Sections", Study No. 4, Solids Mechanics Division, University of Waterloo, Waterloo, Ontario, 167 pp.

Sheikh, S.A., Uzumeri, S.M. 1980. "Strength and Ductility of Tied Concrete Columns", Proceedings, ASCE, V. 106, ST5, pp. 1079-1102

Siohara, H. 1998. "A new model for joint shear failure of reinforced concrete interior beam-to-column joint", Journal of the School of Engineering, The University of Tokyo, Vol. XLV.

Soliman, M. T. M., Yu, C. W. 1967. "The Flexural Stress-Strain Relationships of Concrete Confined by Rectangular transverse reinforcement", Magazine of Concrete Research, Vol. 19, No. 61, pp. 223-238.

Spacone E, Filippou FC, Taucer FF. 1996a. "Fiber beam-column model for nonlinear analysis of R/C frames": part1. Formulation. Earthquake engineering & Structural Dynamics, Vol. 25, No. 7, pp. 711-725.

Stone, W. C., Cheok, G. C. 1989. "Inelastic Behavior of Full-Scale Bridge Columns Subjected to Cyclic Loading", NIST Building Science Series 166, National Institute of Standards and Technology, Gaitherburg, M. D.

Vebo, A., Gali, A. 1977. "Moment-Curvature relation of Reinforced Concrete Slabs", Journal of the Structural Division, ASCE, V. 103, No. ST3, pp. 515-531.

Xiao, Y., Esmaeily-G, A. 2002. "Seismic behavior of reinforced concrete columns subjected to variable axial loads". Seventh U.S. National Conference on Earthquake Engineering (7NCEE): Theme: Urban Earthquake Risk [electronic resource], Earthquake Engineering Research Institute, Oakland, California

APPENDIX A

Extract.xls

The DRAIN-2DX output files are usually very large in size, so obtaining the relationship between the applied load and the corresponding displacement for a selected node is rather difficult. In this study because the average size of the output file was about 15 MB, a program (Extract.xls), which is a Visual Basic application in Microsoft-Excel was written to extract the required data for a selected point. When the load-displacement relationship for a point is required, the *RESULT section in the input file should only include the selected point. For example in the example of the exterior joint model because the load-displacement of the beam-tip (node 7) was required the corresponding section in the input file is:

*RESULTS

! nodes 7

NSD   001   7

The program is able to extract the required data related to the load-displacement of the selected point throughout the number of segments in the program. It is important to note that the program DRAIN-2DX allocates numbers from 1 to 9999 to each event in a segment. The program Extract.xls, then extracts every event in the order they are numbered, segment after segment. After the event number "9999" the DRAIN-2DX prints "*****" in front of the events and the program Extract.xls is not able to read the event number, so it is required to set the "Displacement increment per step" and the "displacement increment for analysis segment" parameters, so as to have the maximum event number of 9999. For example if the displacement increment for analysis segment is 150, and the displacement increment per step is 0.01, the total number of events in that segment is 15000. It is recommended to split the displacement increment for analysis segment, which is 150, to two segments of 75.

After the output file is obtained, the word "END" should be printed in the end of the output file. The file should then be saved.

By clicking on the Ectract.xls the program will prompt the user to browse and select the output file. The required data will shortly be stored in a text document on the desktop.

The source code for Extract.xls
Option Explicit
Public TexName As String, DaNum, DaDate
Public Row1, roW2, newFname, xlName, daTime
Public Row(1 To 10000)
'+---
'| 1. Open the original text file, parse first line
'| 2. Parse the second line
'| 3. Write to a new text file in the perferred format
'| 4. Open the new text file and SaveAs XLS
'+---
Sub ExtractSegments()
    Dim i
    Dim TotalLines
    Dim A
    Dim ExtractedLine
    Dim Msg, Ans
    Dim LastSegNumber
    On Error Resume Next
    Msg = "You must put END at the end of the file"& vbCrLf
    Msg = Msg & "To continue select YES otherwise select NO to cancel"
    Ans = MsgBox(Msg, vbYesNo + vbQuestion)
    If Ans = vbNo Then Exit Sub
    Close #1, #2
    TexName = Application.GetOpenFilename
    newFname = Application.Text(Now(), "yyddmm") _ & "file" & Hex(Hour(Now())) &
".txt"   'Write name
    Open ThisWorkbook.Path & "\" & newFname For Output As #2
    Open TexName For Input Access Read As #1
    Do While Not EOF(1) 'Read #1
        For i = 1 To 10000
            Line Input #1, Row(i)
            If Row(i) = "END" Then GoTo Finished
            If Not Mid(Row(i), 5, 1) <= 9 Then Exit For
            If Mid(Row(i), 5, 1) <= 9 Then
                ExtractedLine = Row(i)
                Print #2, ExtractedLine
            End If
        Next i
    Loop   'get the next group
Finished:
    Close #1, #2   'close them up   "openNewF
    MsgBox "Finished writing new file to " _
    & ThisWorkbook.Path & "\" & xlName, vbOKOnly, "Done"
End Sub

A- 2

INPUT DATA FOR THE CIRCULAR COLUMN TEST
(IDARC2D)

CASE STUDY # 1 :
CONTROL DATA
1, 1, 1, 1, 0, 1, 0, 1
ELEMENT TYPES
1, 0, 0, 0, 0, 0, 0, 0, 0, 0
ELEMENT DATA
1, 0, 0, 0, 0, 0, 0, 0, 0
UNIT SYSTEM (KIPS/INCH)
1
FLOOR ELEVATIONS
360.0
DESCRIPTION OF IDENTICAL FRAMES
1
PLAN CONFIGURATION (SINGLE COLUMN LINE)
1
NODAL WEIGHTS
1, 1, 300.0
CODE FOR SPECIFICATION OF USER PROPERTIES
0
CONCRETE PROPERTIES
1, 5.2, 4110.0, 0.2, 0.624, 0.0, 0.0
REINFORCEMENT PROPERTIES
1, 68.9, 103.6, 27438.0, 0.0, 0.0
HYSTERETIC MODELING RULES
1
1,1,9,0,0.1,1,2
MOMENT CURVATURE ENVELOPE GENERATION
0
COLUMN DIMENSIONS
2
1,1,1,1, 360.0,0.0,0.0, 1000.0, 60.0, 2.5, 54.5, 25, 1.69, 0.625, 3.5
COLUMN CONNECTIVITY
1,1,1,1,0,1
ANALYSIS TYPE
4
STATIC ANALYSIS OPTION (Axial Force Only)
0,0,0,1
4,1
Nodal Loads
1, 1, 1, 1, 900.0

Quasistatic Analysis
1
1
1
301
```
    0.0   2.5    0.0  -2.80   0.0   3.5   7.060   3.5   0.0   -3.5
   -7.03  -3.5   0.0   3.50   7.08  3.5    0.0   -3.5  -7.02  -3.5
    0.0   5.0    9.0  10.60   9.0   5.0    0.0   -5.0  -9.0  -10.55
   -9.0  -5.0    0.0   5.0    9.0  10.6    9.0    5.0   0.0   -5.0
   -9.0  -10.55  -9.0  -5.0   0.0   5.0   10.0   13.5  14.08  13.5
   10.0   5.0    0.0  -5.0  -10.0 -13.5  -14.05 -13.5 -10.0   -5.0
    0.0   5.0   10.0  13.5   14.07 13.5   10.0    5.0   0.0   -5.0
  -10.0 -13.5  -14.05 -13.5 -10.0  -5.0
    0.0   5.0   10.0  13.5   14.08 13.5   10.0    5.0   0.0   -5.0
  -10.0 -13.5  -14.08 -13.5 -10.0  -5.0
    0.0   5.0   10.0  13.5   14.08 13.5   10.0    5.0   0.0   -5.0
  -10.0 -13.5  -14.07 -13.5 -10.0  -5.0
    0.0   5.0   10.0  13.5   14.10 13.5   10.0    5.0   0.0   -5.0
  -10.0 -13.5  -14.07 -13.5 -10.0  -5.0
    0.0   5.0   10.0  13.5   14.10 13.5   10.0    5.0   0.0   -5.0
  -10.0 -13.5  -14.07 -13.5 -10.0  -5.0
    0.0   5.0   10.0  13.5   14.12 13.5   10.0    5.0   0.0   -5.0
  -10.0 -13.5  -14.07 -13.5 -10.0  -5.0
    0.0   5.0   10.0  13.5   14.12 13.5   10.0    5.0   0.0   -5.0
  -10.0 -13.5  -14.07 -13.5 -10.0  -5.0
    0.0   5.0   10.0  13.5   14.12 13.5   10.0    5.0   0.0   -5.0
  -10.0 -13.5  -14.07 -13.5 -10.0  -5.0
    0.0   5.0   10.0  13.5   14.12 13.5   10.0    5.0   0.0   -5.0
  -10.0 -13.5  -14.07 -13.5 -10.0  -5.0
    0.0   5.0   10.0  13.5   14.10 13.5   10.0    5.0   0.0   -5.0
  -10.0 -13.5  -14.07 -13.5 -10.0  -5.0
    0.0   5.0   10.0  16.0   17.66 15.5   10.0    5.0   0.0   -5.0
  -10.0 -15.5  -17.66 -15.5 -10.0  -5.0
    0.0   5.0   10.0  16.0   17.66 15.5   10.0    5.0   0.0   -5.0
  -10.0 -15.5  -17.66 -15.5 -10.0  -5.0
    0.0   5.0   10.0  16.0   17.66 15.5   10.0    5.0   0.0   -5.0
  -10.0 -15.5  -17.66 -15.5 -10.0  -5.0
    0.0   6.0   12.0  20.0   21.30 20.0   12.0    6.0   0.0   -6.0
  -12.0 -20.0  -21.19 -20.0 -12.0  -6.0
    0.0   6.0   12.0  20.0   21.32 20.0   12.0    6.0   0.0   -6.0
  -12.0 -20.0  -21.27 -20.0 -12.0  -6.0   0.0
 0.05
```

SNAPSHOT OUTPUT
0,
0,0,0,0,0
OUTPUT CONTROL
1,6,1
CYC1.OUT
MISCELLANEOUS OUTPUT INFORMATION
1,0,0,0,0,0
COLUMN OUTPUT
1

INPUT DATA FOR EXTERIOR BEAM-COLUMN JOINT TEST #6
(IDARC2D)

CASE STUDY # 6:
CONTROL DATA
 2,1,2,2,0,0,0,1
ELEMENT TYPES
2,2,0,0,0,0,0,0,0,0
ELEMENT DATA
3,2,0,0,0,0,2,0,0
UNITS SYSTEM : KN - MM
2
FLOOR ELEVATIONS
500,2100
DESCRIPTION OF IDENTICAL FRAMES
1
PLAN CONFIGURATION: NO OF COLUMN LINES
3
NODAL WEIGHTS
1,1, 22.24, 22.24, 22.24
2,1, 0 ,1,0
CODE FOR SPECIFICATION OF USER PROPERTIES
0
CONCRETE PROPERTIES
1, 0.0401 ,30, 0, 0.0, 0.0, 0.0
2, 0.1,0,0,0,0,0
REINFORCEMENT PROPERTIES
1, 0.45, 0.6, 0, 0, 0
2, 0.47, 0.6, 0, 0, 0
HYSTERETIC MODELING RULES
1
1, 1,1,.52,.92,1,2
MOMENT CURVATURE ENVELOPE GENERATION
0
COLUMN DIMENSIONS
1
1,1,1,0,1600, 228, 0
    1, 406, 305   ,43 ,2560 ,9.5,127,0.5
    1, 406, 305   ,43 ,2560 ,9.5,127,0.5
1
2,2,1,0,500 , 0, 228
    1, 1500, 1500, 50, 2560, 11.3, 50, 1
    1, 1500, 1500, 50, 2560, 11.3, 50, 1

```
BEAM MOMENT CURVATURE ENVELOPE GENERATION
0
BEAM DIMENSIONS
1,1,2, 2170,750, 203
    1, 457.0, 305.0 ,305.0, 0, 43, 1161, 1161, 9.5, 150
    1, 457.0, 305.0 ,305.0, 0, 43, 1161, 1161, 9.5, 150
1,1,2, 2170,203, 750
    1, 457.0, 305.0 ,305.0, 0, 43, 1161, 1161, 9.5, 150
    1, 457.0, 305.0 ,305.0, 0, 43, 1161, 1161, 9.5, 150
COLUMN CONNECTIVITY
1,1,1,2,1,2
2,2,1,3,0,1
3,2,1,1,0,1
BEAM CONNECTIVITY
1,1,1,1,1,2
2,1,1,1,2,3
MOMENT RELEASES
1,1,2,2
2,1,3,2
ANALYSIS TYPE
4
STATIC ANALYSIS OPTION
0,1,0,0
1,1
nodal lateral load
1,1,1,642.18
QUASI-STATIC CYCLIC ANALYSIS
1
1
2
480
 0   5   0   -5
 0   5   0   -5
 0   5   0   -5
 0   5   10   5   0   -5   -10   -5
 0   5   10   5   0   -5   -10   -5
 0   5   10   5   0   -5   -10   -5
 0   5   10   15   20   15   10   5   0   -5   -10   -15   -20   -15  -10  -5
 0   5   10   15   20   15   10   5   0   -5   -10   -15   -20   -15  -10  -5
 0   5   10   15   20   15   10   5   0   -5   -10   -15   -20   -15  -10  -5
 0   5   10   15   20   25   30   25   20   15   10   5
 0  -5  -10  -15  -20  -25  -30  -25  -20  -15  -10  -5
 0   5   10   15   20   25   30   25   20   15   10   5
 0  -5  -10  -15  -20  -25  -30  -25  -20  -15  -10  -5
```

```
0  5  10  15  20  25  30  25  20  15  10  5
0  -5  -10  -15  -20  -25  -30  -25  -20  -15  -10  -5
0  5  10  15  20  25  30  35  38  35  30  25  20  15  10  5
0  -5  -10  -15  -20  -25  -30  -35  -38  -35  -30  -25  -20  -15  -10  -5
0  5  10  15  20  25  30  35  38  35  30  25  20  15  10  5
0  -5  -10  -15  -20  -25  -30  -35  -38  -35  -30  -25  -20  -15  -10  -5
0  5  10  15  20  25  30  35  38  35  30  25  20  15  10  5
0  -5  -10  -15  -20  -25  -30  -35  -38  -35  -30  -25  -20  -15  -10  -5
0  5  10  15  20  25  30  35  40  49  40  35  30  25  20  15  10  5
0  -5  -10  -15  -20  -25  -30  -35  -40  -49  -40 -35  -30  -25  -20  -15  -10  -5
0  5  10  15  20  25  30  35  40 49  40  35  30  25  20  15  10  5
0  -5  -10  -15  -20  -25  -30  -35  -40 -49 -40 -35  -30  -25  -20  -15  -10  -5
0  5  10  15  20  25  30  35  40  49  40 35  30  25  20  15  10  5
0  -5  -10  -15  -20  -25  -30  -35  -40  -49 -40  -35  -30  -25  -20  -15  -10  -5
 0  5  10  15  20  25  30  35  40  50  60 50  40 35  30  25  20  15  10  5
0  -5  -10  -15  -20  -25  -30  -35  -40  -50 -60 -50 -40 -35  -30  -25  -20  -15  -10  -5
0  5  10  15  20  25  30  35  40 50  60 50 40  35  30  25  20  15  10  5
0  -5  -10  -15  -20  -25  -30  -35  -40 -50  -60 -50 -50 -35  -30  -25  -20  -15  -10  -5
0  5  10  15  20  25  30  35  40  50  60  50  40 35  30  25  20  15  10  5
0  -5  -10  -15  -20  -25  -30  -35  -40  -50  -60  -50  -40 -35  -30  -25  -20  -15  -10  -5
0.05
SNAPSHOT OUTPUT CONTROL
0
0,0,0,0,0
OUTPUT CONTROL
2,10,1,2
LEVEL1.OUT
level2.out
MISCELLANIOUS OUTPUT
0,0,0,0,0,0
```

```
*STARTXX
  CNNPIER      0 1 1 1         ONE column
*NODECOORDS
! foundation
C    1    0.    0.
! beam-column joint
C    2    0.    9144.
*RESTRAINTS
! fixed supports at foundations
S 111        1
*ELEMENTGROUP
  15   1   1       0.        1 COLUMNS
   1   1   1   1   0   0   0   0   1
! concrete material
   3 2      0  .001
0.0179   .00063
0.0358   .002
0.0072   .035
0.0033   .000157
0.0001   .001453
! steel material
   2    .0001
  .475   .0025
  .62   .01
43
22.5     60750.     C01
67.5     60750.     C01
112.5    60750.     C01
157.5    59298.     C01
190.5    2904.      S01
202.5    59298.     C01
247.5    60750.     C01
292.5    60750.     C01
337.5    59298.     C01
342.9    2904.0     S01
382.5    59298.     C01
427.5    59298.     C01
457.20   2904.0     S01
472.5    59298.     C01
517.5    60750.     C01
562.5    59298.     C01
```

```
571.5    2904.0     S01
607.5    59298.     C01
647.7    3630.      S01
652.5    57120.     C01
685.8    726.0      S01
0.       1904       S01
-22.5    60750.     C01
-67.5    60750.     C01
-112.5   60750.     C01
-157.5   59298.     C01
-190.5   2904.      S01
-202.5   59298.     C01
-247.5   60750.     C01
-292.5   60750.     C01
-337.5   59298.     C01
-342.9   2904.0     S01
-382.5   59298.     C01
-427.5   59298.     C01
-457.20  2904.0     S01
-472.5   59298.     C01
-517.5   60750.     C01
-562.5   59298.     C01
-571.5   2904.0     S01
-607.5   59298.     C01
-647.7   3630.      S01
-652.5   57120.     C01
-685.8   726.0      S01
2.768E11 1.82E6          28.33      11.8
   2
   .15    F01
   .85    E01
   1    1    2    1  1
*RESULTS
! nodes 1 and 2
NSD   001      2
*NODALOAD
 HORN                   UNIT HORIZONTAL LOAD
S   0.    -1.   0.    2
*NODALOAD
 HORZ                   UNIT HORIZONTAL LOAD
S   1.    0.    0.    2
*PARAMETERS
! print only, every event
OS   0   0   -1   0   1000
*STAT
N    HORN     1.
```

```
L   10.   4545.
*STAT
N    HORZ      1.
D   2    0   1   1.      90.0  20   3   5
*STAT
N    HORZ      1.
D   2    0   1   .5      90.0  20   3   5    !--------+180
*STAT
N    HORZ      1.
D   0    2   1   .5      90.0  20   3   5
*STAT
N    HORZ      1.
D   0    2   1   1.      90.0  20   3   5    !------------- 0
*STAT
N    HORZ      1.
D   0    2   1   .5      90.0  20   3   5
*STAT
N    HORZ      1.   `
D   0    2   1   .1      90.0  20   3   5    !-------- -120
*STAT
N    HORZ      1.
D   2    0   1   .5      90.0  20   3   5
*STAT
N    HORZ      1.
D   2    0   1   1.      90.0  20   3   5
!------------------------------------------------------------------
*STAT
N    HORZ      1.
D   2    0   1   1.     100.0  20   3   5
*STAT
N    HORZ      1.
D   2    0   1   .50     40.0  20   3   5    !--------+140
*STAT
N    HORZ      1.
D   2    0   1   .5      60.0  20   3   5
*STAT
N    HORZ      1.
D   2    0   1   .1      60.0  20   3   5    !--------- +260
*STAT
N    HORZ      1.
D   0    2   1   .2      50.0  20   3   5
*STAT
N    HORZ      1.
D   0    2   1   .2      50.0  20   3   5
*STAT
N    HORZ      1.
```

```
D    0      2   1   .5      80.0   20   3  5
*STAT
N    HORZ      1.
D    0      2   1   1.0     80.0   20   3  5  !--------- 0
*STAT
N    HORZ      1.
D    0      2   1   1.      100.0  20   3  5
*STAT
N    HORZ      1.
D    0      2   1   .2      80.0   20   3  5
*STAT
N    HORZ      1.
D    0      2   1   .05     80.0   20   3  5  !--------- -260
*STAT
N    HORZ      1.
D    2      0   1   .2      70.0   20   3  5
*STAT
N    HORZ      1.                                                    `
D    2      0   1   .5      90.0   20   3  5
*STAT
N    HORZ      1.
D    2      0   1   1.0     100.0  20   3  5  !--------+ 0 ---------------------
!------------------------------------------------------------------ 27
*STAT
N    HORZ      1.
D    2      0   1   1.      100.0  20   3  5
*STAT
N    HORZ      1.
D    2      0   1   .5      90.0   20   3  5  !--------+190
*STAT
N    HORZ      1.
D    2      0   1   .2      70.0   20   3  5  !--------+260
*STAT
N    HORZ      1.
D    2      0   1   .1      60.0   20   3  5
*STAT
N    HORZ      1.
D    2      0   1   .05     40.0   20   3  5
*STAT
N    HORZ      1.
D    2      0   1   .02     40.0   20   3  5  !--------- +400
*STAT
N    HORZ      1.
D    0      2   1   .05     50.0   20   3  5
*STAT
N    HORZ      1.
```

```
D    0    2  1  .1     50.0   20  3  5
*STAT
N    HORZ    1.
D    0    2  1  .2     40.0   20  3  5    !--------+260
*STAT
N    HORZ    1.
D    0    2  1  .5     50.0   20  3  5
*STAT
N    HORZ    1.
D    0    2  1  .5     50.0   20  3  5    !--------+160
*STAT
N    HORZ    1.
D    0    2  1  .5     80.0   20  3  5
*STAT
N    HORZ    1.
D    0    2  1  1.     80.0   20  3  5    !--------- +0
*STAT
N    HORZ    1.
D    0    2  1  1.     100.0  20  3  5
*STAT
N    HORZ    1.
D    0    2  1  .5     90.0   20  3  5    !-------- -190
*STAT
N    HORZ    1.
D    0    2  1  .05    70.0   20  3  5
*STAT
N    HORZ    1.
D    0    2  1  .02    70.0   20  3  5    !-------- -330
*STAT
N    HORZ    1.
D    0    2  1  .01    70.0   20  3  5    !--------- -400
*STAT
N    HORZ    1.
D    2    0  1  .02    50.0   20  3  5
*STAT
N    HORZ    1.
D    2    0  1  .02    50.0   20  3  5
*STAT
N    HORZ    1.
D    2    0  1  .04    40.0   20  3  5    !-------- -260
*STAT
N    HORZ    1.
D    2    0  1  .05    50.0   20  3  5
*STAT
N    HORZ    1.
D    2    0  1  .1     50.0   20  3  5
```

```
*STAT
N   HORZ    1.
D   2       0   1   .5      80.0    20   3   5
*STAT
N   HORZ    1.
D   2       0   1   1.      80.0    20   3   5   !--------- 0  !
!------------------------------------------------------------ 64
*STAT
N   HORZ    1.
D   2       0   1   1.      100.0   20   3   5
*STAT
N   HORZ    1.
D   2       0   1   .5      90.0    20   3   5
*STAT
N   HORZ    1.
D   2       0   1   .5      70.0    20   3   5   !--------+260
*STAT
N   HORZ    1'.
D   2       0   1   .1      60.0    20   3   5
*STAT
N   HORZ    1.
D   2       0   1   .05     60.0    20   3   5 !--------+380
*STAT
N   HORZ    1.
D   2       0   1   .05     40.0    20   3   5
*STAT
N   HORZ    1.
D   2       0   1   .05     40.0    20   3   5   !--------- +460
*STAT
N   HORZ    1.
D   0       2   1   .05     50.0    20   3   5
*STAT
N   HORZ    1.
D   0       2   1   .05     50.0    20   3   5
*STAT
N   HORZ    1.
D   0       2   1   .05     50.0    20   3   5
*STAT
N   HORZ    1.
D   0       2   1   .05     50.0    20   3   5
*STAT
N   HORZ    1.
D   0       2   1   .1      40.0    20   3   5   !--------+220
*STAT
N   HORZ    1.
D   0       2   1   .2      50.0    20   3   5
```

```
*STAT
N    HORZ    1.
D    0     2   1   .5      50.0    20   3   5
*STAT
N    HORZ    1.
D    0     2   1   .8      50.0    20   3   5    !--------+70
*STAT
N    HORZ    1.
D    0     2   1   .5      100.0   20   3   5
*STAT
N    HORZ    1.
D    0     2   1   .1      70.0    20   3   5    !--------- -100
*STAT
N    HORZ    1.
D    0     2   1   .1      70.0    20   3   5
*STAT
N    HORZ    1.
D    0     2   1   .5      70.0    20   3   5    !-------- -240`
*STAT
N    HORZ    1.
D    0     2   1   .5      50.0    20   3   5
*STAT
N    HORZ    1.
D    0     2   1   .2      50.0    20   3   5
*STAT
N    HORZ    1.
D    0     2   1   .1      40.0    20   3   5    !-------- -380
*STAT
N    HORZ    1.
D    0     2   1   .05     40.0    20   3   5
*STAT
N    HORZ    1.
D    0     2   1   .05     40.0    20   3   5    !--------- -460
*STAT
N    HORZ    1.
D    2     0   1   .05     50.0    20   3   5
*STAT
N    HORZ    1.
D    2     0   1   .05     50.0    20   3   5
*STAT
N    HORZ    1.
D    2     0   1   .1      50.0    20   3   5
*STAT
N    HORZ    1.
D    2     0   1   .2      50.0    20   3   5
*STAT
```

A-15

```
N    HORZ    1.
D    2    0    1    .3      60.0   20   3   5
*STAT
N    HORZ    1.
D    2    0    1    .5      80.0   20   3   5
*STAT
N    HORZ    1.
D    2    0    1    1.      120.   20   3   5      !--------- 0
!-------------------------------------------------------
*STAT
N    HORZ    1.
D    2    0    1    1.      200.0  20   3   5
*STAT
N    HORZ    1.
D    2    0    1    .50     90.0   20   3   5      !--------+290
*STAT
N    HORZ    1.
D    2    0    1    .5      90.0   20   3   5
*STAT
N    HORZ    1.
D    2    0    1    .5      90.0   20   3   5
*STAT
N    HORZ    1.
D    2    0    1    .1      80.0   20   3   5      !--------- +550
*STAT
N    HORZ    1.
D    0    2    1    .2      200.0  20   3   5
*STAT
N    HORZ    1.
D    0    2    1    .2      200.0  20   3   5
*STAT
N    HORZ    1.
D    0    2    1    .5      80.0   20   3   5
*STAT
N    HORZ    1.
D    0    2    1    1.0     70.0   20   3   5      !--------- 0
*STAT
N    HORZ    1.
D    0    2    1    1.      200.   20   3   5
*STAT
N    HORZ    1.
D    0    2    1    .2      200.   20   3   5
*STAT
N    HORZ    1.
D    0    2    1    .2      80.    20   3   5
*STAT
```

```
N    HORZ    1.
D    0    2    1    .05    70.0    20    3    5    !--------- -550
*STAT
N    HORZ    1.
D    2    0    1    .2     70.0    20    3    5
*STAT
N    HORZ    1.
D    2    0    1    .2     90.0    20    3    5
*STAT
N    HORZ    1.
D    2    0    1    .5     190.    20    3    5
*STAT
N    HORZ    1.
D    2    0    1    1.0    200.0   20    3    5    !--------+ 0 --
*STOP
```

INPUT DATA FOR EXTERIOR BEAM-COLUMN JOINT TEST #6
(DRAIN-2DX)

```
*STARTXX
  PACIFIC        0 1 1 1          ONE column
*NODECOORDS
! foundation
C    1    0    0.
! beam-column joint
C    2    0.   300.
! beam-column joint
C    3    0.   1422.
C    8    228.5    203.  -1
C    9    -457.   0.   -1
C   10    0.   -406.  -1
C   11    457.   0.   -1
! COLUMN TOP
C    4    0.   1422.
! column middle
C    5    0.   2842.
!BEAM START
C    6    0    1422.
C   12    228.5    203.  -1
C   13    -457.   0.   -1
C   14    0.   -406.  -1
C   15    457.   0.   -1
!BEAM END
C    7    1600    1422.
!dummy nodes (The corners of 2 connectors)
C   32    228.5    1625.
C   33    -228.5   1625.
C   34    -228.5   1219.
C   35    228.5    1219.
C   36    228.5    1625.
C   37    -228.5   1625.
C   38    -228.5   1219.
C   39    228.5    1219.
C   42    228.5    1625.
C   43    -228.5   1625.
C   44    -228.5   1219.
C   45    228.5    1219
C   46    228.5    1625.
C   47    -228.5   1625.
C   48    -228.5   1219.
```

```
C    49    228.5    1219
C    52    228.5    1625.
C    53   -228.5    1625.
C    54   -228.5    1219.
C    55    228.5    1219
C    56    228.5    1625.
C    57   -228.5    1625.
C    58   -228.5    1219.
C    59    228.5    1219
*RESTRAINTS
! fixed supports at foundations
S 110       1
S 100       5
*SLAVING
! MAKE CONNECTION RIGID
S 111    3    4
S 111    3    8    11    1
S 111    6    12    15    1
S 110    32    52
S 110    33    53
S 110    34    54
S 110    35    55
S 110    36    56
S 110    37    57
S 110    38    58
S 110    39    59
*ELEMENTGROUP
   2   1   0
   2   0   2
   1   1.E9    .1    25.    52.08    4.   4.   2.
   2   1.E9    .1    25.    52.08    4.   4.   2.
   1   1    1.E9    1.E9
   2   1    1.E9    1.E9
1    32       33    1    1       1   1
2    53       34    1    1       1   1
3    54       35    1    1       1   1
4    52       55    3    1       1   1
5    36       37    1    1       1   1
6    57       38    1    1       1   1
7    58       39    1    1       1   1
8    56       59    3    1       1   1
*ELEMENTGROUP
   4   1   0       0.       ROTATIONAL CONNECTIONS
   4
   1   .5e9    .0005    2.E9    2.E9    .1    1    0
   2   .5e9    .0005    2.E9    2.E9    .1    2    0
```

```
3     .5E9    .0005    2.E9    2.E9    .1    1    0
4     .5E9    .0005    2.E9    2.E9    .1    2    0
1     12      32       0       1
2     12      32       0       2
3     9       33       0       1
4     9       33       0       2
5     15      35       0       1
6     15      35       0       2
7     10      34       0       1
8     10      34       0       2
9     14      38       0       1
10    14      38       0       2
11    13      37       0       1
12    13      37       0       2
13    8       36       0       1
14    8       36       0       2
15    11      39       0       1
16    '11     39       0       2
17    32      42       0       3
18    32      42       0       4
19    33      43       0       3
20    33      43       0       4
21    34      44       0       3
22    34      44       0       4
23    35      45       0       3
24    35      45       0       4
25    36      46       0       3
26    36      46       0       4
27    37      47       0       3
28    37      47       0       4
29    38      48       0       3
30    38      48       0       4
31    39      49       0       3
32    39      49       0       4
*ELEMENTGROUP
15    1    1         0.        1 COLUMNS
 4    3    3    2    0    0    0    0    4
! concrete material FOR COLUMN
  3 2       0   .0001
0.0200    .00067
0.0401    .002
0.00802   .017
.003534   .00016
0.0001    .00145
```

```
! concrete material FOR BEAM
  3 2      .5   .0001
0.0200   .00067
0.0401   .002
0.00802  .017
.003534  .00016
0.0001   .00145
! concrete material FOR joint
  2 2      .5   .0001
0.0401   .002
0.008    .030
.003534  .9558
0.0001   1.90146
! concrete material FOR JOINT
  2 2      0.   .0001
0.0401   .002
0.0165   .05
0.003534 .95
0.0001   1.946
! COLUMN BASE REINFORCEMENT
  2    .0001
  .47  .00235
  .65  .1
! COLUMN REINFORCEMENT
  2    .0001
  .47  .00235
  .65  .1
! BEAM REINFORCEMENT
  2    .0001
  .45  .00225
  .63  .1
 41      ! COLUMN
 5.71   3484.63   C01
17.14   3484.63   C01
28.56   3484.63   C01
39.99   3484.63   C01
51.41   3484.63   C01
62.84   3484.63   C01
74.26   3484.63   C01
85.69   3484.63   C01
97.11   3484.63   C01
108.54  3484.63   C01
119.96  3484.63   C01
131.39  3484.63   C01
```

```
142.81    3484.63    C01
154.24    3484.63    C01
165.66    3484.63    C01
179.09    4646.44    C01
188.51    1161.00    S02
197.94    4646.44    C01
211.36    3484.63    C01
222.79    3484.63    C01
0.        1161.      S02
-5.71     3484.63    C01
-17.14    3484.63    C01
-28.56    3484.63    C01
-39.99    3484.63    C01
-51.41    3484.63    C01
-62.84    3484.63    C01
-74.26    3484.63    C01
-85.69    3484.63    C01
-97.11    3484.63    C01
-108.54   3484.63    C01
-119.96   3484.63    C01
-131.39   3484.63    C01
-142.81   3484.63    C01
-154.24   3484.63    C01
-165.66   3484.63    C01
-179.09   4646.44    C01
-188.51   1161.00    S02
-197.94   4646.44    C01
-211.36   3484.63    C01
-222.79   3484.63    C01
 40    ! BEAM
5.        3095.      C02
15.       3095.      C02
25.       3095.      C02
35.       3095.      C02
45.       3095.      C02
55.       3095.      C02
65.       3095.      C02
75.       3095.      C02
85.       3095.      C02
95.       3095.      C02
105.      3095.      C02
115.      3095.      C02
125.      3095.      C02
135.      3095.      C02
145.      3095.      C02
155.      3365.      C02
```

```
165.    2560.   S03
175.    3365.   C02
185.    3095.   C02
195.    3095.   C02
-5.     3095.   C02
-15.    3095.   C02
-25.    3095.   C02
-35.    3095.   C02
-45.    3095.   C02
-55.    3095.   C02
-65.    3095.   C02
-75.    3095.   C02
-85.    3095.   C02
-95.    3095.   C02
-105.   3095.   C02
-115.   3095.   C02
-125.   3095.   C02
-135.   3095.   C02
-145.   3095.   C02
-155.   3365.   C02
-165.   2560.   S03
-175.   3365.   C02
-185.   3095.   C02
-195.   3095.   C02
10
2.5     665.    C04
7.5     665.    C04
12.5    567.5   C03
17.5    567.5   C03
2       8.0     S02
-2      7.0     S03
-2.5    665.    C04
-7.5    665.    C04
-12.5   567.5   C03
-17.5   567.5   C03
2.42587E9 1.39385E5    30.00    14.4
1.7001E9  1.2383E5     30.00    14.4
2
  .10   F01
  .90   E01
2
  .90   E01
  .10   F01
2
  .10   F02
  .90   E02
```

```
1
  1.0    F03
   1     1     2      1  1
   2     2     3      1  2
   3     4     5      1  1
   4     6     7      1  3
   5    42    44      2  4
   6    43    45      2  4
   7    46    48      2  4
   8    47    49      2  4
*RESULTS
! nodes 1 and 2
NSD  001       7
*NODALOAD
 HORZ                    UNIT HORIZONTAL LOAD
S  0.   -1.    0.     7
*NODALOAD
 HORP                    UNIT HORIZONTAL LOAD
S  0.   -1.    0.     5
*NODALOAD
 HORN                    UNIT HORIZONTAL LOAD
S  0.    1.    0.     7
*PARAMETERS
! print only, every event
OS     0   0  -1   0  50000
*STAT
N    HORP     1.
L   10.0    644.  5
*STAT
N    HORZ     1.
L    2.     22.  5
*STAT
N    HORN     1.
L    2.     22.  5
*STAT
N    HORN     1.
L    2.     22.  5
*STAT
N    HORZ     1.
L    2.     22.  5
*STAT
N    HORZ     1.
L    2.     44.  5
*STAT
N    HORN     1.
L    2.     44.  5
```

```
*STAT
N    HORN    1.
L    2.    44.  5
*STAT
N    HORZ    1.
L    2.    44.  5
*STAT
N    HORZ    1.
L    2.    66.  5
*STAT
N    HORN    1.
L    2.    66.  5
*STAT
N    HORN    1.
L    2.    66.  5
*STAT
N    HORZ    1.
L    2.    66.  5
*STAT
N    HORZ    1.
L    2.    88.  5
*STAT
N    HORN    1.
L    2.    88.  5
*STAT
N    HORN    1.
L    2.    88.  5
*STAT
N    HORZ    1.
L    2.    88.  5
*STAT
N    HORN    1.
L    2.    110.  5
*STAT
N    HORZ    1.
L    2.    110.  5
*STAT
N    HORZ    1.
L    2.    110.  5
*STAT
N    HORN    1.
L    2.    110.  5
*STAT
N    HORN    1.
L    2.    129.  5
*STAT
```

```
N    HORZ      1.
L    2.    129.  5
*STAT
N    HORZ      1.
L    2.    129.  5
*STAT
N    HORN      1.
L    2.    129.  5
*STAT
N    HORN      1.
D    7     0    2   .1    10.0    20   3   5
*STAT
N    HORN      1.
D    0     7    2   .1    10.0    20   3   5
*STAT
N    HORN      1.
D    0     7    2   .1    10.0    20   3   5
*STAT
N    HORN      1.
D    7     0    2   .1    10.0    20   3   5
*STAT
N    HORN      1.
D    7     0    2   .1    20.0    40   99  5
*STAT
N    HORN      1.
D    0     7    2   .1    20.0    40   99  5
*STAT
N    HORN      1.
D    0     7    2   .1    20.0    40   99  5
*STAT
N    HORN      1.
D    7     0    2   .1    20.0    40   99  5 !17
*STAT
N    HORN      1.
D    7     0    2   .07   24.0    40   99  5
*STAT
N    HORN      1.
D    7     0    2   .02    6.     40   99  5
*STAT
N    HORN      1.
D    0     7    2   .02   15.0    40   99  5
*STAT
N    HORN      1.
D    0     7    2   .02   15.0    20   99  99
*STAT
N    HORN      1.
```

```
D    0     7   2   .06    24.0    40   99   5
*STAT
N    HORN      1.
D    0     7   2   .002    4.    20   99   99    !15
*STAT
N    HORN      1.
D    0     7   2   .005    2.    20   99   99
*STAT
N    HORN      1.
D    7     0   2   .03    30.0    20   99   99
*STAT
N    HORN      1.
D    7     0   2   .01    13.0    40   99   99
*STAT
N    HORN      1.
D    7     0   2   .04    10.    40   99   99
*STAT
N    HORN      1.                          `
D    7     0   2   .04    10.    40   99   99
*STAT
N    HORN      1.
D    0     7   2   .01    33.0    40   99   99
*STAT
N    HORN      1.
D    0     7   2   .01    33.0    40   99   99
*STAT
N    HORN      1.
D    7     0   2   .02    33.0    40   99   99
*STAT
N    HORN      1.
D    7     0   2   .08    37.0    40   99   99
*STAT
N    HORN      1.
D    0     7   2   .08    37.0    40   99   99
*STAT
N    HORN      1.
D    0     7   2   .08    37.0    40   99   99
*STAT
N    HORN      1.
D    7     0   2   .08    37.0    40   99   99
*STAT
N    HORN      1.
D    7     0   2   .08    45.0    40   99   99
*STAT
N    HORN      1.
D    0     7   2   .08    45.0    40   99   99
```

```
*STAT
N    HORN    1.
D    0      7    2    .08    45.0    40  99  99
*STAT
N    HORN    1.
D    7      0    2    .08    45.0    40  99  99
*STAT
N    HORN    1.
D    7      0    2    .08    52.0    40  99  99
*STAT
N    HORN    1.
D    0      7    2    .08    52.0    40  99  99
*STAT
N    HORN    1.
D    0      7    2    .08    52.0    40  99  99
*STAT
N    HORN    1.
D    7      0    2    .08    52.0    40  99  99
*STAT
N    HORN    1.
D    7      0    2    .06    60.0    40  99  99
*STAT
N    HORN    1.
D    0      7    2    .06    60.0    40  99  99
*STAT
N    HORN    1.
D    0      7    2    .06    60.0    40  99  99
*STAT
N    HORN    1.
D    7      0    2    .06    60.0    40  99  99
*STOP
```